

Automatically Bounding the Taylor Remainder Series: Tighter Bounds and New Applications

Matthew Streeter and Joshua V. Dillon

{mstreeter, jvdillon}@google.com

Abstract

Taylor polynomials play a central role in optimization and machine learning, in part because they can be easily computed using automatic differentiation. In many places where Taylor polynomials are used, it would be advantageous to also have a bound on the remainder series, but techniques for generating such bounds automatically are not as mature as automatic differentiation, and their potential has been less fully explored.

In this work, we present a new algorithm for automatically bounding the Taylor remainder series. In the special case of a scalar function $f : \mathbb{R} \rightarrow \mathbb{R}$, our algorithm takes as input a reference point x_0 , trust region $[a, b]$, and integer $k \geq 1$, and returns an interval I such that $f(x) - \sum_{i=0}^{k-1} \frac{1}{i!} f^{(i)}(x_0)(x - x_0)^i \in I(x - x_0)^k$ for all $x \in [a, b]$. As in automatic differentiation, the function f is provided to the algorithm in symbolic form, and must be composed of known atomic functions.

At a high level, our algorithm has two steps:

1. For a variety of commonly-used functions (e.g., exp, log, relu, softplus), we derive *sharp* polynomial upper and lower bounds on the Taylor remainder series.
2. We recursively combine the bounds for the atomic functions using an interval arithmetic variant of Taylor-mode automatic differentiation.

Our algorithm can make efficient use of machine learning hardware accelerators, and we provide an open source implementation in JAX.¹

We then turn our attention to applications. Most notably, we use our new machinery to create the first *universal* majorization-minimization optimization algorithms: algorithms that iteratively minimize an arbitrary loss using a majorizer that is derived *automatically*, rather than by hand. Applied to machine learning, this leads to architecture-specific optimizers for training deep networks that converge from any starting point, without hyperparameter tuning. Our experiments show that for some optimization problems, these hyperparameter-free optimizers outperform *tuned* versions of gradient descent, Adam, and AdaGrad.

We also show that our automatically-derived bounds can be used for verified global optimization and numerical integration, and to prove sharper versions of Jensen’s inequality.

¹<http://github.com/google/autobound>

Contents

1	Introduction	3
1.1	Outline	4
1.2	An End-to-End Example	5
1.3	Summary of Related Work	6
2	Sharp Taylor Enclosures in One Dimension	7
2.1	Definitions and Notation	8
2.2	Non-Sharp Taylor Enclosures via Bounded Derivatives	9
2.3	Functions with Monotone Derivative	10
2.3.1	Examples	11
2.4	Functions with Even-Symmetric Hessian	12
2.5	Comparison to Taylor Enclosures Based on Derivative Bounds	13
2.6	Related Work	13
2.7	Future Work	13
3	Taylor Enclosures for Arbitrary Univariate Functions	14
3.1	Background: Taylor Mode Automatic Differentiation	14
3.2	Definitions and Notation	15
3.3	The AutoBound1D Algorithm	16
3.3.1	Interval Polynomial Extensions of Atomic Functions	17
3.3.2	Pseudocode and Example	19
3.3.3	Tightness of Automatically-Derived Bounds	23
3.3.4	Limitations	23
3.4	Related Work	24
4	Generalization to Multivariate Functions	25
4.1	Definitions and Notation	25
4.1.1	Operational Semantics for Tensor Intervals	27
4.1.2	Extended Functions	27
4.2	The AutoBound Algorithm	28
4.2.1	Tensor Interval Extensions of Atomic Functions	28
4.2.2	Tensor Interval Polynomial Extensions of Atomic Functions	30
4.2.3	Pseudocode and Analysis	34
4.3	An Implementation in JAX	35
4.4	Future Work	35
5	Automatically Deriving MM Optimization Algorithms	37
5.1	Background: MM Optimization Algorithms	38
5.2	Universal MM Optimization Algorithms	38
5.2.1	Using AutoBound to Derive Majorizers	39

5.2.2	SafeRate: Determining a Safe Learning Rate	39
5.2.3	SafeCombination: Combining Multiple Update Directions	40
5.2.4	Theoretical Guarantees	41
5.3	Experiments	43
5.3.1	Optimizers	43
5.3.2	One-Dimensional Problems	44
5.3.3	Random Regression Problems	47
5.3.4	Multi-Layer Perceptrons	50
5.3.5	Tightness of Automatically-Derived Majorizers	53
5.3.6	Summary	56
5.4	Related Work	56
5.5	Future Work	57
6	Additional Applications	58
6.1	Verified Global Optimization	58
6.1.1	Experiment	58
6.2	Verified Numerical Integration	59
6.2.1	Algorithm Description	59
6.2.2	Experiment	60
6.3	Automatically Sharpening Jensen’s Inequality	61
6.3.1	Experiment	62
7	Summary and Conclusions	63
Appendices		70
A	Proofs	70
A.1	Sharp Taylor Enclosures in One Dimension	70
A.1.1	Proof of Theorem 1	70
A.1.2	Proof of Theorem 2	73
A.1.3	Proof of Theorem 3	76
A.2	Taylor Enclosures for Arbitrary Univariate Functions	77
A.3	Generalization to Multivariate Functions	80
A.3.1	Bilinear Operations on Tensor Intervals	81
A.3.2	Proof of Theorem 7	83
A.3.3	Proof of Theorem 8	84
A.3.4	Proof of Theorem 9	86
A.4	Proof of Theorems 10 and 11	86
A.5	Proof of Theorem 12	88
B	Implementation Details	89
B.1	Computing the SafeRate Learning Rate	89
B.2	Optimizing a Non-Convex Quadratic Over a Hyperrectangle	89

Chapter 1

Introduction

Taylor polynomials are among the most widely used tools in science and engineering. They play a central role in numerical optimization, where first and second-order Taylor polynomials are used to iteratively minimize a scalar-valued function. Because Taylor polynomials can be computed using automatic differentiation, numerical optimizers can be easily applied to very complex functions, such as the training losses used to fit modern machine learning models.

However, a Taylor polynomial provides only a local approximation of a function's behavior, with no guarantees on the accuracy of this approximation at points far from the point x_0 at which derivatives are computed. In applications, this lack of error information is often compensated for by the addition of knobs, whose values must be tuned experimentally. For example, in gradient-based optimization, trial and error is often required to find a value of the learning rate hyperparameter that is large enough to yield sufficiently fast progress but small enough to avoid divergence. Though automated methods for bounding the Taylor remainder series exist, they are less mature than automatic differentiation, and have been less widely used.

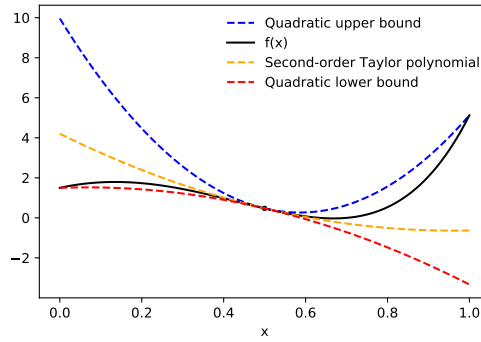


Figure 1.1: Automatically-derived quadratic upper and lower bounds for the function $f(x) = \frac{3}{2} \exp(3x) - 25x^2$, centered at $x_0 = \frac{1}{2}$, and valid over the interval $[0, 1]$.

In this work, we present algorithms for automatically bounding the Taylor remainder series. Applied to a univariate function $f : \mathbb{R} \rightarrow \mathbb{R}$, our algorithms will take as input a trust region $[a, b]$, a reference point $x_0 \in [a, b]$, and a polynomial degree $k \geq 1$, and will output an interval I such that

$$f(x) \in \underbrace{\left(\sum_{i=0}^{k-1} \frac{1}{i!} f^{(i)}(x_0) (x - x_0)^i \right)}_{\text{Degree } k-1 \text{ Taylor polynomial}} + \underbrace{I(x - x_0)^k}_{\text{Remainder bound}} \quad \forall x \in [a, b] \quad (1.1)$$

where I depends on x_0 , k , and $[a, b]$, and is derived from the symbolic expression for f . Note that the right hand side of (1.1) is an interval, defined according to the semantics of interval arithmetic,¹ and therefore gives both upper and lower bounds on $f(x)$. Figure 1.1 depicts the upper and lower bounds our algorithm produces for the function $f(x) = \frac{3}{2} \exp(3x) - 25x^2$ at $x_0 = \frac{1}{2}$, over the trust region $[0, 1]$, with $k = 2$ (which yields quadratic bounds).

We will also be able to compute bounds for vector-variate functions, and the form of these bounds will generalize (1.1) in a natural way.

Among other applications, bounds of this form will allow us to automatically derive majorization-minimization (MM) optimization algorithms. In particular, if we set $k = 2$, the upper bound in (1.1) is a quadratic majorizer, which can be minimized to obtain a point x_1 such that $f(x_1) \leq f(x_0)$. This process can be repeated to further reduce the loss, until a fixed point is reached.

We pay special attention to making the interval I as tight as possible, as this leads to better performance in applications (e.g., faster reduction of the loss in MM optimization). To encourage others to experiment with our bounds and to find new applications, we provide an open source implementation in JAX.

1.1 Outline

We first present our new approach to automatically bounding the Taylor remainder series.

- In Chapter 2, we show how to compute *sharp* Taylor enclosures (i.e., bounds of the form in (1.1)) when f has specific properties, such as a monotonically increasing or decreasing k th derivative, or an even-symmetric Hessian. This allows us to compute sharp Taylor enclosures for many elementary functions, such as \exp and \log , as well as commonly-used neural network activation functions such as relu and softplus .
- In Chapter 3, we present the AutoBound1D algorithm, which recursively combines sharp Taylor enclosures for atomic univariate functions and elementary binary operations, in order to obtain Taylor enclosures for arbitrary compositions of these functions.
- Chapter 4 presents the AutoBound algorithm, which generalizes the results of Chapter 3 to multivariate functions. Because the Taylor series for a multivariate function cannot be expressed in standard matrix calculus notation, we must define an appropriate alternative, and this chapter is more notation-heavy than the others. We take care to ensure that AutoBound can make efficient use of modern automatic differentiation frameworks, and discuss our open source implementation in JAX.

We then turn our attention to applications.

- In Chapter 5, we show that the AutoBound algorithm can be used to create loss-function-specific majorization-minimization (MM) algorithms, which minimize a loss function by iteratively minimizing a locally-tight (typically quadratic) upper bound on the loss. We define two algorithms: SafeRate computes a learning rate that is guaranteed to reduce the loss, and SafeCombination generalizes this by computing a linear combination of user-supplied update directions. We then evaluate these algorithms experimentally. On some optimization problems, such as randomly-generated linear regression problems with non-normally-distributed errors, we find that our hyperparameter-free algorithms dramatically outperform *tuned* versions of gradient descent, Adam, and AdaGrad.
- In Chapter 6, we demonstrate three additional applications of AutoBound: globally optimizing a loss function via branch and bound, computing upper and lower bounds on the value of an integral, and automatically proving sharper versions of Jensen’s inequality.

Finally, Chapter 7 summarizes our work and presents conclusions.

¹The product of an interval $I = [\underline{I}, \bar{I}]$, and a scalar z is defined as $Iz \triangleq \{\alpha z : \alpha \in I\} = [\min\{\underline{I}z, \bar{I}z\}, \max\{\underline{I}z, \bar{I}z\}]$.

1.2 An End-to-End Example

Though presenting the AutoBound algorithm in full generality will require a fair amount of notation, much of the intuition behind the algorithm can be conveyed through a simple example.

Toward this end, suppose we want to come up with quadratic upper and lower bounds on a univariate function $f : \mathbb{R} \rightarrow \mathbb{R}$, defined by

$$f(x) = \exp(x^2). \quad (1.2)$$

Further suppose that we require the bounds to be tight at the point $x_0 = 0.2$, and only require these bounds to be valid for $x \in [-0.5, 0.5]$ (the *trust region*).

As in automatic differentiation, we begin by writing the value of $f(x)$ as a sequence of equations, where each equation gives the value of an intermediate variable as an elementary function of one or more intermediate variables:

$$\begin{aligned} v_0 &= x \\ v_1 &= v_0^2 \\ v_2 &= \exp(v_1). \end{aligned} \quad (1.3)$$

We then compute the values of the intermediate variables at $x = x_0 = 0.2$:

$$\begin{aligned} v_0^{(0)} &= 0.2 \\ v_1^{(0)} &= 0.04 \\ v_2^{(0)} &= 1.0408. \end{aligned} \quad (1.4)$$

Here and throughout the example, numeric values are shown with 5 significant digits.

Next, given our knowledge that $x \in [-0.5, 0.5]$, we compute intervals that enclose the possible values of all the intermediate variables. Using the rules of interval arithmetic, we obtain

$$\begin{aligned} v_0 &\in [-.5, .5] \\ v_1 &\in [0, .25] \\ v_2 &\in [1, 1.2841]. \end{aligned} \quad (1.5)$$

We are now in a position to compute quadratic upper and lower bounds on each intermediate variable, as a function of $x - x_0$. For v_0 , we have the trivial equality

$$v_0 = x_0 + 1 \cdot (x - x_0) = .2 + 1 \cdot (x - .2). \quad (1.6)$$

Note that this equality provides (tight) upper and lower bounds on v_0 , and that these bounds are affine (and hence trivially quadratic) in terms of $x - x_0$.

To obtain quadratic upper and lower bounds for $v_1 = v_0^2$, we square the polynomial on the right hand side of (1.6), to obtain

$$v_1 = 0.04 + 0.4 \cdot (x - .2) + 1 \cdot (x - .2)^2. \quad (1.7)$$

We now consider $v_2 = \exp(v_1)$. To bound v_2 by quadratics, we require quadratic bounds on the \exp function. In Chapter 2 we will develop theory that lets us produce sharp polynomial bounds of arbitrary degree for \exp and other functions. For now, we will take it on faith that for $v_1^{(0)} = 0.04$ (calculated in (1.4)) and $v_1 \in [0, .25]$ (calculated in (1.5)),

$$\exp(v_1) \in 1.0408 + 1.0408 \cdot \left(v_1 - v_1^{(0)}\right) + [0.51353, 0.55883] \cdot \left(v_1 - v_1^{(0)}\right)^2. \quad (1.8)$$

Plugging in the expression for v_1 from (1.7), plugging in $v_1^{(0)} = 0.04$, and expanding gives a quartic polynomial bound in terms of $x - x_0$:

$$\begin{aligned} \exp(v_1) &\in 1.0408 + 0.41632 \cdot (x - x_0) + [1.1230, 1.1302] (x - x_0)^2 \\ &\quad + [0.41083, 0.44706] (x - x_0)^3 + [0.51353, 0.55883] (x - x_0)^4. \end{aligned} \quad (1.9)$$

To obtain a bound that is quadratic (rather than quartic) in terms of $x - x_0$, we again use knowledge of the fact that $x \in [-.5, .5]$ to infer that $x - x_0 \in [-.7, .3]$ (recall $x_0 = 0.2$), and therefore $(x - x_0)^3 \in [-.7, .3](x - x_0)^2$, while $(x - x_0)^4 \in [0, .49](x - x_0)^2$. Making these substitutions, and collecting terms yields the quadratic bounds:

$$\exp(v_1) \in 1.0408 + 0.41632 \cdot (x - x_0) + [0.81728, 1.5382] (x - x_0)^2. \quad (1.10)$$

Figure 1.2 plots the function $f(x) = \exp(x^2)$, together with the quadratic upper and lower bounds we have just derived.

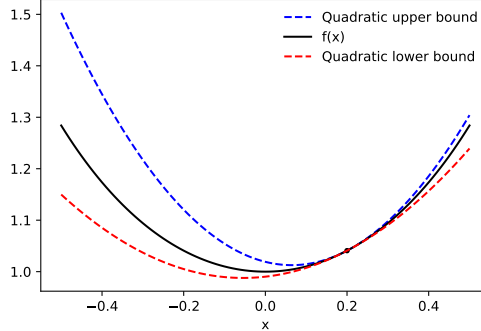


Figure 1.2: Quadratic upper and lower bounds for the function $f(x) = \exp(x^2)$, centered at $x_0 = 0.2$, and valid over the interval $[-0.5, 0.5]$.

1.3 Summary of Related Work

We now give a high-level summary of related work, deferring a more detailed discussion to the separate related work sections that appear in each chapter.

At a high level, our AutoBound algorithm can be viewed as a generalization of Taylor-mode automatic differentiation, which is itself a generalization of forward-mode automatic differentiation. For a comprehensive introduction to these and other automatic differentiation techniques, see [28].

Our work is closely related to an earlier line of work on *Taylor models* [55, 56, 57, 58], which developed an algorithm that, like AutoBound, can be viewed as a variant of Taylor-mode automatic differentiation that makes use of interval arithmetic. However, in Taylor models, the Taylor remainder series is simply bounded by an interval, whereas, as shown in (1.1), we bound the Taylor remainder series by a product of an interval and $(x - x_0)^k$. The latter form of bound is necessary for automatically deriving MM optimizers, and can offer advantages in other applications. Additionally, as discussed further in §3.3, we produce tighter bounds (i.e., narrower intervals) than would be obtained from a direct generalization of previous work on Taylor models, by deriving *sharp* Taylor enclosures for a variety of atomic functions, and by recursively combining the resulting interval polynomials in a tighter way.

The work on sharp Taylor enclosures we present in Chapter 2 was inspired by [17], which introduced the notion of sharp quadratic majorizers for one-dimensional functions, and derived closed-form majorizers for a number of common functions. We generalize their results by considering arbitrary-degree polynomials (rather than just quadratics), and derive tighter bounds by only requiring the bounds to be valid over a user-specified trust region. In addition to making the bounds tighter, the use of a trust region allows us to compute bounds for functions such as \exp , which are not globally upper bounded by any finite degree polynomial.

Chapter 2

Sharp Taylor Enclosures in One Dimension

In this chapter we introduce *sharp Taylor enclosures*, and develop theory that can be used to compute them for various elementary one-dimensional functions of interest.

The main ideas can be illustrated with a simple example. Suppose we are interested in the behavior of the \exp function around the point $x_0 = \frac{1}{2}$. Using the second degree Taylor polynomial, we may obtain the approximation

$$\exp(x) \approx \sqrt{e} + \sqrt{e} \left(x - \frac{1}{2} \right) + 0.82436 \left(x - \frac{1}{2} \right)^2 \quad \text{for } x \approx \frac{1}{2}. \quad (2.1)$$

The approximation is tight at $x = \frac{1}{2}$, but its error grows exponentially for $x \gg x_0$.

In some applications, we would prefer to have polynomial upper and/or lower bounds, rather than a polynomial approximation. Because $\exp(x)$ grows faster than any polynomial, no polynomial upper bound can hold for all $x \in \mathbb{R}$. However, if we only require the bounds to hold for x belonging to some finite interval, the theory developed in this chapter will allow us to compute the tightest polynomial bounds that are valid over that interval. For example, we will be able to show

$$\exp(x) \in \sqrt{e} + \sqrt{e} \left(x - \frac{1}{2} \right) + [0.70255, 1.4522] \left(x - \frac{1}{2} \right)^2 \quad \text{for } x \in [0, 2]. \quad (2.2)$$

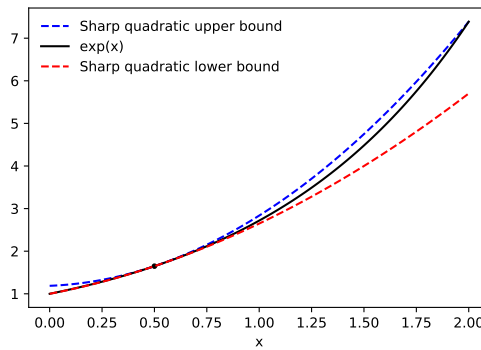


Figure 2.1: The sharp quadratic Taylor enclosure of $\exp(x)$, at $x_0 = \frac{1}{2}$, and valid over the interval $[0, 2]$.

The expression on the right hand side of (2.2) defines what we call a *Taylor enclosure*, which is similar to a Taylor polynomial except that the maximum-degree coefficient is an interval (rather than a scalar). A

Taylor enclosure is called *sharp* if this interval is as narrow as possible, as is the case in (2.2). A Taylor enclosure can be thought of as a function that returns an interval, or equivalently, as a pair of real-valued functions, one of which returns a lower bound and one of which returns an upper bound.

Figure 2.1 illustrates the sharp quadratic Taylor enclosure of \exp , centered at $x_0 = \frac{1}{2}$, and valid over the trust region $[0, 2]$. Observe that the upper bound is tight at two points: $x = x_0$, and $x = 2$, the maximum value in the trust region. Likewise the lower bound is tight at $x = x_0$ and at $x = 0$, the minimum value in the trust region. Having the lower and upper bounds be tight at two (or more) points is a general feature of sharp quadratic bounds [17].

In this chapter, we will develop theory that lets us compute sharp Taylor enclosures of arbitrary degree for one-dimensional functions with certain nice properties. In particular:

1. In §2.3, we show how to compute sharp Taylor enclosures for functions whose $(k + 1)$ st derivative is monotonically increasing or decreasing (such as \exp or \log).
2. In §2.4, we show how to compute sharp Taylor enclosures for functions whose Hessian is even-symmetric (such as softplus, relu , and a number of other commonly-used neural network activation functions).

For functions that do not have either of these special properties, we discuss in §2.2 an alternative method for computing Taylor enclosures using derivative bounds, with the caveat that the results are in general not sharp.

2.1 Definitions and Notation

For a j -times differentiable function $f : \mathbb{R} \rightarrow \mathbb{R}$, and a scalar $x_0 \in \mathbb{R}$, we denote the degree j Taylor polynomial of f at x_0 by

$$T_j(x; f, x_0) \triangleq \sum_{i=0}^j \frac{1}{i!} f^{(i)}(x_0) (x - x_0)^i. \quad (2.3)$$

We denote the corresponding remainder term by

$$R_j(x; f, x_0) \triangleq f(x) - T_j(x; f, x_0). \quad (2.4)$$

Consistent with this definition, we define $T_{-1}(x; f, x_0) \triangleq 0$ and $R_{-1}(x; f, x_0) \triangleq f(x)$.

We denote the set of closed real intervals by $\mathbb{IR} \triangleq \{[a, b] : a, b \in \mathbb{R}, a \leq b\}$. For an interval $I \in \mathbb{IR}$, we use \underline{I} and \bar{I} to denote the left and right endpoints, so that $I = [\underline{I}, \bar{I}]$. The product of an interval $I \in \mathbb{IR}$ and scalar $\alpha \in \mathbb{R}$ is defined as $I\alpha \triangleq \{\alpha x : x \in I\}$, and αI is defined identically. Observe that if $\alpha \geq 0$, $I\alpha = [\alpha \underline{I}, \alpha \bar{I}]$, while if $\alpha \leq 0$, $I\alpha = [\alpha \bar{I}, \alpha \underline{I}]$.

With this notation in place, we can now define Taylor enclosures.

Definition 1 (Taylor enclosure). *If, for some $(k - 1)$ -times differentiable function $f : \mathbb{R} \rightarrow \mathbb{R}$, scalar $x_0 \in \mathbb{R}$, and trust region $[a, b] \in \mathbb{IR}$, an interval $I \in \mathbb{IR}$ satisfies*

$$R_{k-1}(x; f, x_0) \in I(x - x_0)^k \quad \forall x \in [a, b]$$

then the function $F : \mathbb{R} \rightarrow \mathbb{IR}$ defined by

$$F(x) = T_{k-1}(x; f, x_0) + I(x - x_0)^k$$

is a degree k Taylor enclosure of f at x_0 over $[a, b]$.

Observe that if F is a degree k Taylor enclosure of f at x_0 over $[a, b]$, then $f(x) \in F(x)$ for all $x \in [a, b]$.

Of all the intervals I that define a Taylor enclosure, there is a unique narrowest interval, whose end points are given by the following proposition.

Proposition 1. For a $(k-1)$ -times differentiable function $f : \mathbb{R} \rightarrow \mathbb{R}$, scalar $x_0 \in \mathbb{R}$, and trust region $[a, b]$, an interval $I \in \mathbb{IR}$ defines a degree k Taylor enclosure of f at x_0 over $[a, b]$ if and only if

$$I \leq \inf_{x \in [a, b] \setminus \{x_0\}} \left\{ \frac{R_{k-1}(x; f, x_0)}{(x - x_0)^k} \right\}$$

and

$$\bar{I} \geq \sup_{x \in [a, b] \setminus \{x_0\}} \left\{ \frac{R_{k-1}(x; f, x_0)}{(x - x_0)^k} \right\}.$$

Proposition 1 follows from Definition 1 using elementary properties of interval arithmetic; see Appendix A for a formal proof.

Proposition 1 shows that there is a unique sharp Taylor enclosure, defined formally in Definition 2.

Definition 2 (Sharp Taylor enclosure). For a $(k-1)$ -times differentiable function $f : \mathbb{R} \rightarrow \mathbb{R}$, scalar $x_0 \in \mathbb{R}$, and trust region $[a, b]$, the degree k sharp Taylor enclosure of f at x_0 over $[a, b]$ is the Taylor enclosure defined by the interval

$$I_k^*(f, x_0, [a, b]) \triangleq \left[\inf_{x \in [a, b] \setminus \{x_0\}} \left\{ \frac{R_{k-1}(x; f, x_0)}{(x - x_0)^k} \right\}, \sup_{x \in [a, b] \setminus \{x_0\}} \left\{ \frac{R_{k-1}(x; f, x_0)}{(x - x_0)^k} \right\} \right].$$

2.2 Non-Sharp Taylor Enclosures via Bounded Derivatives

Before attempting to derive *sharp* Taylor enclosures, we review a well-known way to derive (possibly non-sharp) Taylor enclosures using bounds on derivatives.

Suppose we desire a degree k Taylor enclosure of a function $f : \mathbb{R} \rightarrow \mathbb{R}$, valid over $[a, b]$, and tight at $x_0 \in [a, b]$, and further suppose that f is k times differentiable (rather than merely $k-1$ times differentiable, as required by Definition 1). Then, using the Lagrange form of the Taylor remainder series and the mean value theorem [3], for any $x \in \mathbb{R}$ there exists a y in the closed interval between x_0 and x , such that

$$R_{k-1}(x; f, x_0) = f^{(k)}(y) \frac{(x - x_0)^k}{k!}. \quad (2.5)$$

Because $x_0, x \in [a, b]$ we have $y \in [a, b]$ also, and thus

$$R_{k-1}(x; f, x_0) \in \left[\inf_{y \in [a, b]} \{f^{(k)}(y)\}, \sup_{y \in [a, b]} \{f^{(k)}(y)\} \right] \frac{(x - x_0)^k}{k!}. \quad (2.6)$$

Equation (2.6) thus defines a Taylor enclosure of f at x_0 over $[a, b]$.

In special cases, the end points of the interval in (2.6) can be computed in closed form. For example, if $f^{(k)}$ is monotonically increasing, the interval in (2.6) simplifies to $[f^{(k)}(a), f^{(k)}(b)]$. Even in these special cases, however, the resulting Taylor enclosure will not be sharp in general. For example, if used to compute a Taylor enclosure of \exp at $x_0 = \frac{1}{2}$ over the trust region $[0, 2]$, this method yields the Taylor enclosure

$$\exp(x) \in \sqrt{e} + \sqrt{e} \left(x - \frac{1}{2} \right) + [0.5, 3.6945] \left(x - \frac{1}{2} \right)^2 \quad \text{for } x \in [0, 2]. \quad (2.7)$$

In contrast, as shown in (2.2), the sharp Taylor enclosure is defined by the interval $[0.70255, 1.4522]$, which gives significantly tighter upper and lower bounds. A more extreme example of non-sharpness arises when computing a quadratic upper bound for the relu function. As long as $0 \in [a, b]$, the interval in (2.6) is $[0, \infty]$, leading to a vacuous upper bound. In contrast, the sharp Taylor enclosure will give a finite upper bound as long as $x \neq x_0$.

If $f^{(k)}$ is not known to have any special properties (such as being monotonically increasing or decreasing), an interval that encloses the interval on the right hand side of (2.6) can be obtained by first deriving an

expression for $f^{(k)}(y)$ (e.g., using automatic differentiation), and then evaluating this expression using interval arithmetic [31, 32, 40, 62]. Given an interval that contains y (here $[a, b]$), this procedure provides an interval that is guaranteed to contain $f^{(k)}(y)$ for all $y \in [a, b]$, and hence contains the interval on the right hand side of (2.6). Note, however, that the resulting interval depends on the expression for $f^{(k)}(y)$, and may be much wider than the interval in (2.6), introducing an additional source of non-sharpness.

2.3 Functions with Monotone Derivative

We will now show that the interval defining the sharp Taylor enclosure of f (at some $x_0 \in \mathbb{R}$ over some trust region $[a, b] \in \mathbb{IR}$) can be computed in closed form in the special case where $f^{(k)}$ is monotonically increasing or monotonically decreasing. Among other things, this will let us compute sharp Taylor enclosures for \exp over any interval, for \log over any interval $[a, b]$ with $a > 0$, and for the reciprocal function over any $[a, b]$ with $0 \notin [a, b]$.

To build intuition, we will first show that if $f'(x)$ is monotonically increasing, then the degree 1 sharp Taylor enclosure of f is defined by the interval

$$I_1^*(f, x_0, [a, b]) = \left[\frac{R_0(a; f, x_0)}{a - x_0}, \frac{R_0(b; f, x_0)}{b - x_0} \right]. \quad (2.8)$$

To see this, observe that if f' is monotonically increasing, then for $k = 1$ and $x \neq x_0$ we have

$$\begin{aligned} \frac{d}{dx} \frac{R_{k-1}(x; f, x_0)}{(x - x_0)^k} &= \frac{d}{dx} \frac{f(x) - f(x_0)}{x - x_0} \\ &= \frac{f'(x)}{x - x_0} - \frac{f(x) - f(x_0)}{(x - x_0)^2} \\ &= \frac{1}{(x - x_0)^2} ((x - x_0)f'(x) - (f(x) - f(x_0))) \\ &= \frac{1}{(x - x_0)^2} \int_{y=x_0}^x f'(x) - f'(y) dy \\ &\geq 0. \end{aligned} \quad (2.9)$$

Thus, for $k = 1$, we see that if f' is monotonically increasing, then $\frac{R_{k-1}(x; f, x_0)}{(x - x_0)^k}$ is also monotonically increasing. Therefore, by Definition 2, the end points of $I_k^*(f, x_0, [a, b])$ are $\inf_{x \in [a, b]} \left\{ \frac{R_{k-1}(x; f, x_0)}{(x - x_0)^k} \right\} = \frac{R_{k-1}(a; f, x_0)}{(a - x_0)^k}$ and $\sup_{x \in [a, b]} \left\{ \frac{R_{k-1}(x; f, x_0)}{(x - x_0)^k} \right\} = \frac{R_{k-1}(b; f, x_0)}{(b - x_0)^k}$, respectively. Plugging in $k = 1$ then gives (2.8).

We will generalize this result to obtain the following theorem, which allows us to compute a sharp degree k Taylor enclosure of any function whose k th derivative is monotonically increasing or decreasing.

Theorem 1. *Let $f : \mathbb{R} \rightarrow \mathbb{R}$ be a function that is k -times differentiable over an interval $[a, b]$, for $k \geq 0$. If $f^{(k)}$ is monotonically increasing over $[a, b]$, then for $x_0 \in (a, b)$, the degree k sharp Taylor enclosure of f at x_0 over $[a, b]$ is given by $I_k^*(f, x_0, [a, b]) = \left[\frac{R_{k-1}(a; f, x_0)}{(a - x_0)^k}, \frac{R_{k-1}(b; f, x_0)}{(b - x_0)^k} \right]$. If $f^{(k)}$ is monotonically decreasing over $[a, b]$, we instead have $I_k^*(f, x_0, [a, b]) = \left[\frac{R_{k-1}(b; f, x_0)}{(b - x_0)^k}, \frac{R_{k-1}(a; f, x_0)}{(a - x_0)^k} \right]$.*

In the special case $k = 0$, Theorem 1 says that if f is monotonically increasing, then $I_0^*(f, x_0, [a, b]) = [f(a), f(b)]$, recovering the trivial fact that if f is monotonically increasing, then $[f(a), f(b)]$ is the narrowest interval that contains $\{f(x) : x \in [a, b]\}$. In the special case $k = 1$, Theorem 1 recovers the result we just derived.

We now outline the proof of Theorem 1 for arbitrary k . First note that, to prove the theorem, it suffices to show that if $f^{(k)}$ is monotonically increasing (resp. decreasing), then $\frac{d}{dx} \frac{R_{k-1}(x; f, x_0)}{(x - x_0)^k}$ is non-negative (resp. non-positive) for $x \in [a, b]$. The first step in showing this is to write $\frac{d}{dx} \frac{R_{k-1}(x; f, x_0)}{(x - x_0)^k}$ as a weighted integral of $f^{(k)}$. To do so, we use the following two propositions.

Proposition 2. For any j -times differentiable function $f : \mathbb{R} \rightarrow \mathbb{R}$,

$$\frac{d}{dx} R_j(x; f, x_0) = R_{j-1}(x; f', x_0).$$

Note that the proposition is valid for $j = 0$, in which case it simply says $\frac{d}{dx} R_0(x; f, x_0) = f'(x)$ (recall that we define $R_{-1}(x; f', x_0) \triangleq f'(x)$). Proposition 2 is straightforward to prove, and a formal proof is given in Appendix A.

We will also use the well-known integral form of the Taylor remainder series [3].

Proposition 3 (Integral form of Taylor remainder series). For any function $f : \mathbb{R} \rightarrow \mathbb{R}$, and any integer $j \geq 0$, where $f^{(j)}$ is absolutely continuous over the closed interval between x_0 and x ,

$$R_j(x; f, x_0) = \int_{t=x_0}^x f^{(j+1)}(t) \frac{1}{j!} (x-t)^j dt.$$

Taking the derivative $\frac{d}{dx} \frac{R_{k-1}(x; f, x_0)}{(x-x_0)^k}$, and applying Propositions 2 and 3, we obtain the following lemma, whose proof is given in Appendix A.

Lemma 1. For any function $f : \mathbb{R} \rightarrow \mathbb{R}$, and any integer $k \geq 2$, where $f^{(k-1)}$ is absolutely continuous over the closed interval between x_0 and x ,

$$\frac{d}{dx} \frac{R_{k-1}(x; f, x_0)}{(x-x_0)^k} = \frac{1}{(x-x_0)^{k+1}} \int_{t=x_0}^x f^{(k)}(t) \left((x-x_0) \frac{1}{(k-2)!} (x-t)^{k-2} - \frac{k}{(k-1)!} (x-t)^{k-1} \right) dt.$$

The final and most involved step of the proof is to carefully analyze the sign of the expression given in Lemma 1 to show that if $f^{(k)}$ is monotonically increasing (decreasing), then $\frac{R_{k-1}(x; f, x_0)}{(x-x_0)^k}$ is monotonically increasing (decreasing) as well. This is proved in Lemma 2, from which Theorem 1 immediately follows. The proof is given in Appendix A.

Lemma 2. Let $f : \mathbb{R} \rightarrow \mathbb{R}$ be a function that is k times differentiable over the interval $[a, b]$, for $k \geq 0$. If $f^{(k)}$ is monotonically increasing (decreasing) over $[a, b]$, then for $x_0 \in (a, b)$, $\frac{R_{k-1}(x; f, x_0)}{(x-x_0)^k}$ is monotonically increasing (decreasing) over $[a, b]$.

2.3.1 Examples

We conclude this section by using Theorem 1 to derive sharp Taylor enclosures for a few functions of interest.

The \exp function has k th derivative $\exp^{(k)}(x) = \exp(x)$, which is monotonically increasing for all x . Thus, by Theorem 1,

$$\begin{aligned} I_k^*(\exp, x_0, [a, b]) &= \left[\frac{R_{k-1}(a; \exp, x_0)}{(a-x_0)^k}, \frac{R_{k-1}(b; \exp, x_0)}{(b-x_0)^k} \right] \\ &= \left[\frac{\exp(a) - \sum_{i=0}^{k-1} \frac{1}{i!} \exp(x_0) (a-x_0)^i}{(a-x_0)^k}, \frac{\exp(b) - \sum_{i=0}^{k-1} \frac{1}{i!} \exp(x_0) (b-x_0)^i}{(b-x_0)^k} \right]. \end{aligned} \quad (2.10)$$

The \log function has k th derivative $\log^{(k)}(x) = (-1)^{k-1} \frac{(k-1)!}{x^k}$. Thus, for $x > 0$, $\log^{(k)}$ is monotonically decreasing if k is odd, and monotonically increasing if k is even. Theorem 1 thus gives a sharp Taylor enclosure at x_0 over $[a, b]$ for any $x_0, a > 0$.

The function $f(x) = |x|$ has first derivative $f^{(1)}(x) = \text{sign}(x)$, which is monotonically increasing for all x . Thus, taking $k = 1$, the sharp degree 1 Taylor enclosure is defined by an interval whose end points are $\frac{\text{sign}(a) - \text{sign}(x_0)}{a-x_0}$ and $\frac{\text{sign}(b) - \text{sign}(x_0)}{b-x_0}$.

Finally, consider the function $f(x) = x^p$, for some integer p . The k th derivative is $f^{(k)}(x) = x^{p-k} \prod_{i=0}^{k-1} (p-i)$. If $p-k$ is non-negative and odd, then x^{p-k} is increasing for all x , and $\prod_{i=0}^k (p-i)$ is positive, so $f^{(k)}$ is increasing for all x . If $p-k$ is non-negative and even, then x^{p-k} is increasing for $x \geq 0$, and decreasing for $x \leq 0$, and $\prod_{i=0}^{k-1} (p-i)$ is positive, so $f^{(k)}$ is increasing for $x \geq 0$ and decreasing for $x \leq 0$.

Table 2.1 summarizes these results.

Table 2.1: Sharp degree k Taylor enclosures for functions with monotone k th derivative.

FUNCTION f	CONDITIONS	$I_k^*(f, x_0, [a, b])$	$\overline{I}_k^*(f, x_0, [a, b])$
exp	NONE	$\frac{\exp(a) - \sum_{i=0}^{k-1} \frac{1}{i!} \exp(x_0) (a-x_0)^i}{(a-x_0)^k}$	$\frac{\exp(b) - \sum_{i=0}^{k-1} \frac{1}{i!} \exp(x_0) (b-x_0)^i}{(b-x_0)^k}$
log	$a \geq 0, k = 0$	$\log(a)$	$\log(b)$
	$a \geq 0, k \text{ ODD}$	$\frac{\log(b) - \log(x_0) - \sum_{i=1}^{k-1} \frac{(-1)^{i+1}}{i b^i} (b-x_0)^i}{(b-x_0)^k}$	$\frac{\log(a) - \log(x_0) - \sum_{i=1}^{k-1} \frac{(-1)^{i+1}}{i a^i} (a-x_0)^i}{(a-x_0)^k}$
	$a \geq 0, k \text{ EVEN}$	$\frac{\log(a) - \log(x_0) - \sum_{i=1}^{k-1} \frac{(-1)^{i+1}}{i a^i} (a-x_0)^i}{(a-x_0)^k}$	$\frac{\log(b) - \log(x_0) - \sum_{i=1}^{k-1} \frac{(-1)^{i+1}}{i b^i} (b-x_0)^i}{(b-x_0)^k}$
$x \mapsto x $	$k = 1$	$\frac{\text{sign}(a) - \text{sign}(x_0)}{a-x_0}$	$\frac{\text{sign}(b) - \text{sign}(x_0)}{b-x_0}$
$x \mapsto x^p \text{ FOR } p \in \mathbb{Z}$	$d \leq p-1, p-k \text{ ODD OR } a \geq 0$	$\frac{a^p - \sum_{i=0}^{k-1} \frac{1}{i!} a^{p-i} \prod_{j=0}^{i-1} p-j}{(a-x_0)^k}$	$\frac{b^p - \sum_{i=0}^{k-1} \frac{1}{i!} b^{p-i} \prod_{j=0}^{i-1} p-j}{(b-x_0)^k}$
	$k \leq p-1, p-k \text{ EVEN, } b \leq 0$	$\frac{b^p - \sum_{i=0}^{k-1} \frac{1}{i!} b^{p-i} \prod_{j=0}^{i-1} p-j}{(b-x_0)^k}$	$\frac{a^p - \sum_{i=0}^{k-1} \frac{1}{i!} a^{p-i} \prod_{j=0}^{i-1} p-j}{(a-x_0)^k}$

2.4 Functions with Even-Symmetric Hessian

Many commonly-used neural network activation functions, such as ReLU [63], GELU [33], SiLU (a.k..a. Swish) [24, 71] and Softplus, have Hessians that are even-symmetric (meaning $f''(x) = f''(-x) \forall x \in \mathbb{R}$). In this section we derive Taylor enclosures for functions with even symmetric Hessians. Unlike the results in the previous section, here we will only consider quadratic Taylor enclosures ($k = 2$), which are the most relevant in a neural network optimization context.

Our main result is the following theorem.

Theorem 2. *Let $f : \mathbb{R} \rightarrow \mathbb{R}$ be a twice-differentiable function, and suppose for some $\alpha > 0$, f'' is even symmetric over $[-\alpha, \alpha]$ (meaning $f''(x) = f''(-x) \forall x \in [-\alpha, \alpha]$), and f'' is decreasing over $[0, \alpha]$. Then, the sharp quadratic Taylor enclosure of f over $[a, b] \subseteq [-\alpha, \alpha]$ at $x_0 \in (a, b)$ is given by:*

$$I_2^*(f, x_0, [a, b]) = \left[\min \left\{ \frac{R_1(a; f, x_0)}{(a-x_0)^2}, \frac{R_1(b; f, x_0)}{(b-x_0)^2} \right\}, \frac{R_1(c; f, x_0)}{(c-x_0)^2} \right]$$

where $c \triangleq \min \{b, \max \{-x_0, a\}\}$.

To prove Theorem 2, we analyze the minimum and maximum possible values of the ratio $r(x) \triangleq \frac{R_1(x; f, x_0)}{(x-x_0)^2}$ for $x \in [a, b]$, which by definition are the end points of the interval $I_2^*(f, x_0, [a, b])$. To do so, we first use Lemma 1 to write $r'(x)$ in terms of a weighted integral of $f''(t)$, and then carefully analyze the sign of the resulting expression in order to show that $r(x)$ is maximized at $x = -x_0$, decreasing for $x > -x_0$, and increasing for $x < -x_0$. This implies that the minimum value of $r(x)$ for $x \in [a, b]$ is either $r(a)$ or $r(b)$ (whichever is smaller), while the maximum value is $r(c)$, where c is the point in $[a, b]$ that is closest to $-x_0$, yielding the expression given in Theorem 2. The full proof is given in Appendix A.

Figure 2.2 plots a number of commonly-used activation functions whose Hessian is even symmetric.

For the Hard SiLU, LeakyReLU, ReLU, and Softplus functions, the Hessian is monotonically decreasing for $x \geq 0$, and Theorem 2 can be used to derive a sharp quadratic Taylor enclosure for any trust region $[a, b]$. For GELU and SiLU (a.k.a. Swish), Theorem 2 can be used so long as the trust region $[a, b]$ does not include the regions far from the origin in which the Hessian is non-monotonic (for trust regions not satisfying this condition, bounds on the Hessian can be used to derive a non-sharp quadratic Taylor enclosure, as discussed in §2.2). Finally, it is worth noting that the Log Sigmoid activation function (not shown in Figure 2.2) is equivalent to the function $x \mapsto -\text{Softplus}(-x)$, and thus its sharp quadratic Taylor enclosure can be derived from the one for Softplus.

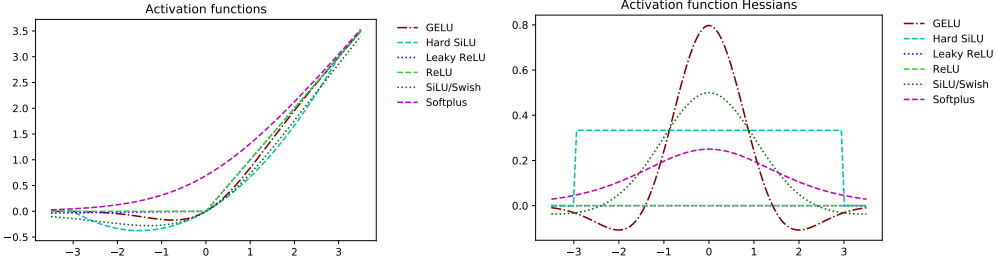


Figure 2.2: Some commonly-used neural network activation functions (left) and their Hessians (right).

2.5 Comparison to Taylor Enclosures Based on Derivative Bounds

How much better are sharp Taylor enclosures than the non-sharp Taylor enclosures discussed in §2.2, obtained via bounds on the range of the k th derivative? The following theorem shows that asymptotically (as the size of the trust region approaches zero), the interval defining the sharp Taylor enclosure is at least $k + 1$ times narrower than an interval based on this range. The proof is given in Appendix A.

Theorem 3. *For any analytic function $f : \mathbb{R} \rightarrow \mathbb{R}$, any integer $k > 0$, and any $x_0 \in \mathbb{R}$,*

$$\lim_{\epsilon \rightarrow 0} \frac{\text{width}(I_k^{\text{Lagrange}}(f, [x_0, x_0 + \epsilon]))}{\text{width}(I_k^*(f, x_0, [x_0, x_0 + \epsilon]))} = \binom{k + \ell}{\ell}$$

where $I_k^{\text{Lagrange}}(f, [a, b]) \triangleq \frac{1}{k!} \left[\inf_{y \in [a, b]} \{f^{(k)}(y)\}, \sup_{y \in [a, b]} \{f^{(k)}(y)\} \right]$, ℓ is the smallest positive integer such that $f^{(k+\ell)}(x_0) \neq 0$, and for any interval $I = [\underline{I}, \bar{I}]$, we define $\text{width}(I) \triangleq \bar{I} - \underline{I}$. Furthermore, both $I_k^{\text{Lagrange}}(f, [x_0, x_0 + \epsilon])$ and $I_k^*(f, x_0, [x_0, x_0 + \epsilon])$ have width $O(\epsilon^\ell)$ (as $\epsilon \rightarrow 0$).

2.6 Related Work

The work in this chapter was inspired by a paper by de Leeuw and Lange [17], who introduced the notion of sharp quadratic majorizers for one-dimensional functions, and derived closed-form majorizers for a number of common functions. Using our terminology, deriving a sharp quadratic majorizer for a function $f : \mathbb{R} \rightarrow \mathbb{R}$ is equivalent to deriving the upper bound of a degree 2 sharp Taylor enclosure, over the trust region $[a, b] = [-\infty, \infty]$. Thus, our results generalize those of [17] in three ways: by deriving polynomial bounds of arbitrary degree, by providing both upper and lower bounds, and by deriving the tightest bounds that are valid over an arbitrary trust region. We note that the use of a finite trust region is essential for computing Taylor enclosures for functions such as \exp , which asymptotically grow faster than any fixed degree polynomial.

Extending the results of de Leeuw and Lange in a different direction, Browne and McNicholas [10] derived sharp quadratic majorizers for multivariate functions. Generalizing their results to take into account a trust region would be an interesting area of future work.

2.7 Future Work

Our results suggest several possibilities for future work. Perhaps the most obvious one is to develop theory that applies to additional one-dimensional functions. For example, we do not currently have a way to compute sharp Taylor enclosures for periodic functions, such as sine or cosine. It would also be nice to generalize Theorem 2 to Taylor enclosures of degree > 2 .

Finally, it would be very interesting to derive sharp Taylor enclosures for multivariate functions, perhaps building on the results of Browne and McNicholas [10].

Chapter 3

Taylor Enclosures for Arbitrary Univariate Functions

In Chapter 2, we developed theory that allowed us to derive *sharp* Taylor enclosures for univariate functions with certain mathematical properties. In this chapter, we will consider the problem of deriving Taylor enclosures for *arbitrary* functions that can be written in terms of atomic univariate functions, plus the elementary binary operations of addition, subtraction, multiplication, division, and exponentiation. As an example, having already derived sharp Taylor enclosures for \exp , we would like to be able to derive a Taylor enclosure of the function

$$f(x) = \frac{\exp(x)}{2+x}. \quad (3.1)$$

To do so, we will see that it suffices to come up with rules for performing various operations on *interval polynomials*. We develop such rules in §3.3, after first reviewing relevant background knowledge.

3.1 Background: Taylor Mode Automatic Differentiation

The algorithm we will develop in this chapter can be thought of as a generalization of Taylor-mode automatic differentiation, and to understand our algorithm it may be helpful to first review this method.

Applied to a univariate function $f : \mathbb{R} \rightarrow \mathbb{R}$, Taylor mode automatic differentiation computes the coefficients of the degree k Taylor polynomial of f at some point $x_0 \in \mathbb{R}$, which is equivalent to computing $f^{(i)}(x_0)$ for $i \in \{0, 1, \dots, k\}$.

One can think of Taylor mode automatic differentiation as an evaluation of f using overloaded operators whose input and output are Taylor polynomials, rather than scalars. A key insight behind this approach is that the degree k Taylor polynomial for a composite function $f(x) = g(h(x))$ at x_0 can be obtained by first computing the degree k Taylor polynomial for h at x_0 , then plugging it into the degree k Taylor polynomial for g at $h(x_0)$, then expanding the result and dropping all terms of degree $> k$. Thus, if $f = \sigma_1 \circ \sigma_2 \circ \dots \circ \sigma_n$, where each σ_i is an atomic function (whose Taylor polynomial can be computed in closed form), we can compute a Taylor polynomial for f recursively, at each step plugging the Taylor polynomial for $\sigma_{i+1} \circ \sigma_{i+2} \circ \dots \circ \sigma_n$ into the Taylor polynomial for σ_i . Thus can be thought of as evaluating f on the identity polynomial, using an extended version of each σ_i that inputs and outputs Taylor polynomials rather than scalars. This approach can be extended to functions composed of operations that take two or more arguments.

For a formal treatment of Taylor mode automatic differentiation and additional discussion, see [7, 28].

3.2 Definitions and Notation

As in §2.1, we denote the set of closed real intervals by $\mathbb{IR} \triangleq \{[a, b] : a, b \in \mathbb{R}, a \leq b\}$, and mathematical expressions containing intervals represent sets according to the usual rules of interval arithmetic.

Definition 3 (Interval polynomial). *A degree k interval polynomial is a function $F : \mathbb{R} \rightarrow \mathbb{IR}$, of the form:*

$$F(z) = \sum_{i=0}^k F_{[i]} z^i$$

where each coefficient $F_{[i]} \in \mathbb{IR} \cup \mathbb{R}$ is either an interval or a scalar.

For any interval polynomial F , we use $F_{[i]}$ to denote its i th coefficient (starting at $i = 0$, so that $F(z) = \sum_{i=0}^k F_{[i]} z^i$, where k is the degree of F). We use $\mathbb{IP}(k)$ to denote the set of degree k interval polynomials.

Definition 4 (Interval polynomial enclosure). *A degree k interval polynomial $F \in \mathbb{IP}(k)$ is an enclosure for a function $f : \mathbb{R} \rightarrow \mathbb{R}$ over an interval $Z \in \mathbb{IR}$ if*

$$f(z) \in F(z) \quad \forall z \in Z.$$

As an example, the interval polynomial $F(z) = z + [0, 1]z^2$ is a degree 2 interval polynomial enclosure of the function $f(z) = z + \sin(z)z^2$ over the interval $Z = [0, \pi]$.

Note that a *Taylor enclosure* (defined previously in Definition 1) is a particular kind of interval polynomial enclosure, namely one in which all but the last coefficient is a scalar. Although we are mainly interested in deriving Taylor enclosures, the machinery we develop in this chapter will be applicable to arbitrary interval polynomial enclosures (including those with more than one interval coefficient).

The key to our recursive algorithm will be to define, for each atomic scalar-valued function of interest, an *interval polynomial extension* that inputs and outputs interval polynomials rather than scalars. The formal definition of an interval polynomial extension ends up being somewhat technical, but is immediately followed by a concrete example designed to make it more clear.

Definition 5 (Interval polynomial extension). *For integers $n > 0$ and $k \geq 0$, and an n -argument scalar-valued function $f : \mathbb{R}^n \rightarrow \mathbb{R}$, the function $F : \mathbb{IP}(k)^n \rightarrow \mathbb{IP}(k)$ is an interval polynomial extension of f over trust regions $Y_1, Y_2, \dots, Y_n, Z \in \mathbb{IR}$ iff. the following condition holds: For any $z \in Z$, any interval polynomials $P_1, P_2, \dots, P_n \in \mathbb{IP}(k)$, and any $y_1, y_2, \dots, y_n \in \mathbb{R}$ with $y_i \in Y_i$ and $y_i \in P_i(z)$ for all i , we have*

$$f(y_1, y_2, \dots, y_n) \in F(P_1, P_2, \dots, P_n)(z).$$

Example. Definition 5 is rather subtle, and in particular it may not be obvious why it should require trust regions for both the arguments of f and the independent variable z . To illustrate the definition, consider the function $f : \mathbb{R} \rightarrow \mathbb{R}$, defined by

$$f(y) \triangleq \begin{cases} y^2 & \text{if } y \in [-1, 1] \\ |y| & \text{otherwise.} \end{cases} \quad (3.2)$$

Let $F : \mathbb{IP}(2) \rightarrow \mathbb{IP}(2)$ be defined by

$$F(A) = A_{[0]}^2 + 2A_{[0]}A_{[1]}z + \left(A_{[1]}^2 + 2A_{[1]}A_{[2]}[0, .5] + A_{[2]}^2[0, .25]\right)z^2. \quad (3.3)$$

Then, F is a degree 2 interval polynomial extension of f over the trust regions $Y = [-1, 1]$ and $Z = [0, .5]$. This is true because, for any $z \in Z$, any degree 2 interval polynomial $A(z) \triangleq A_{[0]} + A_{[1]}z + A_{[2]}z^2$, and any

$y \in Y$ with $y \in A(z)$,

$$\begin{aligned}
f(y) &= y^2 && \text{because } y \in [-1, 1] \\
&\in (A_{[0]} + A_{[1]}z + A_{[2]}z^2)^2 && \text{because } y \in A(z) \\
&\subseteq A_{[0]}^2 + 2A_{[0]}A_{[1]}z + z^2 \left(A_{[1]}^2 + 2A_{[1]}A_{[2]}z + A_{[2]}^2 z^2 \right) \\
&\subseteq A_{[0]}^2 + 2A_{[0]}A_{[1]} + z^2 \left(A_{[1]}^2 + 2A_{[1]}A_{[2]}[0, .5] + A_{[2]}^2[0, .25] \right) && \text{because } z \in [0, .5] \\
&= F(A).
\end{aligned} \tag{3.4}$$

Given an arbitrary function f which is composed of atomic functions for which we have derived interval polynomial extensions, we will be able to recursively compute a Taylor enclosure of f by evaluating f on the identity polynomial using the extended functions. The validity of this approach is captured in the following proposition, which follows immediately from the definitions given so far.

Proposition 4. *Consider a function $f : \mathbb{R} \rightarrow \mathbb{R}$ of the form $f(z) = \text{op}(a_1(z), a_2(z), \dots, a_n(z))$, and an arbitrary trust region $Z \in \mathbb{IR}$, and let the following conditions hold:*

1. For all i , we have $a_i(z) \in Y_i$ for all $z \in Z$.
2. For all i , P_i is an interval polynomial enclosure of a_i over Z .
3. Op is an interval polynomial extension of op over Y_1, Y_2, \dots, Y_n and Z .

Then, the interval polynomial $F \triangleq \text{Op}(P_1, P_2, \dots, P_n)$ is enclosure of f over Z .

Proof. Consider some arbitrary $z \in Z$, and let $y_i = a_i(z)$. By conditions 1 and 2, $y_i \in Y_i$ and $y_i \in P_i(z)$. Thus, using condition 3 and Definition 5:

$$f(z) = \text{op}(y_1, y_2, \dots, y_n) \in \text{Op}(P_1, P_2, \dots, P_n)(z) = F(z). \tag{3.5}$$

Because $z \in Z$ was arbitrary, it follows that F is an interval polynomial enclosure of f over Z . \square

3.3 The AutoBound1D Algorithm

We now present an new algorithm, AutoBound1D, for deriving a Taylor enclosure of an arbitrary univariate function $f : \mathbb{R} \rightarrow \mathbb{R}$ that can be written in terms of commonly-used atomic functions. In Chapter 4, we generalize this algorithm to handle multivariate functions.

At a high level, AutoBound1D is similar to the algorithm defined in previous work on Taylor models [55, 56, 57, 58], in that both algorithms compose interval polynomials in a manner analogous to Taylor mode automatic differentiation. However, there are several critical differences:

1. AutoBound1D produces bounds of the form $R_{k-1}(x; f, x_0) \in I(x - x_0)^k$, in contrast to Taylor model bounds of the form $R_{k-1}(x; f, x_0) \in I$. This makes it possible for the bounds derived by AutoBound1D to be used as the basis of a majorization-minimization algorithm (see Chapter 5), and has potential advantages in other applications as well (see Chapter 6).
2. Where available, we use *sharp* Taylor enclosures for the atomic functions (obtained using the theory developed in Chapter 2), whereas previous work on Taylor models made use of looser enclosures based on derivative bounds, similar to the baseline method discussed in §2.2.
3. When composing two interval polynomials, we use a dedicated rule that produces tighter bounds than the simpler approach of repeatedly applying an interval polynomial multiplication rule.

The remainder of this section is organized as follows. In §3.3.1 we define interval polynomial extensions of various commonly used functions. In §3.3.2 we present pseudocode for AutoBound1D, prove its correctness, and give a worked example.

3.3.1 Interval Polynomial Extensions of Atomic Functions

The AutoBound1D algorithm will derive a Taylor enclosure of a function $f : \mathbb{R} \rightarrow \mathbb{R}$ by evaluating f using *interval polynomial extensions* of the atomic functions of which f is composed. As formalized in Definition 5, these extended functions input and output interval polynomials of some fixed degree k , with the output interval polynomial satisfying a natural inclusion property that guarantees correctness of the algorithm.

In the following subsections, we define interval polynomial extensions of scalar arithmetic operations (such as addition and multiplication) and of arbitrary non-linear scalar functions (such as \exp or \log).

To do so, we will use the following basic properties of interval arithmetic [62], which we state without proof. For intervals $X, Y, Z \in \mathbb{IR}$, and a scalar $\alpha \in \mathbb{R}$, we have

$$X + Y = Y + X \tag{3.6}$$

$$\alpha(X + Y) = \alpha X + \alpha Y \tag{3.7}$$

$$X(Y + Z) \subseteq XY + XZ. \tag{3.8}$$

Note that (3.8) does not hold with equality. As a counterexample, if $X = [-3, 3]$, $Y = [1, 1]$, and $Z = [-1, -1]$, then $X(Y + Z) = [0, 0]$, while $XY + XZ = [-3, 3] + [-3, 3] = [-6, 6]$.

In the subsections that follow, we state our extended functions in terms of two generic interval polynomials:

$$A(z) = \sum_{i=1}^k A_{[i]} z^i, \quad B(z) = \sum_{i=1}^k B_{[i]} z^i. \tag{3.9}$$

Background: Bounding the Range of an Interval Polynomial

Our interval polynomial extensions will be defined in terms of a function `RangeBound`, which bounds the range of an interval polynomial over a given trust region. That is, for any interval polynomial P and interval $Z \in \mathbb{IR}$,

$$z \in Z \implies P(z) \subseteq \text{RangeBound}(P, Z). \tag{3.10}$$

A simple way to bound the range of an interval polynomial is to evaluate the interval polynomial at Z using interval arithmetic, defining

$$\text{RangeBound}(P, Z) \triangleq \sum_{i=0}^{\text{degree}(P)} P_{[i]} Z^i. \tag{3.11}$$

However, there are a variety of other possibilities which make different tradeoffs between tightness and computation. See [74] for a numerical comparison of several different approaches, and see [59] for discussion of two approaches that have proven useful in global optimization algorithms.

Addition, Subtraction, and Multiplication

For interval polynomials $A(z) = \sum_{i=1}^k A_{[i]} z^i$ and $B(z) = \sum_{i=1}^k B_{[i]} z^i$, we have the following equalities:

$$A(z) + B(z) = \sum_{i=0}^k (A_{[i]} + B_{[i]}) z^k \tag{3.12}$$

$$A(z) - B(z) = \sum_{i=0}^k (A_{[i]} - B_{[i]}) z^k. \tag{3.13}$$

These equalities follow from the commutativity property (3.6) and the distributivity property (3.7). Because the right hand sides are degree k interval polynomials, these equalities immediately define interval polynomial extensions of the scalar addition and subtraction operations (over any trust regions).

For scalar multiplication, we first use the sub-distributivity property (3.8) to write

$$A(z)B(z) \subseteq \sum_{i=0}^k \sum_{j=0}^k A_{[i]} B_{[j]} z^{i+j}. \quad (3.14)$$

To define an interval polynomial extension of scalar multiplication, we must enclose the degree $2k$ interval polynomial on the right hand side of (3.14) by a degree k polynomial. To do so, we collect the terms of degree $\geq k$ in a single polynomial, then use a RangeBound function satisfying (3.10) to reduce the degree of this polynomial to k . Letting $S \triangleq \{(i, j) : i, j \in \{0, 1, \dots, k\}\}$, for $z \in Z$ we have:

$$\begin{aligned} A(z)B(z) &\subseteq \left(\sum_{(i,j) \in S: i+j < k} A_{[i]} B_{[j]} z^{i+j} \right) + z^k \left(\sum_{(i,j) \in S: i+j \geq k} A_{[i]} B_{[j]} z^{i+j-k} \right) \\ &\subseteq \left(\sum_{(i,j) \in S: i+j < k} A_{[i]} B_{[j]} z^{i+j} \right) + z^k \cdot \text{RangeBound} \left(\sum_{(i,j) \in S: i+j \geq k} A_{[i]} B_{[j]} z^{i+j-k}, Z \right). \end{aligned} \quad (3.15)$$

Equation (3.15) defines an interval polynomial extension of scalar multiplication for any trust regions Y_1, Y_2 and Z , with the result depending only on Z .

We note that equations (3.12), (3.13), and (3.14) appeared previously in a paper by Rokne [73], along with a rule for interval polynomial division.

Exponentiation with a Non-Negative Integer Exponent

We now consider computing $A(z)^p$, for an integer $p \geq 0$. For $p \in \{0, 1\}$ this is trivial. For $p \geq 2$, a natural approach is to simply apply the multiplication rule $p - 1$ times. However, this approach produces an unnecessarily loose bound. For example, consider squaring the degree 0 interval polynomial $A(z) = [-3, 3]$. Using the multiplication rule gives

$$A(z)A(z) = [-3, 3] \cdot [-3, 3] = [-9, 9]. \quad (3.16)$$

In contrast, using the exponentiation rule for interval arithmetic gives $A(z)^2 = [-3, 3]^2 = [0, 9]$.

To obtain a tighter bound than the one given by repeated multiplication, we use the exponentiation rule (rather than the product rule) for interval arithmetic whenever possible. For example, in the case where $p = 2$ and $k = 2$, for $z \in Z$ we have

$$\begin{aligned} A(z)^2 &= (A_{[0]} + A_{[1]}z + A_{[2]}z^2)^2 \\ &\subseteq A_{[0]}^2 + 2A_{[0]}A_{[1]}z + z^2 (2A_{[0]}A_{[2]} + A_{[1]}^2 + 2A_{[1]}A_{[2]}z + A_{[2]}^2 z^2) \\ &\subseteq A_{[0]}^2 + 2A_{[0]}A_{[1]}z + z^2 \cdot \text{RangeBound} (2A_{[0]}A_{[2]} + A_{[1]}^2 + 2A_{[1]}A_{[2]}z + A_{[2]}^2 z^2, Z). \end{aligned} \quad (3.17)$$

By computing the intervals $A_{[0]}^2$, $A_{[1]}^2$, and $A_{[2]}^2$ using the exponentiation rule (rather than the product) rule, we obtain a tighter result than would be obtained by computing $A(z)^2$ using (3.15). This approach generalizes naturally to other k and p .

Arbitrary Univariate Functions

We next define an interval polynomial extension of an arbitrary function $\sigma : \mathbb{R} \rightarrow \mathbb{R}$ for which a Taylor enclosure is known. This immediately provides interval polynomial extensions of the all functions considered in Chapter 2, including \exp , \log , $x \mapsto x^p$, and various neural network activation functions.

To define the extended function, we first consider the problem of composing two interval polynomials. We immediately have

$$A(B(z)) = \sum_{i=0}^k A_{[i]}(B(z))^i. \quad (3.18)$$

Thus, for $z \in Z$, we could obtain an enclosure of $A(B(z))$ by applying the rule for non-negative integer exponentiation k times, and summing the results. However, we can obtain a tighter enclosure by first rewriting $A(B(z))$ as a degree k^2 polynomial, then enclosing it by a degree k polynomial using a single call to RangeBound, as in (3.15). As in Taylor-mode automatic differentiation, this can be implemented efficiently using Faà di Bruno's formula [7]. We denote the resulting enclosure by $A \circ_Z B$.

Applied to an input polynomial P , the extended function will compute a degree k Taylor enclosure of σ , and then compose it with the polynomial $P - P_{[0]}$. To define it formally, for any $y_0 \in \mathbb{R}$ and $Y \in \mathbb{IR}$, let $\mathcal{T}_k(\sigma, y_0, Y)$ denote the known degree k Taylor enclosure of σ at y_0 over Y . The degree k interval polynomial extension of σ over trust regions Y_1 and Z is defined by:

$$\Sigma(P) = \mathcal{T}_k(\sigma, P_{[0]}, Y_1) \circ_Z (P - P_{[0]}) \quad (3.19)$$

where $P_{[0]}$ denotes the degree 0 term of P (here assumed to be a scalar), and we use $A \circ_Z B$ to denote interval polynomial composition that is valid for $z \in Z$, as described in the previous paragraph.

Exponentiation with a fractional or negative exponent

For $p \in \mathbb{R}$, where p is not an integer or $p < 0$, we define $A(z)^p$ as the application of the nonlinear function $x \mapsto x^p$ to the interval polynomial $A(z)$ using (3.19).

Division

Having defined interval polynomial extensions of multiplication and exponentiation, we simply treat division as multiplication by the reciprocal:

$$\frac{A(z)}{B(z)} \triangleq A(z)B(z)^{-1} \quad (3.20)$$

where $B(z)^{-1}$ is defined as the application of the nonlinear function $x \mapsto x^{-1}$ to $B(z)$ using (3.19).

Note that if it is possible for $B(z)$ to be 0 (i.e., $0 \in Y_2$) then (3.19) will produce an interval polynomial with infinite coefficients, and the right hand side of (3.20) will have coefficients that are either infinite or indeterminate (i.e, NaN), as appropriate, depending on the coefficients of $A(z)$.

Summary

Table 3.1 summarizes the interval polynomial extensions we have derived for addition, multiplication, and arbitrary univariate functions.

For simplicity, we have omitted the extensions for subtraction, division, and exponentiation with a constant exponent, which can be defined in terms of the extensions given in the table.

3.3.2 Pseudocode and Example

We now formally present the AutoBound1D algorithm.

The algorithm takes as input a function $f : \mathbb{R} \rightarrow \mathbb{R}$, represented as a *symbolic expression*. A symbolic expression is a sequence of equations, each of which gives the value of some intermediate variable as an atomic function of other intermediate variables.

We use \mathbb{O} to denote the set of atomic univariate functions that may appear in a symbolic expression. To keep our pseudocode as simple as possible, we will assume that the only binary operations that appear in a symbolic expression are $+$ and \times . Functions containing subtraction or division can be converted to this

Table 3.1: Interval polynomial extensions of atomic functions.

FUNCTION	DEGREE k INTERVAL POLYNOMIAL EXTENSION OVER Y_1, Y_2, \dots AND Z
$\sigma(a, b) = a + b$	$\Sigma(A, B) \triangleq (A_{[0]} + B_{[0]}, A_{[1]} + B_{[1]}, \dots, A_{[k]} + B_{[k]})$
$\sigma(a, b) = ab$	$\Sigma(A, B) = Q$, WHERE $Q_{[j]} = \begin{cases} \sum_{l, m: l+m=j} A_{[l]} B_{[m]} & j < k \\ \text{RangeBound} \left(\sum_{l, m: l+m \geq k} A_{[l]} B_{[m]} z^{l+m-k}, Z \right) & j = k. \end{cases}$
UNIVARIATE σ	$\Sigma(A) = P \circ_Z (A - A_{[0]})$ (SEE §3.3.1), WHERE P IS A DEGREE k TAYLOR ENCLOSURE OF σ AT $A_{[0]}$ OVER Y_1 .

form as a preprocessing step, using the relations $x - y = x + (-y)$ and $\frac{x}{y} = xy^{-1}$. Functions containing exponentiation can also be converted to this form so long as each exponent is a constant, by letting \mathbb{O} contain a univariate function $x \mapsto x^p$ for each distinct exponent p .

Definition 6 (Symbolic expression). *A symbolic expression is a pair $(\mathcal{V}, \mathcal{E})$, where $\mathcal{V} = (v_0, v_1, \dots, v_n)$ is a tuple of intermediate variables, and $\mathcal{E} = (e_1, e_2, \dots, e_n)$ is a tuple of equations, where $e_i = (\sigma_i, L_i)$, $\sigma_i \in \mathbb{O}$ is an atomic function, and L_i is a tuple of intermediate variables, of the same length as the number of arguments that σ_i takes.*

In a symbolic expression, v_0 represents the input to the function, and v_n represents the output. As an example, the function $f(x) = \sqrt{\exp(x)}$ can be represented by the symbolic expression $(\mathcal{V}, \mathcal{E})$ where $\mathcal{V} = (v_0, v_1, v_2)$ and $\mathcal{E} = ((\exp, (v_0)), (\text{sqrt}, (v_1)))$, representing the equations:

$$\begin{aligned} v_0 &= x \\ v_1 &= \exp(v_0) \\ v_2 &= \sqrt{v_1}. \end{aligned} \tag{3.21}$$

We now describe AutoBound1D. Given as input an integer k , a trust region $[a, b] \in \mathbb{IR}$, a reference point $x_0 \in [a, b]$, and a symbolic expression $(\mathcal{V}, \mathcal{E})$ with $\mathcal{V} = (v_0, v_1, v_2, \dots, v_n)$, AutoBound1D computes intervals Y_0, Y_1, \dots, Y_n such that

$$v_i(x) \in Y_i \quad \forall x \in [a, b] \tag{3.22}$$

where $v_i(x)$ denotes the value of the intermediate variable v_i as a function of the independent variable x . The intervals Y_i are obtained from the equations in \mathcal{E} using the rules of interval arithmetic.

In parallel, the algorithm computes degree k interval polynomials P_0, P_1, \dots, P_n (represented as tuples of coefficients) such that

$$v_i(x) \in P_i(x - x_0) \quad \forall x \in [a, b]. \tag{3.23}$$

The interval polynomials P_i are obtained from the equations in \mathcal{E} , using the interval polynomial extensions of the atomic functions (summarized in Table 3.1). The algorithm returns P_n , which is a Taylor enclosure of the function $f : \mathbb{R} \rightarrow \mathbb{R}$ defined by the symbolic expression $(\mathcal{V}, \mathcal{E})$, at x_0 over $[a, b]$.

Theorem 4 shows that AutoBound1D returns the coefficients of a Taylor enclosure of the function f represented by the symbolic expression provided as input to the algorithm.

Theorem 4. *Assume that the table Σ provided as a hyperparameter to AutoBound1D contains interval polynomial extensions of each primitive function in \mathbb{O} . (That is, for any primitive function $\sigma : \mathbb{R}^m \rightarrow \mathbb{R} \in \mathbb{O}$, integer $k > 0$, and intervals $Y_1, Y_2, \dots, Y_m, Z \in \mathbb{IR}$, the function $F(z) = \Sigma[\sigma, k](z; Y_1, Y_2, \dots, Y_m, Z)$ is an interval polynomial extension of σ over Y_1, Y_2, \dots, Y_m and Z .)*

Then, when given as input a symbolic expression $(\mathcal{V}, \mathcal{E})$, an interval $[a, b] \in \mathbb{IR}$, a scalar $x_0 \in [a, b]$, and a target degree $k > 0$, AutoBound1D returns a tuple containing the coefficients of a degree k interval polynomial P_n that satisfies:

$$f(x) \in P_n(x - x_0) \quad \forall x \in [a, b]$$

where $f : \mathbb{R} \rightarrow \mathbb{R}$ is the function represented by the symbolic expression $(\mathcal{V}, \mathcal{E})$. Furthermore, if the first $k - 1$ coefficients of P_n are scalars (which is the case when Σ is set to its default value), then P_n is a Taylor enclosure of f at x_0 over $[a, b]$.

The proof of Theorem 4 uses induction to show that invariants (3.22) and (3.23) are maintained at each step of the algorithm. Applying invariant (3.23) with $i = n$ then proves the first claim in the theorem. The second claim (that P_n is a Taylor enclosure if its first $k - 1$ coefficients are scalars) follows from an analysis of the behavior of P_n as $x \rightarrow x_0$. A formal proof is given in Appendix A.

Algorithm AutoBound1D (a simplified algorithm for one-dimensional functions).

Hyperparameters:

1. A table Σ , such that for any function $\sigma : \mathbb{R}^m \rightarrow \mathbb{R} \in \mathbb{O}$ and integer $k > 0$, the function

$$F(z) = \Sigma[\sigma, k](z; Y_1, Y_2, \dots, Y_m, Z)$$

is a degree k interval polynomial extension of σ over trust regions Y_1, Y_2, \dots, Y_m and Z .

2. A function RangeBound , such that for any interval polynomial P and interval Z , $z \in Z \implies P(z) \subseteq \text{RangeBound}(P, Z)$.

The default value of Σ is given in Table 3.1, and the default value of RangeBound is given by (3.11).

Input: a symbolic expression $(\mathcal{V}, \mathcal{E})$, scalar $x_0 \in \mathbb{R}$, interval $[a, b] \in \mathbb{IR}$, and target degree $k \in \mathbb{Z}_{>0}$.

Output: a tuple of coefficients that define a degree k Taylor enclosure of $f : \mathbb{R} \rightarrow \mathbb{R}$ at x_0 over $[a, b]$, where f is the function represented by the symbolic expression $(\mathcal{V}, \mathcal{E})$.

Let $\mathcal{V} = (v_0, v_1, \dots, v_n)$, and let $\mathcal{E} = ((\sigma_1, L_1), (\sigma_2, L_2), \dots, (\sigma_n, L_n))$.

Set $P_0 \leftarrow (x_0, 1)$, $Y_0 \leftarrow [a, b]$, and $Z \leftarrow [a - x_0, b - x_0]$.

for i from 1 to n **do**

 Let j_q be the index of the q th variable in L_i , and let m be the length of L_i (so $L_i = (v_{j_1}, v_{j_2}, \dots, v_{j_m})$).

 Set $P_i \leftarrow \Sigma[\sigma_i, k](P_{j_1}, P_{j_2}, \dots, P_{j_m}; Y_{j_1}, Y_{j_2}, \dots, Y_{j_m}, Z)$.

 Set $Y_i^{(0)} \leftarrow \sigma_i(Y_{j_1}, Y_{j_2}, \dots, Y_{j_m})$. {Apply σ_i to interval arguments using interval arithmetic.}

 Set $Y_i^{(1)} \leftarrow \text{RangeBound}(P_i, Z)$.

 Set $Y_i \leftarrow Y_i^{(0)} \cap Y_i^{(1)}$.

Return P_n .

Example

We now trace through a run of AutoBound1D, using it to compute a quadratic Taylor enclosure of the function $f(x) = \frac{\exp(x)}{x+2}$ at $x_0 = 0$ over $[0, 2]$. Evidently, the value of f can be computed using the sequence of equations:

$$\begin{aligned} v_0 &= x \\ v_1 &= 2 + v_0 \\ v_2 &= \exp(v_0) \\ v_3 &= v_1^{-1} \\ v_4 &= v_2 v_3 \end{aligned} \tag{3.24}$$

which corresponds to the symbolic expression with intermediate variables $(v_0, v_1, v_2, v_3, v_4)$ and equations $((\text{plus_two}, (v_0)), (\exp, (v_0)), (\text{reciprocal}, (v_1)), (\times, (v_1, v_3)))$.

Given $x_0 = 0$ and the trust region $[-1, 1]$ as input, AutoBound1D initializes

$$\begin{aligned} P_0 &= (0, 1) \\ Y_0 &= [-1, 1] \\ Z &= [-1, 1]. \end{aligned} \tag{3.25}$$

The value of P_0 represents the coefficients of the trivial Taylor enclosure $x = x_0 + 1 \cdot (x - x_0)$, while the value of Y_0 reflects the assumption $x \in [-1, 1]$, and the value of Z reflects the assumption $x - x_0 \in [-1, 1]$.

On iteration $i = 1$, the algorithm processes the equation (plus_two, (v_0)). The interval polynomial extension of the plus_two function simply adds 2 to the 0th coefficient of the polynomial, yielding

$$\begin{aligned} P_1 &= (2 + (P_0)_{[0]}, (P_0)_{[1]}) = (2, 1) \\ Y_1^{(0)} &= 2 + Y_0 = [1, 3] \\ Y_1^{(1)} &= \text{RangeBound}(P_1, Z) = 2 + 1 \cdot Z = [1, 3] \\ Y_1 &= [1, 3] \cap [1, 3] = [1, 3]. \end{aligned} \tag{3.26}$$

The value of Y_1 reflects the fact that $x \in [-1, 1]$ implies $2 + x \in [1, 3]$, while the value of P_1 reflects the fact that $x_0 = 0$ implies $2 + x = 2 + 1 \cdot (x - x_0)$.

On iteration $i = 2$, the algorithm processes the equation (exp, (v_0)). Applied to the polynomial P_0 , the interval polynomial extension of exp over trust regions Y_0 and Z returns $Q \circ_Z P_0$, where Q is the sharp quadratic Taylor enclosure of exp at $(P_0)_{[0]} = 0$ over $Y_0 = [-1, 1]$. According to Theorem 1, $Q = (1, 1, [\frac{1}{e}, e - 2])$. Because $P_0 = (0, 1)$, $Q \circ_Z P_0 = Q$, and therefore,

$$\begin{aligned} P_2 &= \left(1, 1, \left[\frac{1}{e}, e - 2\right]\right) \\ Y_2^{(0)} &= \exp(Y_0) = \left[\frac{1}{e}, e\right] \\ Y_2^{(1)} &= \text{RangeBound}(P_2, Z) = [0, e] \\ Y_2 &= \left[\frac{1}{e}, e\right]. \end{aligned} \tag{3.27}$$

On iteration $i = 3$, the algorithm processes the equation (reciprocal, (v_1)). Proceeding as in the previous iteration, we obtain

$$\begin{aligned} P_3 &= \left(\frac{1}{2}, -\frac{1}{4}, \left[\frac{1}{12}, \frac{1}{4}\right]\right) \\ Y_3 &= \left(\frac{1}{3}, 1\right). \end{aligned} \tag{3.28}$$

Finally, on iteration $i = 4$, the algorithm applies the interval polynomial extension of the product function to the polynomials P_2 and P_3 to obtain

$$P_4 = \left(\frac{1}{2}, \frac{1}{4}, \left[\frac{3}{4e} - \frac{5}{12}, \frac{3e}{4} - \frac{1}{4e} - \frac{5}{4}\right]\right). \tag{3.29}$$

We conclude

$$\begin{aligned} f(x) &\in \frac{1}{2} + \frac{1}{4}(x - x_0) + \left[\frac{3}{4e} - \frac{5}{12}, \frac{3e}{4} - \frac{1}{4e} - \frac{5}{4}\right](x - x_0)^2 \\ &\approx \frac{1}{2} + \frac{1}{4}(x - x_0) + [-0.14076, 0.69674](x - x_0)^2. \end{aligned} \tag{3.30}$$

In contrast, as shown in [78], applying the baseline interval arithmetic approach to the same function f at x_0 over $[-1, 1]$ produces the substantially looser Taylor enclosure:

$$f(x) \in \frac{1}{2} + \frac{1}{4}(x - x_0) + [-2.64, 4.04](x - x_0)^2. \quad (3.31)$$

Figure 3.1 plots the quadratic Taylor enclosures given by (3.30) and (3.31). Note that, although the enclosure returned by AutoBound1D improves significantly over the baseline, it is not sharp, as is generally the case when the input is a non-trivial composite function.

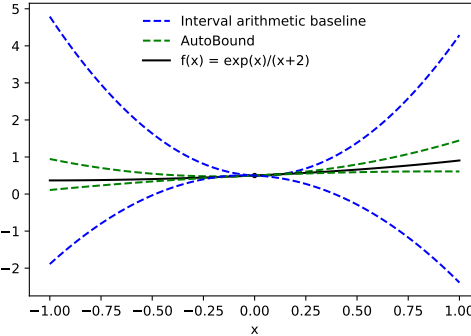


Figure 3.1: Quadratic Taylor enclosures for $f(x) = \frac{\exp(x)}{2+x}$ at $x_0 = 0$ over $[-1, 1]$, as derived by AutoBound and by the baseline interval arithmetic method [78].

3.3.3 Tightness of Automatically-Derived Bounds

How tight are the Taylor enclosures returned by AutoBound1D? We have not yet developed theory that answers this question in full generality. However, in the special case where f is a polynomial, the following theorem shows that AutoBound1D improves on the classical interval arithmetic baseline (discussed in §2.2) by a factor of at least $k + 1$. Note the similarity to Theorem 3, which is algorithm-agnostic.

Theorem 5. *Let $f(x) = \sum_{i=0}^n \alpha_i x^i$, and let k be a positive integer such that for some $l > 0$, $\alpha_{k+l} \neq 0$. Let ℓ be the smallest positive integer such that $\alpha^{k+\ell} \neq 0$. Then,*

$$\lim_{\epsilon \rightarrow 0} \frac{\text{width}(I_{\text{IntervalArithmetic}}(f, k, [-\epsilon, \epsilon]))}{\text{width}(I_{\text{AutoBound}}(f, k, [-\epsilon, \epsilon], 0))} = \binom{k+\ell}{\ell}$$

where $I_{\text{IntervalArithmetic}}(f, k, [a, b])$ is the interval obtained by evaluating $\frac{1}{k!} f^{(k)}$ over the interval $[a, b]$ according to the rules of interval arithmetic, and $I_{\text{AutoBound}}(f, k, [a, b], 0)$ is the degree k coefficient of the polynomial returned by AutoBound1D given the same arguments.

3.3.4 Limitations

The most obvious limitation of AutoBound1D is that it applies only to univariate functions. We devote Chapter 4 to generalizing the algorithm to multivariate functions.

A more subtle limitation of the algorithm is that, although it can be applied to univariate functions that make use of bilinear operations (such as matrix multiplications or convolutions), each scalar product used to compute the output of the bilinear operation must have a dedicated equation in the symbolic expression, which is impractical when using software frameworks such as TensorFlow [1], PyTorch [68], or JAX [9]. This limitation is removed as part of the generalization to multivariate functions in Chapter 4.

Finally, AutoBound1D cannot compute a Taylor enclosure of functions such as $f(x) = x^x$, where the independent variable appears in both a base and an exponent. Fortunately, such functions do not typically arise in the applications of interest. (In contrast, functions such as $f(x) = x^p$ for fixed $p \in \mathbb{R}$ are supported, because $x \mapsto x^p$ can be treated as an atomic function.)

3.4 Related Work

At a high level, our AutoBound1D algorithm can be seen as a variant of Taylor mode automatic differentiation that uses interval arithmetic. A different variant of Taylor mode automatic differentiation that uses interval arithmetic has been presented in the literature on *Taylor models* [55, 56, 57, 58]. A Taylor model is equivalent to a Taylor remainder series bound of the form $R_{k-1}(x; f, x_0) \in I$, where I is an interval. The algorithm for computing a Taylor model for a function f can be thought of as evaluating f using a set of extended operators that input and output (P, I) pairs, where P is a Taylor polynomial and I is an interval that bounds the remainder term. As discussed in §3.3, AutoBound1D differs from previous work on Taylor models in three ways: (i) by producing bounds of the form $R_{k-1}(x; f, x_0) \in I(x - x_0)^k$, which allows the bounds to be used as the basis of an MM optimizer (see Chapter 5), (ii) by using sharp Taylor enclosures to obtain tighter bounds, and (iii) by composing interval polynomials in a tighter way, further tightening the bounds.

Other noteworthy approaches that use interval polynomials to bound functions include Boundary Arithmetic [21, 22, 48] and Ultra Arithmetic [41, 42, 43, 44]. See [66] for a discussion of the history of these methods and their limitations, and see [58] for additional discussion and a comparison to Taylor Models.

More recently, [20] presented a prototype of a constraint solver that performs arithmetic operations on Chebyshev polynomials. Like our approach, this work involves evaluating a function using polynomial extensions of various operations. However, the use of Chebyshev polynomials makes the details of these operations different from ours, and the presentation in [20] considers only a limited set of operations (addition, multiplication, exponentiation, and absolute value).

An alternative approach, discussed in detail §2.2, is to compute an interval that defines a degree k Taylor enclosure by evaluating an expression for $f^{(k)}(x_0)$ using interval arithmetic. Though elegant, this approach has some inherent limitations which can cause it to quickly produce enormous intervals [58]. In the experiments of [58], these intervals were observed to be up to a factor of 10^{42} wider than the ones obtained using Taylor models.

Another approach to bounding the Taylor remainder series uses a variant of Cauchy's estimate to bound the Taylor coefficients, and thereby to bound the remainder term [64]. However, this approach requires maximizing functions over the complex plane via global optimization methods (e.g., branch and bound), and is not a practical alternative to the approach we present here.

Chapter 4

Generalization to Multivariate Functions

In this chapter, we generalize the AutoBound1D algorithm to handle multivariate functions. To accomplish this, there are two distinct problems we must solve:

1. We must make the algorithm work with multivariate interval polynomials, rather than scalar interval polynomials.
2. In order to make efficient use of modern machine learning frameworks, we must ensure that the output of our algorithm can be computed using a small number of widely-supported operations on tensors.

Toward these ends, we introduce the notion of a *tensor interval*: an interval whose end points are tensors rather than scalars. When then define *tensor interval polynomials*, which generalize interval polynomials by allowing the coefficients of the polynomial to be tensor intervals rather than scalar intervals.

With these concepts in place, elementwise operations on tensor interval polynomials, such as addition, subtraction, and (elementwise) multiplication, use simple rules analogous to the rules given in Chapter 3 for scalar interval polynomials. We also derive a rule for composing two tensor interval polynomials, which generalizes the rule for scalar interval polynomials.

For bilinear operations, such as matrix multiplications and convolutions, the situation is more subtle. Because any bilinear operation can be written as a large number of scalar additions and multiplications, we could in principle handle bilinear operations using the existing addition and multiplication rules. However, doing so would produce an impractically large (and inefficient) computation graph, with a vertex for each scalar multiplication (and potentially millions of vertices overall), which would prevent us from being able to make effective use of machine learning compilers (such as XLA) and automatic differentiation frameworks (e.g., TensorFlow, PyTorch, JAX). To work around this, we derive rules for enclosing the result of this hypothetical computation in a (potentially wider) tensor interval that can be computed using a small number of standard operations on tensors. These rules are analogous to, but different from, the rules for Interval Bound Propagation [27], which provides an efficient way to enclose the results of interval arithmetic on tensors.

4.1 Definitions and Notation

As is standard in the machine learning literature, we use the term *tensor* to denote a multidimensional array of real numbers (without requiring that the elements of the array define a physical tensor). We use bold capital symbols such as \mathbf{A} to denote tensors.

We use $\text{shape}(\mathbf{A})$ to denote the shape of tensor \mathbf{A} , a tuple of non-negative integers. Tuples can be multiplied by integers as in python, so for example if \mathbf{A} has shape $(3, 5)$, then $2 * \text{shape}(\mathbf{A}) = (3, 5, 3, 5)$.

We use $\text{indices}(\mathbf{A})$ to denote the set of tuples of integers that index the elements of \mathbf{A} . For example, if $\text{shape}(\mathbf{A}) = (3, 5)$, then $\text{indices}(\mathbf{A}) = \{(i, j) \in \mathbb{Z}^2 : 0 \leq i < 3, 0 \leq j < 5\}$.

To define tensor polynomials, we must first define appropriate inner and outer products. If \mathbf{A} is a tensor of rank r , and \mathbf{B} is a tensor of rank $q \leq r$, the inner product $\langle \mathbf{A}, \mathbf{B} \rangle$ is a tensor of rank $r - q$, whose elements are defined by

$$\langle \mathbf{A}, \mathbf{B} \rangle_{i_1, i_2, \dots, i_{r-q}} \triangleq \sum_{(j_1, j_2, \dots, j_q) \in \text{indices}(\mathbf{B})} \mathbf{A}_{i_1, i_2, \dots, i_{r-q}, j_1, j_2, \dots, j_q} \mathbf{B}_{j_1, j_2, \dots, j_q}. \quad (4.1)$$

Observe that if \mathbf{a} and \mathbf{b} are vectors, $\langle \mathbf{a}, \mathbf{b} \rangle$ is the usual dot product, while if \mathbf{A} is a matrix and \mathbf{b} is a vector, then $\langle \mathbf{A}, \mathbf{b} \rangle$ is the usual matrix-vector product.

If \mathbf{A} is a tensor of rank r , and \mathbf{B} is a tensor of rank s , the outer product $\mathbf{A} \otimes \mathbf{B}$ is a tensor of rank $r + s$, whose elements are defined by

$$(\mathbf{A} \otimes \mathbf{B})_{i_1, i_2, \dots, i_r, j_1, j_2, \dots, j_s} = \mathbf{A}_{i_1, i_2, \dots, i_r} \mathbf{B}_{j_1, j_2, \dots, j_s}. \quad (4.2)$$

For an integer $k \geq 0$, we use $\mathbf{A}^{\otimes k}$ to denote a repeated outer product: for $k > 0$, $\mathbf{A}^{\otimes k} \triangleq \mathbf{A} \otimes \mathbf{A}^{\otimes k-1}$, while $\mathbf{A}^{\otimes 0} \triangleq 1$. Observe that if \mathbf{A} has rank r , then $\mathbf{A}^{\otimes k}$ has rank kr .

With this notation in hand, we can now define a *tensor polynomial*.

Definition 7 (Tensor polynomial). *A degree k tensor polynomial is a function \mathbf{A} from tensors of some input shape I to tensors of some output shape O , defined by coefficients $\mathbf{A}_{[0]}, \mathbf{A}_{[1]}, \dots, \mathbf{A}_{[k]}$, where $\mathbf{A}_{[j]}$ has shape $O + j * I$. For a tensor \mathbf{Z} of shape I , the value of $\mathbf{A}(\mathbf{Z})$ is given by*

$$\mathbf{A}(\mathbf{Z}) = \sum_{j=0}^k \langle \mathbf{A}_{[j]}, \mathbf{Z}^{\otimes j} \rangle. \quad (4.3)$$

To define tensor *interval* polynomials, we must generalize our inner and outer products to work with *tensor intervals*, which we now define.

Definition 8 (Tensor interval). *For tensors $\mathbf{A}, \mathbf{B} \in \mathbb{R}^{n_1 \times n_2 \times \dots \times n_k}$, the tensor interval $[\mathbf{A}, \mathbf{B}]$ is the set of tensors $\{\mathbf{X} \in \mathbb{R}^{n_1 \times n_2 \times \dots \times n_k} : \mathbf{A} \leq \mathbf{X} \leq \mathbf{B}\}$, where the inequality is elementwise.*

We use calligraphic symbols such as \mathcal{A} to denote tensor intervals. Following the conventions for scalar intervals, we use $\underline{\mathcal{A}}$ and $\bar{\mathcal{A}}$ to denote the left and right endpoints of a tensor interval \mathcal{A} . We use $r(\mathcal{A}) \triangleq \frac{\bar{\mathcal{A}} - \underline{\mathcal{A}}}{2}$ to denote the radius of \mathcal{A} , and $m(\mathcal{A}) \triangleq \frac{\bar{\mathcal{A}} + \underline{\mathcal{A}}}{2}$ to denote the midpoint.

Indexing a tensor interval gives a scalar interval, for example if \mathcal{A} has rank r , then $\mathcal{A}_{i_1, i_2, \dots, i_r}$ denotes the scalar interval $[\underline{\mathcal{A}}_{i_1, i_2, \dots, i_r}, \bar{\mathcal{A}}_{i_1, i_2, \dots, i_r}]$. With this indexing convention in place, the inner product definition (4.1) immediately generalizes to the case where one or both arguments are tensor intervals (rather than tensors). The outer product definition (4.2) generalizes similarly. We can now define a tensor interval polynomial in terms of these generalized inner and outer products.

Definition 9 (Tensor interval polynomial). *A tensor interval polynomial is a function \mathcal{A} from tensors of some input shape I to tensors of some output shape O , defined by coefficients $\mathcal{A}_{[0]}, \mathcal{A}_{[1]}, \dots, \mathcal{A}_{[k]}$, where $\mathcal{A}_{[j]}$ is a tensor interval of shape $O + j * I$. For a tensor \mathbf{Z} of shape I , the value of $\mathcal{A}(\mathbf{Z})$ is given by*

$$\mathcal{A}(\mathbf{Z}) = \sum_{j=0}^k \langle \mathcal{A}_{[j]}, \mathbf{Z}^{\otimes j} \rangle. \quad (4.4)$$

In the derivations that follow, we will also need to consider a generalized outer product that treats the first n indices of \mathbf{A} and \mathbf{B} as “batch” indices. If \mathbf{A} is a tensor of rank r , and \mathbf{B} is a tensor of rank s , where the first n elements of $\text{shape}(\mathbf{A})$ match the first n elements of $\text{shape}(\mathbf{B})$, then $\mathbf{A} \otimes_n \mathbf{B}$ denotes a tensor of rank $r + s - n$, whose elements are defined by

$$(\mathbf{A} \otimes_n \mathbf{B})_{b_1, b_2, \dots, b_n, i_1, i_2, \dots, i_{r-n}, j_1, j_2, \dots, j_{s-n}} = \mathbf{A}_{b_1, b_2, \dots, b_n, i_1, i_2, \dots, i_{r-n}} \mathbf{B}_{b_1, b_2, \dots, b_n, j_1, j_2, \dots, j_{s-n}}. \quad (4.5)$$

Observe that setting $n = 0$ recovers (4.2), so that $\mathbf{A} \otimes_0 \mathbf{B} = \mathbf{A} \otimes \mathbf{B}$. Like equation (4.2), equation (4.5) extends naturally to the case where one or both arguments are tensor intervals.

4.1.1 Operational Semantics for Tensor Intervals

Tensor intervals have the same operational semantics as scalar intervals. Formally, for an n -argument operation op , we define

$$\text{op}(\mathcal{A}_1, \mathcal{A}_2, \dots, \mathcal{A}_n) \triangleq \{\text{op}(\mathbf{A}_1, \mathbf{A}_2, \dots, \mathbf{A}_n) : \mathbf{A}_i \in \mathcal{A}_i \ \forall i \in \{1, 2, \dots, n\}\}. \quad (4.6)$$

The right hand side of (4.6) need not be expressible as a tensor interval, though in many cases it will be. Under this definition, the rules for adding, subtracting, multiplying, and exponentiating tensor intervals mirror the corresponding rules for interval arithmetic. In particular,

$$\mathcal{A} + \mathcal{B} \triangleq \{\mathbf{A} + \mathbf{B} : \mathbf{A} \in \mathcal{A}, \mathbf{B} \in \mathcal{B}\} = [\underline{\mathcal{A}} + \underline{\mathcal{B}}, \bar{\mathcal{A}} + \bar{\mathcal{B}}]. \quad (4.7)$$

Similarly,

$$\mathcal{A} \odot \mathcal{B} = [\min \{\underline{\mathcal{A}} \odot \underline{\mathcal{B}}, \underline{\mathcal{A}} \odot \bar{\mathcal{B}}, \bar{\mathcal{A}} \odot \underline{\mathcal{B}}, \bar{\mathcal{A}} \odot \bar{\mathcal{B}}\}, \max \{\underline{\mathcal{A}} \odot \underline{\mathcal{B}}, \underline{\mathcal{A}} \odot \bar{\mathcal{B}}, \bar{\mathcal{A}} \odot \underline{\mathcal{B}}, \bar{\mathcal{A}} \odot \bar{\mathcal{B}}\}] \quad (4.8)$$

where the min and max are elementwise. The rule for computing the elementwise power \mathcal{A}^k is similarly an elementwise application of the usual interval arithmetic rule.

Note that the inner product of two tensor intervals was already defined by (4.1) in terms of scalar interval additional and multiplication, and thus does not have these semantics by definition. However, we will see that the tensor interval inner product operation *extends* the tensor inner product operation, in a sense to be made precise in the next section.

4.1.2 Extended Functions

The key to our algorithm will be to define extended versions of various atomic functions, which operate on tensor interval polynomials rather than tensors. The first step is to define *tensor interval extensions* of these functions.

Definition 10 (Tensor interval extension). *Let op be a function that takes n tensor arguments. A tensor interval extension of op is a function Op that takes n tensor interval arguments of the same shapes as the corresponding arguments of op , such that for any tensor intervals $\mathcal{A}_1, \mathcal{A}_2, \dots, \mathcal{A}_n$,*

$$\text{op}(\mathcal{A}_1, \mathcal{A}_2, \dots, \mathcal{A}_n) \subseteq \text{Op}(\mathcal{A}_1, \mathcal{A}_2, \dots, \mathcal{A}_n)$$

where the set on the left hand side is defined by (4.6). If this condition holds with equality, Op is said to be an exact tensor interval extension of op .

The tensor interval inner product defined by (4.1) is a tensor interval extension of the corresponding tensor inner product. Furthermore, when the second argument is a tensor (rather than a tensor interval), this extension is exact, as shown in the following proposition. A formal proof is given in Appendix A.

Proposition 5. *The tensor interval inner product defined by (4.1) extends the tensor inner product defined by (4.1). That is, for any tensor intervals \mathcal{A} and \mathcal{B} of appropriate shapes,*

$$\{\langle \mathbf{A}, \mathbf{B} \rangle : \mathbf{A} \in \mathcal{A}, \mathbf{B} \in \mathcal{B}\} \subseteq \langle \mathcal{A}, \mathcal{B} \rangle.$$

Furthermore, when the second argument is a tensor (or a singleton tensor interval) this extension is exact: for any tensor interval \mathcal{A} and tensor \mathbf{B} of appropriate shapes,

$$\{\langle \mathbf{A}, \mathbf{B} \rangle : \mathbf{A} \in \mathcal{A}\} = \langle \mathcal{A}, \mathbf{B} \rangle.$$

We are now ready to define tensor interval *polynomial* extensions. Our definition will directly generalize Definition 5, which applied to scalar interval polynomials. See the discussion surrounding Definition 5 for an example that illustrates the definition, and the role that the different trust regions play.

Definition 11 (Tensor interval polynomial extension). *Let op be a function that takes n tensor arguments. A function Op , which takes n degree k tensor interval polynomial arguments, is said to be a tensor interval polynomial extension of op over trust regions $\mathcal{Y}_1, \mathcal{Y}_2, \dots, \mathcal{Y}_n$ and \mathcal{Z} (each of which is a tensor interval) iff. the following condition holds: for any tensor $\mathbf{Z} \in \mathcal{Z}$, any tensor interval polynomials $\mathcal{P}_1, \mathcal{P}_2, \dots, \mathcal{P}_n$, and any tensors $\mathbf{Y}_1, \mathbf{Y}_2, \dots, \mathbf{Y}_n$, with $\mathbf{Y}_i \in \mathcal{Y}_i$ and $\mathbf{Y}_i \in \mathcal{P}_i(\mathbf{Z})$ for all i , we have*

$$\text{op}(\mathbf{Y}_1, \mathbf{Y}_2, \dots, \mathbf{Y}_n) \in \text{Op}(\mathcal{P}_1, \mathcal{P}_2, \dots, \mathcal{P}_n)(\mathbf{Z}).$$

4.2 The AutoBound Algorithm

We are now ready to present the AutoBound algorithm, which derives a Taylor enclosure of a multivariate function f composed of known atomic functions. This section is organized as follows:

- In §4.2.1, we define tensor interval extensions of various atomic functions.
- In §4.2.2, we define tensor interval *polynomial* extensions of these same functions.
- In §4.2.3 we give pseudocode for the AutoBound algorithm and provide a proof of correctness.

4.2.1 Tensor Interval Extensions of Atomic Functions

We begin by deriving tensor interval extensions of various atomic functions. For arithmetic operations (such as addition and multiplication) and elementwise unary functions (such as \exp and \log) these rules mirror the usual rules for interval arithmetic. For bilinear operations, we extend and generalize previous results on Interval Bound Propagation [27].

Binary Arithmetic Operations

The rules for elementwise addition, multiplication, and exponentiation given in §4.1.1 immediately define exact tensor interval extensions of the corresponding operations. For example, the function $F(\mathcal{A}, \mathcal{B}) = \mathcal{A} + \mathcal{B} = [\underline{\mathcal{A}} + \underline{\mathcal{B}}, \bar{\mathcal{A}} + \bar{\mathcal{B}}]$ is an exact tensor interval extension of the function $f(\mathbf{A}, \mathbf{B}) = \mathbf{A} + \mathbf{B}$.

Elementwise Functions

A function f is said to be *elementwise* if it applies some univariate function $\sigma : \mathbb{R} \rightarrow \mathbb{R}$ to each element of a tensor independently, and returns a tensor of the same shape. If f returns a tensor of rank r , a tensor interval extension of f is then given by

$$F(\mathcal{X})_{i_1, i_2, \dots, i_r} \triangleq \left[\inf_{x \in \mathcal{X}_{i_1, i_2, \dots, i_r}} \{\sigma(x)\}, \sup_{x \in \mathcal{X}_{i_1, i_2, \dots, i_r}} \{\sigma(x)\} \right]. \quad (4.9)$$

If σ is monotonically increasing, this definition simplifies to $F(\mathcal{X}) \triangleq [f(\underline{\mathcal{X}}), f(\bar{\mathcal{X}})]$. Similarly, if f is monotonically decreasing, it simplifies to $F(\mathcal{X}) \triangleq [f(\bar{\mathcal{X}}), f(\underline{\mathcal{X}})]$.

Bilinear Operations

We now define tensor interval extensions for arbitrary bilinear operations (e.g., matrix multiplication, convolution). These tensor interval extensions will not be exact, and instead will make various tradeoffs between tightness and computation.

Because any bilinear operation can be written as a sequence of scalar multiplications and additions, we can in principle define a tensor interval extension using the rules for scalar interval arithmetic. To define this extension formally, let \mathbf{b} be an arbitrary bilinear function. It can be shown that, because \mathbf{b} is bilinear, there exists a tensor \mathbf{W} such that

$$\mathbf{b}(\mathbf{X}, \mathbf{Y}) = \langle \langle \mathbf{W}, \mathbf{X} \rangle, \mathbf{Y} \rangle. \quad (4.10)$$

Using Proposition 5, it follows that for any tensor intervals \mathcal{X} and \mathcal{Y} with $\mathbf{X} \in \mathcal{X}$ and $\mathbf{Y} \in \mathcal{Y}$,

$$\mathbf{b}(\mathbf{X}, \mathbf{Y}) \in \langle \langle \mathbf{W}, \mathcal{X} \rangle, \mathcal{Y} \rangle \triangleq \mathbf{B}(\mathcal{X}, \mathcal{Y}). \quad (4.11)$$

Thus, \mathbf{B} is a tensor interval extension of \mathbf{b} .

Although \mathbf{B} is a perfectly reasonable tensor extension of \mathbf{b} , and $\mathbf{B}(\mathcal{X}, \mathcal{Y})$ can in principle be computed efficiently, $\mathbf{B}(\mathcal{X}, \mathcal{Y})$ is not efficiently computable in machine learning frameworks such as TensorFlow, which do not have first-class support for intervals. To make efficient use of such frameworks, we would like to define a tensor interval extension of \mathbf{b} that can be computed in terms of a small number of calls to \mathbf{b} itself.

In the special case where either \mathcal{A} or \mathcal{B} is a singleton tensor interval (i.e., a tensor interval whose left and right endpoints are identical) previous work on Interval Bound Propagation [27] provides a tensor interval extension that requires just two calls to \mathbf{b} . The following proposition generalizes this result to define a tensor interval extension that requires four calls to \mathbf{b} in general, but only requires two calls in the special case where either \mathcal{A} or \mathcal{B} is a singleton.

Proposition 6. *Let $\mathbf{b}(\mathbf{X}, \mathbf{Y}) = \langle \langle \mathbf{W}, \mathcal{X} \rangle, \mathcal{Y} \rangle$ be a bilinear operation, where $\mathbf{W} \geq \mathbf{0}$ (elementwise). Then, for any tensor intervals \mathcal{A} and \mathcal{B} , and any tensors $\mathbf{A} \in \mathcal{A}$, $\mathbf{B} \in \mathcal{B}$,*

$$\mathbf{b}(\mathbf{A}, \mathbf{B}) \in \mathbf{b}(m(\mathcal{A}), m(\mathcal{B})) + [-1, 1](\mathbf{b}(r(\mathcal{A}), |m(\mathcal{B})|) + \mathbf{b}(|m(\mathcal{A})|, r(\mathcal{B})) + \mathbf{b}(r(\mathcal{A}), r(\mathcal{B})))$$

where the functions m and r were defined in §4.1, and return the midpoint and radius of a tensor interval, respectively.

If $\underline{\mathcal{A}} = \bar{\mathcal{A}}$, this can be simplified to:

$$\mathbf{b}(\underline{\mathcal{A}}, \mathbf{B}) \in \mathbf{b}(m(\mathcal{A}), m(\mathcal{B})) + [-1, 1]\mathbf{b}(|m(\mathcal{A})|, r(\mathcal{B})) \quad \forall \mathbf{B} \in \mathcal{B}$$

while if $\underline{\mathcal{B}} = \bar{\mathcal{B}}$, it can be simplified to

$$\mathbf{b}(\mathbf{A}, \underline{\mathcal{B}}) \in \mathbf{b}(m(\mathcal{A}), m(\mathcal{B})) + [-1, 1]\mathbf{b}(r(\mathcal{A}), |m(\mathcal{B})|) \quad \forall \mathbf{A} \in \mathcal{A}.$$

We also provide an alternative tensor interval extension that produces a tighter interval at the cost of additional computation. This result is based on the following lemma.

Lemma 3. *For intervals $[\underline{x}, \bar{x}]$ and $[\underline{y}, \bar{y}]$,*

$$[\underline{x}, \bar{x}] \cdot [\underline{y}, \bar{y}] \subseteq [\underline{x}^+ \underline{y}^+ + \bar{x}^+ \underline{y}^- + \underline{x}^- \bar{y}^+ + \bar{x}^- \bar{y}^-, \bar{x}^+ \bar{y}^+ + \underline{x}^+ \bar{y}^- + \bar{x}^- \underline{y}^+ + \underline{x}^- \bar{y}^-]$$

where for $z \in \mathbb{R}$, we define $z^+ \triangleq \max\{z, 0\}$ and $z^- \triangleq \min\{z, 0\}$.

To understand the uses and limitations of Lemma 3, it is useful to compare it to the product rule for interval arithmetic, namely

$$[\underline{x}, \bar{x}] \cdot [\underline{y}, \bar{y}] = [\min\{\underline{x}\underline{y}, \underline{x}\bar{y}, \bar{x}\underline{y}, \bar{x}\bar{y}\}, \max\{\underline{x}\underline{y}, \underline{x}\bar{y}, \bar{x}\underline{y}, \bar{x}\bar{y}\}]. \quad (4.12)$$

It can be shown that if $0 \notin [\underline{x}, \bar{x}]$, or if $0 \notin [\underline{y}, \bar{y}]$, then the interval given by Lemma 3 coincides with the interval given by the product rule. But if $0 \in [\underline{x}, \bar{x}]$ and $0 \in [\underline{y}, \bar{y}]$, the interval given by Lemma 3 can be looser. For example, if $[\underline{x}, \bar{x}] = [-2, 3]$ and $[\underline{y}, \bar{y}] = [-5, 7]$, then the product rule gives $[\underline{x}, \bar{x}] \cdot [\underline{y}, \bar{y}] = [-15, 21]$, but Lemma 3 gives $[\underline{x}, \bar{x}] \cdot [\underline{y}, \bar{y}] \subseteq [0 + 3 \cdot -5 + -2 \cdot 7 + 0, 3 \cdot 7 + 0 + 0 + -2 \cdot -5] = [-29, 31]$.

The virtue of Lemma 3 is that, unlike the product rule (4.12), it gives an interval that is *linear* as a function of \underline{x}^+ , \bar{x}^+ , \underline{y}^- , and \bar{y}^+ . This linearity allows us to prove the following theorem, which defines an alternative tensor interval extension of an arbitrary bilinear operation.

Theorem 6. *Let \mathbf{b} be a bilinear function. For tensor intervals \mathcal{A}, \mathcal{B} , and tensors $\mathbf{A} \in \mathcal{A}$, $\mathbf{B} \in \mathcal{B}$,*

$$\begin{aligned} \mathbf{b}(\mathbf{A}, \mathbf{B}) \in & \left[\mathbf{b}(\underline{\mathcal{A}}^+, \underline{\mathcal{B}}^+) + \mathbf{b}(\bar{\mathcal{A}}^+, \underline{\mathcal{B}}^-) + \mathbf{b}(\underline{\mathcal{A}}^-, \bar{\mathcal{B}}^+) + \mathbf{b}(\bar{\mathcal{A}}^-, \bar{\mathcal{B}}^-), \right. \\ & \left. \mathbf{b}(\bar{\mathcal{A}}^+, \bar{\mathcal{B}}^+) + \mathbf{b}(\underline{\mathcal{A}}^+, \bar{\mathcal{B}}^-) + \mathbf{b}(\bar{\mathcal{A}}^-, \underline{\mathcal{B}}^+) + \mathbf{b}(\underline{\mathcal{A}}^-, \underline{\mathcal{B}}^-) \right] \end{aligned}$$

where for any tensor \mathbf{Z} we define $\mathbf{Z}^+ \triangleq \max\{\mathbf{Z}, \mathbf{0}\}$ and $\mathbf{Z}^- \triangleq \min\{\mathbf{Z}, \mathbf{0}\}$ (and the minimum and maximum are elementwise).

Summary

The following table summarizes the tensor interval extensions of atomic functions that we have derived in this section. The first three rows are simply element-wise versions of the corresponding rules from interval arithmetic. The remaining rows give the tensor interval extensions of bilinear operations presented in equation (4.11), Proposition 6, and Theorem 6.

Table 4.1: Tensor interval extensions of atomic functions.

FUNCTION	TENSOR INTERVAL EXTENSION(S)
$f(\mathbf{X}, \mathbf{Y}) = \mathbf{X} + \mathbf{Y}$	$F(\mathcal{X}, \mathcal{Y}) = [\underline{\mathcal{X}} + \underline{\mathcal{Y}}, \bar{\mathcal{X}} + \bar{\mathcal{Y}}]$
$f(\mathbf{X}, \mathbf{Y}) = \mathbf{X} \odot \mathbf{Y}$	$F(\mathcal{X}, \mathcal{Y}) = [\min \{\underline{\mathcal{A}} \odot \underline{\mathcal{B}}, \underline{\mathcal{A}} \odot \bar{\mathcal{B}}, \bar{\mathcal{A}} \odot \underline{\mathcal{B}}, \bar{\mathcal{A}} \odot \bar{\mathcal{B}}\}, \max \{\underline{\mathcal{A}} \odot \bar{\mathcal{B}}, \bar{\mathcal{A}} \odot \bar{\mathcal{B}}, \bar{\mathcal{A}} \odot \underline{\mathcal{B}}, \bar{\mathcal{A}} \odot \bar{\mathcal{B}}\}]$
ANY ELEMENTWISE f ($f(\mathbf{X})_{i_1, i_2, \dots, i_r} = \sigma(\mathbf{X}_{i_1, i_2, \dots, i_r})$)	$F(\mathcal{X})_{i_1, i_2, \dots, i_r} \triangleq [\inf_{x \in \mathcal{X}_{i_1, i_2, \dots, i_r}} \{\sigma(x)\}, \sup_{x \in \mathcal{X}_{i_1, i_2, \dots, i_r}} \{\sigma(x)\}]$
ANY BILINEAR f ($f(\mathbf{X}, \mathbf{Y}) = \langle \langle \mathbf{W}, \mathbf{X} \rangle, \mathbf{Y} \rangle$)	$\begin{aligned} F(\mathcal{X}, \mathcal{Y}) &= \langle \mathcal{X}, \langle \mathbf{W}, \mathcal{Y} \rangle \rangle \\ F(\mathcal{X}, \mathcal{Y}) &= f(m(\mathcal{X}), m(\mathcal{Y})) \\ &\quad + [-1, 1] (f(r(\mathcal{X}), m(\mathcal{Y})) + f(m(\mathcal{X}) , r(\mathcal{Y}))) + f(r(\mathcal{X}), r(\mathcal{Y}))) \\ F(\mathcal{X}, \mathcal{Y}) &= [f(\underline{\mathcal{X}}^+, \underline{\mathcal{Y}}^+) + f(\bar{\mathcal{X}}^+, \underline{\mathcal{Y}}^-) + f(\underline{\mathcal{X}}^-, \bar{\mathcal{Y}}^+) + f(\bar{\mathcal{X}}^-, \bar{\mathcal{Y}}^-), \\ &\quad f(\bar{\mathcal{X}}^+, \bar{\mathcal{Y}}^+) + f(\underline{\mathcal{X}}^+, \bar{\mathcal{Y}}^-) + f(\bar{\mathcal{X}}^-, \underline{\mathcal{Y}}^+) + f(\underline{\mathcal{X}}^-, \bar{\mathcal{Y}}^-)] \end{aligned}$

4.2.2 Tensor Interval Polynomial Extensions of Atomic Functions

Having developed tensor interval extensions of various atomic functions in the previous section, we are now ready to develop tensor interval *polynomial* extensions (see Definition 11) of these same functions. These extended functions will form the basis of the AutoBound algorithm we present in the next section.

Bounding the Range of a Tensor Interval Polynomial

As in §3.3.1, our extended functions will be defined in terms of a function RangeBound, which bounds the range of an arbitrary polynomial over a trust region. Given a tensor interval polynomial \mathcal{P} and a tensor interval \mathcal{Z} as arguments, the RangeBound function returns a tensor interval that satisfies

$$\mathbf{Z} \in \mathcal{Z} \implies \mathcal{P}(\mathbf{Z}) \subseteq \text{RangeBound}(\mathcal{P}, \mathcal{Z}). \quad (4.13)$$

As in §3.3.1, one option for the RangeBound function is to simply evaluate \mathcal{P} at \mathcal{Z} using interval arithmetic, defining

$$\text{RangeBound}(\mathcal{P}, \mathcal{Z}) \triangleq \sum_{i=0}^{\text{degree}(\mathcal{P})} \langle \mathcal{P}_{[i]}, \mathcal{Z}^{\otimes i} \rangle. \quad (4.14)$$

However, as in §3.3.1, other approaches are possible that allow for different tradeoffs between tightness and computation.

Addition

We first consider the problem of adding two degree k tensor interval polynomials, say $\mathcal{A}(\mathbf{Z}) = \sum_{i=0}^k \langle \mathcal{A}_{[i]}, \mathbf{Z}^{\otimes i} \rangle$ and $\mathcal{B}(\mathbf{Z}) = \sum_{i=0}^k \langle \mathcal{B}_{[i]}, \mathbf{Z}^{\otimes i} \rangle$, where $\mathcal{A}(\mathbf{Z})$ and $\mathcal{B}(\mathbf{Z})$ have the same shape. As defined in §4.1.1, tensor interval addition is associative and commutative, and therefore

$$\mathcal{A}(\mathbf{Z}) + \mathcal{B}(\mathbf{Z}) = \sum_{i=0}^k \langle \mathcal{A}_i, \mathbf{Z}^{\otimes i} \rangle + \langle \mathcal{B}_i, \mathbf{Z}^{\otimes i} \rangle. \quad (4.15)$$

Furthermore, it can be shown that for any tensor intervals \mathcal{U} , \mathcal{V} , and tensor \mathbf{W} of appropriate shapes, the inner product defined by (4.1) satisfies¹

$$\langle \mathcal{U}, \mathbf{W} \rangle + \langle \mathcal{V}, \mathbf{W} \rangle = \langle \mathcal{U} + \mathcal{V}, \mathbf{W} \rangle. \quad (4.16)$$

Therefore,

$$\mathcal{A}(\mathbf{Z}) + \mathcal{B}(\mathbf{Z}) = \sum_{i=0}^k \langle \mathcal{A}_i + \mathcal{B}_i, \mathbf{Z}^{\otimes i} \rangle. \quad (4.17)$$

This equation defines an exact tensor interval polynomial extension of addition (over any trust regions).

Multiplication

Recall from (3.8) that interval multiplication is sub-distributive. Likewise, elementwise multiplication of tensor intervals is sub-distributive: for tensor intervals \mathcal{U} , \mathcal{V} , \mathcal{W} ,

$$\mathcal{U} \odot (\mathcal{V} + \mathcal{W}) \subseteq \mathcal{U} \odot \mathcal{V} + \mathcal{U} \odot \mathcal{W}. \quad (4.18)$$

Therefore, for interval polynomials $\mathcal{A}(\mathbf{Z}) = \sum_{i=0}^k \langle \mathcal{A}_{[i]}, \mathbf{Z}^{\otimes i} \rangle$ and $\mathcal{B}(\mathbf{Z}) = \sum_{i=0}^k \langle \mathcal{B}_{[i]}, \mathbf{Z}^{\otimes i} \rangle$, which return tensors of the same shape,

$$\begin{aligned} \mathcal{A}(\mathbf{Z}) \odot \mathcal{B}(\mathbf{Z}) &= \left(\sum_{i=0}^k \langle \mathcal{A}_{[i]}, \mathbf{Z}^{\otimes i} \rangle \right) \odot \left(\sum_{j=1}^k \langle \mathcal{B}_{[j]}, \mathbf{Z}^{\otimes j} \rangle \right) \\ &\subseteq \sum_{i=0}^k \sum_{j=0}^k \langle \mathcal{A}_{[i]}, \mathbf{Z}^{\otimes i} \rangle \odot \langle \mathcal{B}_{[j]}, \mathbf{Z}^{\otimes j} \rangle. \end{aligned} \quad (4.19)$$

To rewrite (4.19) as an interval polynomial, we will use the following proposition, whose proof is given in Appendix A.

Proposition 7. *For a tensor \mathbf{Z} , non-negative integers p and q , length s non-negative integer tuple S , tensor \mathbf{U} of shape $S + p * \text{shape}(\mathbf{Z})$, and tensor \mathbf{V} of shape $S + q * \text{shape}(\mathbf{Z})$,*

$$\langle \mathbf{U}, \mathbf{Z}^{\otimes p} \rangle \odot \langle \mathbf{V}, \mathbf{Z}^{\otimes q} \rangle = \langle \mathbf{U} \otimes_s \mathbf{V}, \mathbf{Z}^{\otimes(p+q)} \rangle.$$

Furthermore, for tensor intervals \mathcal{U} and \mathcal{V} , of the same shape as \mathbf{U} and \mathbf{V} respectively,

$$\langle \mathcal{U}, \mathbf{Z}^{\otimes p} \rangle \odot \langle \mathcal{V}, \mathbf{Z}^{\otimes q} \rangle \subseteq \langle \mathcal{U} \otimes_s \mathcal{V}, \mathbf{Z}^{\otimes(p+q)} \rangle.$$

Applying Proposition 7 to each term of (4.19), and letting s denote the rank of $\mathcal{A}(\mathbf{Z})$ (which by assumption equals the rank of $\mathcal{B}(\mathbf{Z})$), we have

$$\mathcal{A}(\mathbf{Z}) \odot \mathcal{B}(\mathbf{Z}) \subseteq \sum_{i=0}^k \sum_{j=0}^k \langle \mathcal{A}_{[i]} \otimes_s \mathcal{B}_{[j]}, \mathbf{Z}^{\otimes(i+j)} \rangle. \quad (4.20)$$

The right hand side of (4.20) is a degree $2k$ tensor interval polynomial, and therefore does not define a degree k tensor interval extension of elementwise multiplication. To obtain the desired degree k polynomial, we will use the following theorem.

Theorem 7. *For a tensor \mathbf{Z} , non-negative integers p and q , length s non-negative integer tuple S , tensor \mathbf{A} of shape $S + p * \text{shape}(\mathbf{Z})$, tensor \mathbf{B} of shape $S + q * \text{shape}(\mathbf{Z})$, and non-negative integer $k \leq p + q$,*

$$\langle \mathbf{A}, \mathbf{Z}^{\otimes p} \rangle \odot \langle \mathbf{B}, \mathbf{Z}^{\otimes q} \rangle = \langle \langle \mathbf{A} \otimes_s \mathbf{B}, \mathbf{Z}^{\otimes(p+q-k)} \rangle, \mathbf{Z}^{\otimes k} \rangle.$$

¹In contrast, for tensor intervals $\mathcal{U}, \mathcal{V}, \mathcal{W}$, we have only sub-distributivity: $\langle \mathcal{U}, \mathcal{W} \rangle + \langle \mathcal{V}, \mathcal{W} \rangle \subseteq \langle \mathcal{U} + \mathcal{V}, \mathcal{W} \rangle$.

Using Theorem 7 to rewrite (4.20), and letting $\mathbb{Z}_{0:k} \triangleq \{0, 1, \dots, k\}$, we have for $\mathbf{Z} \in \mathcal{Z}$:

$$\begin{aligned}
\mathcal{A}(\mathbf{Z}) \odot \mathcal{B}(\mathbf{Z}) &\subseteq \left(\sum_{\substack{i,j \in \mathbb{Z}_{0:k}: \\ i+j < k}} \langle \mathcal{A}_{[i]} \otimes_s \mathcal{B}_{[j]}, \mathbf{Z}^{\otimes i+j} \rangle \right) + \sum_{\substack{i,j \in \mathbb{Z}_{0:k}: \\ i+j \geq k}} \langle \langle \mathcal{A}_{[i]} \otimes_s \mathcal{B}_{[j]}, \mathbf{Z}^{\otimes(i+j-k)} \rangle, \mathbf{Z}^{\otimes(i+j)} \rangle \\
&\subseteq \left(\sum_{\substack{i,j \in \mathbb{Z}_{0:k}: \\ i+j < k}} \langle \mathcal{A}_{[i]} \otimes_s \mathcal{B}_{[j]}, \mathbf{Z}^{\otimes i+j} \rangle \right) + \\
&\quad \left\langle \text{RangeBound} \left(\sum_{\substack{i,j \in \mathbb{Z}_{0:k}: \\ i+j \geq k}} \langle \mathcal{A}_{[i]} \otimes_s \mathcal{B}_{[j]}, \mathbf{Z}^{\otimes(i+j-k)} \rangle, \mathcal{Z} \right), \mathbf{Z}^{\otimes(i+j)} \right\rangle. \tag{4.21}
\end{aligned}$$

This equation defines an (inexact) tensor interval polynomial extension of elementwise multiplication over trust regions $(\mathcal{Y}_1, \mathcal{Y}_2)$ and \mathcal{Z} (where the trust regions \mathcal{Y}_1 and \mathcal{Y}_2 play no role).

Exponentiation with a Non-Negative Integer Exponent

To compute $\mathcal{A}(\mathbf{Z})^p$, for integer $p \geq 0$, we could simply apply the multiplication rule repeatedly. However, we can obtain a tighter bound by expanding the polynomial, collecting terms, and using the power rule from interval arithmetic, as in §3.3.1.

Elementwise Functions

The rule for applying an elementwise function σ to a tensor interval polynomial $\mathcal{A}(\mathbf{Z}) = \sum_{i=0}^k \langle \mathcal{A}_{[i]}, \mathbf{Z}^{\otimes i} \rangle$ is conceptually simple: we compute a Taylor enclosure (itself a tensor interval polynomial) for σ , then compose it with $\mathcal{A}(\mathbf{Z})$.

To formalize the rule, suppose we wish to define a degree k tensor interval polynomial extension of σ over trust regions \mathcal{Y} and \mathcal{Z} . The first step is to compute a degree k *elementwise* tensor interval polynomial $\mathcal{S}^{\mathcal{Y}}$, satisfying

$$\sigma(\mathbf{Y}) \in \sum_{i=0}^k \mathcal{S}_{[i]}^{\mathcal{Y}} \odot \mathbf{Y}^i \quad \forall \mathbf{Y} \in \mathcal{Y}. \tag{4.22}$$

For many elementwise functions σ of interest (including \exp , \log , and various neural network activation functions), the theory we developed in Chapter 2 can be used to compute the tightest possible choice for the coefficients of $\mathcal{S}^{\mathcal{Y}}$.

It follows immediately from (4.22) (and the operational semantics defined in §4.1.1) that

$$\sigma(\mathcal{A}(\mathbf{Z})) \subseteq \sum_{i=0}^k \mathcal{S}_{[i]}^{\mathcal{Y}} \odot \mathcal{A}(\mathbf{Z})^i. \tag{4.23}$$

We could thus define a tensor interval polynomial extension of σ over \mathcal{Y} and \mathcal{Z} using the tensor interval polynomial extensions of elementwise multiplication and exponentiation defined in the previous section. However, as in §3.3.1, we can define a tighter extension which uses a single call to the `RangeBound` function. We denote this extension by $\mathcal{S}^{\mathcal{Y}} \circ_{\mathcal{Z}} \mathcal{A}$.

Bilinear Operations

In §4.2.1, we gave rules for applying an arbitrary bilinear operation to two tensor intervals. Building on these results, the following theorem provides a rule for applying an arbitrary bilinear operation to a tensor

interval polynomial. For simplicity, we state the theorem for the case of a scalar-valued, vector-variate bilinear operation, however it extends readily to multi-valued operations with arguments of arbitrary shape.

Theorem 8. *Let $\mathbf{b} : \mathbb{R}^n \times \mathbb{R}^m \rightarrow \mathbb{R}$ be a scalar-valued, vector-variate bilinear operation, and let $\mathbf{W} \in \mathbb{R}^{n \times m}$ be its transformation matrix, so that $\mathbf{b}(\mathbf{x}, \mathbf{y}) = \mathbf{x}^\top \mathbf{W} \mathbf{y}$. For any tensor \mathbf{U} whose first dimension has length n , and any tensor \mathbf{V} whose first dimension has length m , define*

$$\text{batched}(\mathbf{U}, \mathbf{V}) \triangleq \sum_{p=1}^n \sum_{q=1}^m \mathbf{W}_{pq} (\mathbf{U}_p \otimes \mathbf{V}_q).$$

Let Batched be a tensor interval extension of batched .

For any degree k tensor interval polynomials \mathcal{A} and \mathcal{B} , let the degree k interval polynomial $\mathcal{Q}(\mathcal{A}, \mathcal{B})$ be defined by:

$$\mathcal{Q}(\mathcal{A}, \mathcal{B})_{[i]} \triangleq \begin{cases} \sum_{l, m \in \mathbb{Z}_{0:k}: l+m=i} \text{Batched}(\mathcal{A}_{[l]}, \mathcal{B}_{[m]}) & i < k \\ \text{RangeBound} \left(\sum_{\substack{l, m \in \mathbb{Z}_{0:k}: \\ l+m \geq k}} \langle \text{Batched}(\mathcal{A}_{[l]}, \mathcal{B}_{[m]}), \mathbf{Z}^{\otimes(l+m-k)} \rangle, \mathcal{Z} \right) & i = k \end{cases}$$

where $\mathbb{Z}_{0:k} \triangleq \{0, 1, \dots, k\}$.

Then, for any degree k tensor interval polynomials \mathcal{A} and \mathcal{B} , and any tensor interval \mathcal{Z} ,

$$\{\mathbf{b}(\mathbf{X}, \mathbf{Y}) : \mathbf{X} \in \mathcal{A}(\mathbf{Z}), \mathbf{Y} \in \mathcal{B}(\mathbf{Z})\} \subseteq \sum_{i=0}^k \langle \mathcal{Q}(\mathcal{A}, \mathcal{B})_{[i]}, \mathbf{Z}^{\otimes i} \rangle \quad \forall \mathbf{Z} \in \mathcal{Z}.$$

Accordingly, for any tensor intervals \mathcal{Y}_1 , \mathcal{Y}_2 , and \mathcal{Z} , \mathcal{Q} is a degree k tensor interval polynomial extension of \mathbf{b} over trust regions $(\mathcal{Y}_1, \mathcal{Y}_2)$ and \mathcal{Z} (where \mathcal{Y}_1 and \mathcal{Y}_2 play no role).

Note that for given bilinear operation \mathbf{b} , Theorem 8 can be used to define various interval polynomial extensions of \mathbf{b} , depending on which tensor interval extension we use for the function batched (as defined in the theorem statement). In particular, the three tensor interval extensions presented in §4.2.1 provide three possible interval polynomial extensions of \mathbf{b} , which make different tradeoffs between computation and tightness.

Table 4.2: Degree k tensor interval polynomial extensions of atomic functions over trust regions $\mathcal{Y}_1, \mathcal{Y}_2, \dots, \mathcal{Y}_n$ and \mathcal{Z} (where n is the number of arguments).

FUNCTION	TENSOR INTERVAL POLYNOMIAL EXTENSION
$f(\mathbf{X}, \mathbf{Y}) = \mathbf{X} + \mathbf{Y}$	$F(\mathcal{A}, \mathcal{B})_{[i]} = \mathcal{A}_{[i]} + \mathcal{B}_{[i]}$
$f(\mathbf{X}, \mathbf{Y}) = \mathbf{X} \odot \mathbf{Y}$	$F(\mathcal{A}, \mathcal{B})_{[i]} = \begin{cases} \sum_{l, m \in \mathbb{Z}_{0:k}: l+m=i} \mathcal{A}_{[l]} \otimes_s \mathcal{B}_{[m]} & i < k \\ \text{RangeBound} \left(\sum_{\substack{l, m \in \mathbb{Z}_{0:k}: \\ l+m \geq k}} \langle \mathcal{A}_{[l]} \otimes_s \mathcal{B}_{[m]}, \mathbf{Z}^{\otimes(l+m-k)} \rangle, \mathcal{Z} \right) & i = k \end{cases}$ WHERE s IS THE COMMON RANK OF $\mathcal{A}(\mathbf{Z})$ AND $\mathcal{B}(\mathbf{Z})$.
ANY ELEMENTWISE f ($f(\mathbf{X})_{i_1, \dots} = \sigma(\mathbf{X}_{i_1, \dots})$)	$F(\mathcal{A}) = \mathcal{S}^{\mathcal{Y}_1} \circ_{\mathcal{Z}} \mathcal{A}$, WHERE $\mathcal{S}^{\mathcal{Y}_1}$ IS AN ELEMENTWISE TENSOR INTERVAL POLYNOMIAL ENCLOSURE OF σ OVER \mathcal{Y}_1 (SEE §4.2.2).
ANY BILINEAR f ($f(\mathbf{X}, \mathbf{Y}) = \langle \langle \mathbf{W}, \mathbf{X} \rangle, \mathbf{Y} \rangle$)	$F(\mathcal{A}, \mathcal{B})_{[i]} = \begin{cases} \sum_{l, m \in \mathbb{Z}_{0:k}: l+m=i} \text{Batched}(\mathcal{A}_{[l]}, \mathcal{B}_{[m]}) & i < k \\ \text{RangeBound} \left(\sum_{\substack{l, m \in \mathbb{Z}_{0:k}: \\ l+m \geq k}} \langle \text{Batched}(\mathcal{A}_{[l]}, \mathcal{B}_{[m]}), \mathbf{Z}^{\otimes(l+m-k)} \rangle, \mathcal{Z} \right) & i = k \end{cases}$ WHERE Batched IS A TENSOR INTERVAL EXTENSION OF THE BATCHED VERSION OF f (SEE THEOREM 8).

Summary

Table 4.2 summarizes the tensor interval polynomial extensions we have just derived.

4.2.3 Pseudocode and Analysis

Having defined rules for applying various functions to tensor interval polynomials, we are now in a position to define the AutoBound algorithm, which computes a Taylor enclosure of an arbitrary vector-variate and vector-valued function f composed of these functions.²

At a high level, the algorithm is simple: given a symbolic expression for a function $f : \mathbb{R}^d \rightarrow \mathbb{R}^s$, a center point $\mathbf{x}_0 \in \mathbb{R}^d$, and a target degree k , we compute the coefficients of a degree k Taylor enclosure of f by *evaluating* f on the identity polynomial, using the tensor interval polynomial extensions of each atomic function. These tensor interval polynomial extensions are defined over trust regions, which are computed by evaluating f using the *tensor interval* extensions of the atomic functions. Pseudocode for the AutoBound algorithm follows.

Algorithm AutoBound

Hyperparameters:

1. A table Σ , such that for any function $\sigma \in \mathbb{O}$:

- $\Sigma[\sigma, 0]$ is a tensor interval extension of σ , and
- for any integer k , $\Sigma[\sigma, k]$ is a function F that defines a degree k interval polynomial extension of σ , over trust regions provided as parameters to F .

2. A function RangeBound, such that for any tensor interval polynomial \mathcal{P} and interval \mathcal{Z} , $\mathbf{Z} \in \mathcal{Z} \implies \mathcal{P}(\mathbf{Z}) \subseteq \text{RangeBound}(\mathcal{P}, \mathcal{Z})$.

The default value of Σ is given in Table 4.2, and the default value of RangeBound is given by (4.14).

Input: a symbolic expression $(\mathcal{V}, \mathcal{E})$ for a function $f : \mathbb{R}^d \rightarrow \mathbb{R}^s$, a center point $\mathbf{x}_0 \in \mathbb{R}^d$, a vector interval $[\mathbf{a}, \mathbf{b}]$, and a target degree $k \in \mathbb{Z}_{>0}$.

Output: the coefficients of a tensor interval polynomial \mathcal{P}_n , such that $f(\mathbf{x}) \in \mathcal{P}_n(\mathbf{x} - \mathbf{x}_0)$ for all $\mathbf{x} \in [\mathbf{a}, \mathbf{b}]$.

Let $\mathcal{V} = \{v_0, v_1, \dots, v_n\}$, and let $\mathcal{E} = \{(\sigma_i, L_i)\}_{i=1}^n$.

Initialize $\mathcal{P}_0 \leftarrow (\mathbf{x}_0, \mathbb{I}_{d \times d})$, $\mathcal{Y}_0 \leftarrow [\mathbf{a}, \mathbf{b}]$, and $\mathcal{Z} \leftarrow [\mathbf{a} - \mathbf{x}_0, \mathbf{b} - \mathbf{x}_0]$.

for i from 1 to n **do**

 Let j_q be the index of the q th variable in L_i , and let m be the length of L_i (so $L_i = (v_{j_1}, v_{j_2}, \dots, v_{j_m})$).

 Set $\mathcal{P}_i \leftarrow \Sigma[\sigma_i, k](\mathcal{P}_{j_1}, \mathcal{P}_{j_2}, \dots, \mathcal{P}_{j_m}; (\mathcal{Y}_{j_1}, \mathcal{Y}_{j_2}, \dots, \mathcal{Y}_{j_m}), \mathcal{Z})$.

 Set $\mathcal{Y}_i^{(0)} \leftarrow \Sigma[\sigma_i, 0](\mathcal{Y}_{j_1}, \mathcal{Y}_{j_2}, \dots, \mathcal{Y}_{j_m})$.

 Set $\mathcal{Y}_i^{(1)} \leftarrow \text{RangeBound}(\mathcal{P}_i, \mathcal{Z})$.

 Set $\mathcal{Y}_i \leftarrow \mathcal{Y}_i^{(0)} \cap \mathcal{Y}_i^{(1)}$.

Return \mathcal{P}_n .

By adjusting the hyperparameter Σ , different tradeoffs can be made between the tightness of the tensor interval polynomial enclosures that AutoBound returns and the computation required to compute their coefficients. For example, for bilinear operations one can use any of the tensor interval extensions defined in Table 4.1.

The following theorem shows that AutoBound always returns a valid tensor interval polynomial enclosure, provided that the hyperparameter Σ satisfies the assumptions stated in the pseudocode. The proof is a straightforward induction, and is given in Appendix A.

²The algorithm can be applied to tensor-variate and tensor-valued functions by appropriate reshaping.

Theorem 9. Assume that the AutoBound hyperparameter Σ has the properties stated in the pseudocode. Then, given as input a symbolic expression $(\mathcal{V}, \mathcal{E})$ defining a function $f : \mathbb{R}^d \rightarrow \mathbb{R}^s$, a vector $\mathbf{x}_0 \in \mathbb{R}^d$, and a target degree k , AutoBound returns the coefficients of a tensor interval polynomial \mathcal{P}_n such that

$$f(\mathbf{x}) \in \mathcal{P}_n(\mathbf{x} - \mathbf{x}_0) \quad \forall \mathbf{x} \in [\mathbf{a}, \mathbf{b}].$$

4.3 An Implementation in JAX

We now briefly describe our implementation of the AutoBound algorithm in JAX [9].

Our implementation is built upon a few libraries which are not specific to JAX, but instead are designed to work with any Numpy-compatible API:

1. a *tensor interval arithmetic* library contains code for performing various operations on tensor intervals, according to the rules defined in §4.2.1, using any Numpy-like API as a back end. The library contains support for elementary arithmetic operations (such as $+$ and $*$), as well as arbitrary bilinear operations (such as matrix multiplications or convolutions).
2. a *tensor interval polynomial arithmetic* library offers similar functionality for tensor interval polynomials, using the rules defined in §4.2.2.
3. a *sharp Taylor enclosure* library contains code for computing sharp Taylor enclosures for various elementwise functions (e.g., \exp , \log , relu , softplus), using the theory developed in Chapter 2.

Building on these libraries, we provide code that allows one to compute a Taylor enclosure for an arbitrary JAX-traceable python function. To do so, the code first converts the python function to a JAX expression (Jaxpr), looks up the sharp Taylor enclosure of elementwise functions used in the Jaxpr, and then combines them according to the AutoBound algorithm, making use of the libraries just described.

One important subtlety is that JAX does not have primitives for certain functions such as softplus . Instead, the softplus function is represented in terms of elementary functions such as \exp and \log . Thus, running our algorithm directly on the Jaxpr would not take advantage of the known sharp Taylor enclosure of softplus , and would instead compute weaker bounds obtained via the sharp Taylor enclosures for \exp and \log . To work around this, our implementation has pattern-matching functionality that allows us to identify uses of the softplus function within a Jaxpr, and to treat them as a single atomic function with a known sharp Taylor enclosure.

Our code is available on GitHub at <http://github.com/google/autobound>.

4.4 Future Work

In the future, we plan to extend the results presented in this chapter in several ways:

1. *Developing a reverse-mode algorithm.* The AutoBound algorithm operates in a manner analogous to forward-mode automatic differentiation, and thus is only efficient when the number of inputs to the function is small. To enable additional applications, it would be very useful to develop a reverse-mode algorithm, which would let us efficiently compute Taylor remainder series bounds for functions with millions of inputs. We provide a brief sketch of the ideas that make a reverse-mode algorithm possible below.
2. *Computing diagonal bounds.* Our bounds on $R_{k-1}(\mathbf{x}; f, \mathbf{x}_0)$ are in terms of $(\mathbf{x} - \mathbf{x}_0)^{\otimes k}$. Thus, the number of coefficients in the bound goes up exponentially with k . In some applications, it would be useful to instead obtain a bound in terms of $(\mathbf{x} - \mathbf{x}_0)^k$, so that the number of coefficients in the bound is independent of k (and linear in the dimension of \mathbf{x}).

3. *Supporting other set arithmetics.* Although we have stated our results in terms of interval arithmetic, the same approach could be used in conjunction with other set arithmetics, for example ellipsoid arithmetic. This may yield tighter (and therefore more useful) bounds.

To outline how a reverse-mode variant of AutoBound would work, consider the function $f : \mathbb{R} \rightarrow \mathbb{R}$ defined by

$$f(x) = \sigma_1(\sigma_2(\sigma_3(x))).$$

AutoBound would compute a Taylor enclosure of f by first computing a Taylor enclosure (say, P_2) for $\sigma_2 \circ \sigma_3$, then composing a Taylor enclosure of σ_1 with P_2 to obtain a Taylor enclosure of f . But it is also possible to work in the other direction, first computing a Taylor enclosure of $\sigma_1 \circ \sigma_2$ (as a function of $\sigma_3(x)$) and then composing it with a Taylor enclosure of σ_3 to obtain a Taylor enclosure of f .

This idea can be generalized to more complex functions, analogous to the work of Wang [79], who presented a generalization of reverse-mode automatic differentiation that computes higher-order derivatives. Furthermore, by combining this approach with the diagonal bounds idea described in item (2), we expect to be able to compute quadratic enclosures of the form $f(\mathbf{x}) \in \nabla f(\mathbf{x})^\top(\mathbf{x} - \mathbf{x}_0) + I(\mathbf{x} - \mathbf{x}_0)^2$ using time and memory comparable to that required to compute the gradient. Such enclosures could be very useful in the context of universal MM optimization algorithms, as we discuss further in §5.5.

Chapter 5

Automatically Deriving MM Optimization Algorithms

Optimization plays a central role in machine learning and statistics. To fit a model, one typically minimizes a loss function $f : \mathbb{R}^n \rightarrow \mathbb{R}$, where f is available in symbolic form, allowing its derivatives to be computed easily via automatic differentiation.

The optimizers used to fit models to data typically fall into one of two categories:

1. *General-purpose optimizers based on Taylor polynomials.* This category includes gradient descent, Newton's method, and many other optimizers.
2. *Majorization-minimization (MM) optimizers.* These methods are based on *majorizers* (locally-tight upper bounds), which have been derived by hand for various loss functions of interest.

MM optimizers are attractive because they converge from any starting point, do not require hyperparameter tuning, and sometimes offer faster rates of convergence than general-purpose methods. MM optimizers have been derived for logistic regression [8], quantile regression [37], support vector machines [30], and many other problems [16, 50]. However, because each new problem requires a non-trivial derivation, MM has not been applicable to more complex loss functions, such as the ones used in deep learning.

In this chapter, we will use AutoBound to derive the upper bounds used in MM optimization algorithms *automatically*, thereby creating general-purpose MM optimizers that are as widely applicable as gradient-based methods. We thereby greatly extend the reach of this decades-old optimization template, making its benefits much more broadly available. Furthermore, we will see that the resulting optimizers perform well on a variety of problems.

Computing a majorizer using AutoBound requires an additional forward pass that uses memory linear in the number of inputs. For this reason, we do not majorize the original loss function (which would require too much memory), but instead seek a majorizer that is valid over a lower-dimensional subspace.

Our first universal MM algorithm, called SafeRate, uses a one-dimensional upper bound to derive a learning rate that is guaranteed to reduce the loss. This learning rate depends on the current iterate \mathbf{x}_t , and therefore adapts during the course of optimization. Our second algorithm, SafeCombination, generalizes this by computing a linear combination of d update directions rather than a single learning rate.

A possible concern with any such approach is that our automatically-derived upper bounds may be too loose, especially for complex losses. Reassuringly, we find that the majorizers used by SafeRate are tight in practice, even for multi-layer perceptrons with up to 64 hidden layers.

Although our universal MM optimizers are significant in their own right, we hope their biggest impact will be as illustrations of an underappreciated fact:

A general-purpose optimizer can automatically compute more than just derivatives.

5.1 Background: MM Optimization Algorithms

Majorization-minimization (MM) is a well-known optimization technique based on a simple idea: by minimizing a locally-tight upper bound on a loss function of interest, we can iteratively reduce the loss. To present the method formally, we will use the following definition.

Definition 12 (Majorization). *Consider a function $f : \mathbb{R}^n \rightarrow \mathbb{R}$. A function $\bar{f} : \mathbb{R}^n \times \mathbb{R}^n \rightarrow \mathbb{R}$ majorizes f if, for any $\mathbf{y} \in \mathbb{R}^n$:*

$$f(\mathbf{x}) \leq \bar{f}(\mathbf{x}, \mathbf{y}) \quad \forall \mathbf{x} \in \mathbb{R}^n \quad (5.1)$$

and furthermore, $\bar{f}(\mathbf{y}, \mathbf{y}) = f(\mathbf{y})$.

If \bar{f} majorizes f , then \bar{f} provides an upper bound on f that is tight at a specified point \mathbf{y} , and valid everywhere. Figure 5.1 illustrates a majorizer for the softplus function.

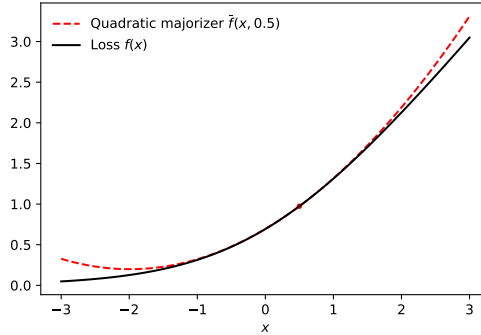


Figure 5.1: The function $f(x) = \log(1 + \exp(x))$, and the quadratic majorizer $\bar{f}(x, y) = f(y) + \nabla f(y)(x - y) + \frac{1}{8}(x - y)^2$, evaluated at $y = \frac{1}{2}$.

Given an arbitrary starting point $\mathbf{x}_0 \in \mathbb{R}^n$, a majorization-minimization algorithm produces a sequence of iterates $\mathbf{x}_0, \mathbf{x}_1, \mathbf{x}_2, \dots$ by setting

$$\mathbf{x}_{t+1} = \operatorname{argmin}_{\mathbf{x} \in \mathbb{R}^n} \{ \bar{f}(\mathbf{x}, \mathbf{x}_t) \}. \quad (5.2)$$

An appealing property of MM is that the loss decreases monotonically: $f(\mathbf{x}_{t+1}) \leq f(\mathbf{x}_t)$ for all t . This follows from the sequence of inequalities:

$$f(\mathbf{x}_{t+1}) \leq \bar{f}(\mathbf{x}_{t+1}, \mathbf{x}_t) \leq \bar{f}(\mathbf{x}_t, \mathbf{x}_t) = f(\mathbf{x}_t) \quad (5.3)$$

where the first inequality holds because \bar{f} majorizes f , and the second inequality holds by definition of \mathbf{x}_{t+1} .

Majorization-minimization is the subject of a large literature, and many different majorizers have been derived for functions with specific properties. For example, if one can show that f is β -smooth (meaning that ∇f has a Lipschitz constant at most β), then it can be shown that f is majorized by the quadratic function $\bar{f}(\mathbf{x}, \mathbf{y}) = f(\mathbf{y}) + \nabla f(\mathbf{y})(\mathbf{x} - \mathbf{y}) + \frac{\beta}{2} \|\mathbf{x} - \mathbf{y}\|_2^2$. However, we are not aware any previous work on automatically deriving majorizers for arbitrary losses. See [16, 50] for textbook treatments of MM.

5.2 Universal MM Optimization Algorithms

We now present two *universal* MM optimization algorithms: MM optimization algorithms that can be applied to any loss that can be written as a composition of elementwise functions (e.g., \exp , \log , relu , softplus), plus the binary operations of addition and multiplication. The term “universal” is ours, and to our knowledge these algorithms are the first MM algorithms that are universal in this sense.

In fact, our first algorithm is a special case of our second one, but we choose to present it separately for pedagogical purposes. Specifically:

- The SafeRate algorithm uses AutoBound to compute a learning rate η_t that is guaranteed to monotonically reduce the loss.
- The SafeCombination algorithm uses AutoBound to compute a vector η_t that specifies a combination of user-supplied update directions that is guaranteed to monotonically reduce the loss.

In both cases, the majorizer is defined over a low-dimensional subspace of the original optimization domain, making the algorithms *majorization-minimization subspace methods*. In addition, the value of the majorizer will be infinite outside a trust region, whose size affects the tightness of the majorizer. In order to speed up convergence, both algorithms use a simple heuristic to adapt the size of the trust region over time.

5.2.1 Using AutoBound to Derive Majorizers

Recall that, when used to compute a degree k Taylor enclosure of a univariate function $f : \mathbb{R} \rightarrow \mathbb{R}$, AutoBound takes as input a point $x_0 \in \mathbb{R}$ and a trust region $[a, b] \subseteq \mathbb{R}$, and returns a tuple whose last element is an interval $I_{k, f, x_0, [a, b]}$ that satisfies

$$f(x) \in \left(\sum_{i=0}^{k-1} \frac{1}{i!} f^{(i)}(x_0) (x - x_0)^i \right) + I_{k, f, x_0, [a, b]} (x - x_0)^k \quad \forall x \in [a, b]. \quad (5.4)$$

Using this interval, we can define a function $\bar{f}(x, x_0)$ that majorizes f :

$$\bar{f}(x, x_0) \triangleq \begin{cases} \left(\sum_{i=0}^k \frac{1}{i!} f^{(i)}(x_0) (x - x_0)^i \right) + \max \left\{ \underline{I}_{k, f, x_0, [a, b]} (x - x_0)^k, \overline{I}_{k, f, x_0, [a, b]} (x - x_0)^k \right\} & x \in [a, b] \\ \infty & x \notin [a, b]. \end{cases} \quad (5.5)$$

The function \bar{f} majorizes f because $\bar{f}(x, x_0) = f(x_0)$ by inspection, and (5.4) implies $f(x) \leq \bar{f}(x, x_0)$.

If k is even, or if $a \geq 0$, we have $(x - x_0)^k \geq 0$ for all $x \in [a, b]$, and the definition of \bar{f} simplifies to

$$\bar{f}(x, x_0) \triangleq \begin{cases} \left(\sum_{i=0}^k \frac{1}{i!} f^{(i)}(x_0) (x - x_0)^i \right) + \overline{I}_{k, f, x_0, [a, b]} (x - x_0)^k & x \in [a, b] \\ \infty & x \notin [a, b]. \end{cases} \quad (5.6)$$

For a vector-variate function $f : \mathbb{R}^d \rightarrow \mathbb{R}$, the situation is similar, except that the end points of $I_{x, f, x_0, [a, b]}$ will be tensors rather than scalars.

5.2.2 SafeRate: Determining a Safe Learning Rate

Iterative methods for optimization, such as gradient descent and Newton's method, optimize a differentiable loss $f : \mathbb{R}^n \rightarrow \mathbb{R}$ by performing a sequence of updates of the form

$$\mathbf{x}_{t+1} = \mathbf{x}_t + \eta_t \mathbf{v}_t \quad (5.7)$$

where \mathbf{v}_t is an update direction and η_t is a step size. To optimize f effectively, we would like to choose \mathbf{v}_t and η_t so as to guarantee convergence to a first-order critical point (or preferably, a local minimum).

Optimization theory provides many methods for choosing \mathbf{v}_t and η_t , which have different theoretical guarantees depending on what assumptions are made about f . If f is convex and the gradient norm is bounded, then setting $\mathbf{v}_t = -\nabla f(\mathbf{x}_t)$ and $\eta_t = \frac{1}{\sqrt{t}}$ guarantees that the loss of the average iterate converges to the global minimum [81]. If f is non-convex but its gradient has a Lipschitz constant of at most β (meaning f is “ β -smooth”), then setting $\mathbf{v}_t = -\nabla f(\mathbf{x}_t)$ and $\eta_t = \frac{1}{\beta}$ guarantees that the loss goes down monotonically

[26]. See the textbooks [65, 67] for an introduction to optimization theory, including classical results on the rates of convergence achieved by different algorithms under various assumptions.

The loss functions used to train neural networks are neither convex nor β -smooth. For such functions, the only globally convergent optimization methods we are aware of involve are classical methods that require line search or trust region adaptation (e.g., [67, chapters 3-4]). Because these classical approaches are based on Taylor polynomials, and have no way of knowing how accurate the Taylor polynomial approximation is at a given \mathbf{x}_t , they require trial and error in order to find a point that reduces the loss.

Using our new machinery, it is possible to find a learning rate that is *guaranteed* to reduce the loss, at the cost of just one additional forward pass. To do so, we use AutoBound to derive a majorizer of the function

$$h_t(\eta) = f(\mathbf{x}_t + \eta \mathbf{v}_t). \quad (5.8)$$

Specifically, given a specified maximum learning rate $\bar{\eta}_t$, we auto-derive a majorizer for h_t as described in §5.2.1 to obtain a polynomial P_t such that

$$h_t(\eta) \leq P_t(\eta) \quad \forall \eta \in [0, \bar{\eta}_t]. \quad (5.9)$$

Note that P_t defines a majorizer of f that is valid for $\mathbf{x} \in \{\mathbf{x}_t + \eta \mathbf{v}_t : \eta \in [0, \bar{\eta}_t]\}$.

We then choose η_t to minimize the majorizer, setting

$$\eta_t = \operatorname{argmin}_{\eta \in [0, \bar{\eta}_t]} \{P_t(\eta)\}. \quad (5.10)$$

The argmin can be found efficiently by computing the roots of a degree $k-1$ polynomial (see Appendix B).

How do we choose the maximum learning rate, $\bar{\eta}_t$? Because $\eta_t \leq \bar{\eta}_t$, choosing $\bar{\eta}_t$ too small will slow down progress. On the other hand, as $\bar{\eta}_t$ increases, \bar{I}_t will also increase, so choosing $\bar{\eta}_t$ very large will also result in a small value of η_t . A simple heuristic, which we will find to be effective in our experiments in §5.3, is to set $\bar{\eta}_1$ to an arbitrary value (say, 1), and then to set:

$$\bar{\eta}_{t+1} = \begin{cases} 2\bar{\eta}_t & \text{if } \eta_t \geq \frac{1}{2}\bar{\eta}_t \\ \frac{1}{2}\bar{\eta}_t & \text{otherwise.} \end{cases} \quad (5.11)$$

We refer to the resulting algorithm as SafeRate, and give pseudocode below.

A few remarks about SafeRate are in order:

1. As written, SafeRate calls AutoBound once per iteration, and passes it a symbolic expression that depends on \mathbf{x}_t and \mathbf{v}_t . However, in an actual implementation, AutoBound is called once up front to return an object (e.g., a TensorFlow tensor) that works for arbitrary \mathbf{x}_t and \mathbf{v}_t . Thus, the overhead of recursively analyzing the symbolic expression for the loss f is incurred once up front, rather than T times.
2. The use of a finite trust region is not necessary for all problems. In particular, for linear or logistic regression, AutoBound is able to compute a quadratic majorizer that is valid over an unbounded trust region. In such cases we may set $\bar{\eta}_1 = \infty$ to effectively disable the use of a finite trust region.

5.2.3 SafeCombination: Combining Multiple Update Directions

The method just discussed for determining a safe learning rate is a special case of a more general method, where a number of possible update directions are provided, and AutoBound is used to determine a linear combination of the update directions that is guaranteed to monotonically reduce the loss.

Concretely, let $\mathbf{U}_t \in \mathbb{R}^{n \times d}$ be a matrix whose columns specify d possible update directions (e.g., the negative gradient, or the update direction used by Adam or AdaGrad). We will perform an update of the form:

$$\mathbf{x}_{t+1} = \mathbf{x}_t + \mathbf{U}_t \boldsymbol{\eta}_t \quad (5.12)$$

Algorithm SafeRate

Parameters:

1. a function \mathcal{O} that, given the current iterate \mathbf{x}_t and observed gradients $\mathbf{g}_1, \mathbf{g}_2, \dots, \mathbf{g}_t$, returns an update direction.
2. a function `PolynomialUpperBound` that, given a function $h : \mathbb{R} \rightarrow \mathbb{R}$, an interval $[a, b]$, and a point $z_0 \in [a, b]$, returns a degree k polynomial P such that $h(z) \leq P(z) \forall z \in [a, b]$, and $P(z_0) = h(z_0)$. (Default version uses `AutoBound` to return a quadratic upper bound.)

Input: a loss $f : \mathbb{R}^n \rightarrow \mathbb{R}$, and an initial point $\mathbf{x}_1 \in \mathbb{R}^n$.

Output: a point $\mathbf{x}_{T+1} \in \mathbb{R}^n$.

```

Initialize  $\bar{\eta}_1 \leftarrow 1$ .
for  $t$  from 1 to  $T$  do
  Set  $\mathbf{g}_t \leftarrow \nabla f(\mathbf{x}_t)$ .
  Set  $\mathbf{v}_t \leftarrow \mathcal{O}(\mathbf{x}_t, \{\mathbf{g}_s\}_{s=1}^t)$ .
  Define  $h_t(\eta) \triangleq f(\mathbf{x}_t + \eta \mathbf{v}_t)$ .
  Set  $P_t \leftarrow \text{PolynomialUpperBound}(h_t, [0, \bar{\eta}_t], 0)$ .
  Set  $\eta_t \leftarrow \text{argmin}_{\eta \in [0, \bar{\eta}_t]} \{P_t(\eta)\}$ .
  Set  $\mathbf{x}_{t+1} \leftarrow \mathbf{x}_t + \eta_t \mathbf{v}_t$ .
  Set  $\bar{\eta}_{t+1} \leftarrow \begin{cases} 2\bar{\eta}_t & \text{if } \eta_t \geq \frac{1}{2}\bar{\eta}_t \\ \frac{1}{2}\bar{\eta}_t & \text{otherwise.} \end{cases}$ 
Return  $\mathbf{x}_{T+1}$ .

```

for some $\boldsymbol{\eta}_t \in [\mathbf{0}, \bar{\boldsymbol{\eta}}_t] \subseteq \mathbb{R}^d$.

The vector $\boldsymbol{\eta}_t$ can be obtained by generalizing equations (5.8) and (5.9) in the natural way, leading to the bound:

$$f(\mathbf{x}_t + \mathbf{U}_t \boldsymbol{\eta}) \leq f(\mathbf{x}_t) + \nabla f(\mathbf{x}_t)^\top \mathbf{U}_t \boldsymbol{\eta} + \boldsymbol{\eta}^\top \bar{\mathbf{I}}_t \boldsymbol{\eta} \quad \forall \boldsymbol{\eta} \in [\mathbf{0}, \bar{\boldsymbol{\eta}}_t] \quad (5.13)$$

for some matrix $\bar{\mathbf{I}}_t \in \mathbb{R}^{d \times d}$.

The usual way to minimize the right hand side of (5.13) would be to set the derivative to zero, but this does not work here for two reasons. First, the bound is only valid for $\boldsymbol{\eta} \in [\mathbf{0}, \bar{\boldsymbol{\eta}}_t]$, and setting the derivative to zero might yield a value outside this hyperrectangle. Second, the matrix $\bar{\mathbf{I}}_t$ is not necessarily positive semidefinite, so setting the derivative to zero does not necessarily give us the global minimum. Nevertheless, the right hand side can be approximately minimized over the hyperrectangle $[\mathbf{0}, \bar{\boldsymbol{\eta}}_t]$ using a variant of conjugate gradient descent, which we describe in Appendix B.

The vector $\bar{\boldsymbol{\eta}}_t$ is determined adaptively using a scheme similar to (5.11), but applied to each of the d components of $\bar{\boldsymbol{\eta}}_t$ independently.

It can be shown that, by setting $d = n$ and letting \mathbf{U}_t be the identity matrix, we obtain a second-order optimizer that can minimize quadratic losses (e.g., least squares linear regression) in one step.

5.2.4 Theoretical Guarantees

Our universal MM algorithms enjoy a number of desirable theoretical guarantees, which we now state. The proofs are given in Appendix A.

First, like other MM optimizers, our universal MM optimizers are guaranteed to monotonically reduce the loss.

Proposition 8. *The iterates of SafeRate and SafeCombination satisfy*

$$f(\mathbf{x}_{T+1}) \leq f(\mathbf{x}_T) \leq \dots \leq f(\mathbf{x}_1).$$

Algorithm SafeCombination

Parameters:

1. a function \mathcal{O} that, given the current iterate \mathbf{x}_t and observed gradients $\mathbf{g}_1, \mathbf{g}_2, \dots, \mathbf{g}_t$, returns an n by d update direction matrix.
2. a function `PolynomialUpperBound` that, given a function $h : \mathbb{R}^d \rightarrow \mathbb{R}$, a vector interval $[\mathbf{a}, \mathbf{b}] \subseteq \mathbb{R}^d$, and a point $\mathbf{z}_0 \in [\mathbf{a}, \mathbf{b}]$, returns a quadratic polynomial P such that $h(\mathbf{z}) \leq P(\mathbf{z}) \forall \mathbf{z} \in [\mathbf{a}, \mathbf{b}]$, and $P(\mathbf{z}_0) = h(\mathbf{z}_0)$. (Default version uses `AutoBound`.)

Input: a loss $f : \mathbb{R}^n \rightarrow \mathbb{R}$, and an initial point $\mathbf{x}_1 \in \mathbb{R}^n$.

Output: a point $\mathbf{x}_{T+1} \in \mathbb{R}^n$.

```

Initialize  $\bar{\boldsymbol{\eta}}_1 \leftarrow \mathbf{1}_d \in \mathbb{R}^d$ .
for  $t$  from 1 to  $T$  do
  Set  $\mathbf{g}_t \leftarrow \nabla f(\mathbf{x}_t)$ .
  Set  $\mathbf{U}_t \leftarrow \mathcal{O}(\mathbf{x}_t, \{\mathbf{g}_s\}_{s=1}^t)$ .
  Define  $h_t(\boldsymbol{\eta}) \triangleq f(\mathbf{x}_t + \mathbf{U}_t \boldsymbol{\eta})$ .
  Set  $P_t \leftarrow \text{PolynomialUpperBound}(h_t, [\mathbf{0}, \bar{\boldsymbol{\eta}}_t], \mathbf{0})$ .
  Set  $\boldsymbol{\eta}_t \leftarrow \text{MinimizeQuadratic}(P_t, [\mathbf{0}, \bar{\boldsymbol{\eta}}_t])$  (see §B.2).
  Set  $\mathbf{x}_{t+1} \leftarrow \mathbf{x}_t + \mathbf{U}_t \boldsymbol{\eta}_t$ .
  For  $i \in \{1, 2, \dots, d\}$ , set  $(\bar{\boldsymbol{\eta}}_{t+1})_i \leftarrow \begin{cases} 2(\bar{\boldsymbol{\eta}}_t)_i & \text{if } (\boldsymbol{\eta}_t)_i \geq \frac{1}{2}(\bar{\boldsymbol{\eta}}_t)_i \\ \frac{1}{2}(\bar{\boldsymbol{\eta}}_t)_i & \text{otherwise.} \end{cases}$ 
Return  $\mathbf{x}_{T+1}$ .

```

The next question we would like to answer is how fast our universal MM optimizers converge. Because we have not yet developed a complete theory around the tightness of the bounds returned by `AutoBound`, we cannot yet answer this question in full generality. However, under the standard assumption of a β -smooth loss, and assuming that the `PolynomialUpperBound` function returns the upper bound that follows from the definition of β -smoothness, we can show our optimizers enjoy convergence guarantees similar to those of backtracking line search [4], but without the need to backtrack or to tune line search hyperparameters. As is standard in non-convex optimization, the guarantees are stated in terms of the minimum gradient norm.

Theorem 10. *Let f , \mathbf{v}_t , and P_t be defined as in the pseudocode for `SafeRate`. Suppose, for some $\beta \geq 1$, f is β -smooth over the level set $\{\mathbf{y} : f(\mathbf{y}) \leq f(\mathbf{x}_1)\}$, and suppose that the `PolynomialUpperBound` function returns*

$$P_t(\boldsymbol{\eta}) = f(\mathbf{x}_t) + \boldsymbol{\eta}^\top \nabla f(\mathbf{x}_t)^\top \mathbf{v}_t + \frac{\beta}{2} \boldsymbol{\eta}^2 (f(\mathbf{x}_t)^\top \mathbf{v}_t)^2.$$

Further suppose $\mathbf{v}_t = -\nabla f(\mathbf{x}_t)$. Then,

$$\min_{1 \leq t \leq T} \left\{ \|\nabla f(\mathbf{x}_t)\|^2 \right\} \leq \frac{2\beta(f(\mathbf{x}_1) - f(\mathbf{x}_{T+1}))}{T}.$$

The same guarantee holds for `SafeCombination`, provided the negative gradient is one of the d update directions.

Lastly, we consider the running time of our algorithms. Both algorithms require an additional forward pass, whose time complexity is some multiple of that required to compute $f(\mathbf{x})$. We state our result in terms of the number of multiplications, which is the dominant term in the time complexity for the loss functions of interest.

Theorem 11. *Let $f : \mathbb{R}^n \rightarrow \mathbb{R}$ be a function such that for any $\mathbf{x} \in \mathbb{R}^n$, computing $f(\mathbf{x})$ requires M_0 multiplications, and calling `DirectionOracle` requires M_1 multiplications. Then, using `AutoBound` as the*

PolynomialUpperBound function, each iteration of *SafeRate* requires $O(M_1 + M_0 k \log(k))$ multiplications, where k is the polynomial degree, and each iteration of *SafeCombination* requires $O(M_1 + M_0 d^\omega)$ multiplications, where $\omega < 2.37286$.

5.3 Experiments

We now compare *SafeRate* and *SafeCombination* to existing optimizers, on both real and synthetic problems.

5.3.1 Optimizers

We compare *SafeRate* and *SafeCombination* to four existing optimizers: Adam [47], AdaGrad [19], gradient descent, and backtracking line search using the Armijo-Goldstein condition [4].

For Adam, AdaGrad, and gradient descent, we consider all learning rates in the set $\{10^i : i \in \mathbb{Z}, -4 \leq i \leq 1\}$, and present results for the best-performing learning rate (learning rates that are powers of 10 outside this grid performed poorly on all problems). Other Adam hyperparameters are left at the default values recommended in the original paper [47].

Backtracking line search refers to a gradient descent optimizer that chooses the learning rate on each step using a backtracking line search first described by Armijo [4]. Starting at a point \mathbf{x} , backtracking line search seeks to find a point \mathbf{x}' that reduces the loss by at least $\frac{\alpha}{2} \|\nabla f(\mathbf{x})\|^2$, where α starts at an initial value $\alpha_0 \in \mathbb{R}$, and is halved until this condition is satisfied. We consider all values of $\alpha_0 \in \{10^i : i \in \mathbb{Z}, -5 \leq i \leq 3\}$, and report results for the value of α_0 that achieved the minimum loss.

These optimizers and hyperparameter grids are summarized in Table 5.1.

Table 5.1: Optimizers used in our experiments.

OPTIMIZER	HYPERPARAMETERS
ADAGRAD [19] (DIAGONAL MATRIX VERSION)	$\eta \in \{10^i : i \in \{10^i : i \in \mathbb{Z}, -4 \leq i \leq 1\}\}$, $\delta = 0$
ADAM [47]	$\eta \in \{10^i : i \in \{10^i : i \in \mathbb{Z}, -4 \leq i \leq 1\}\}$, $\beta_1 = 0.9$, $\beta_2 = 0.999$, $\epsilon = 10^{-8}$
BACKTRACKING LINE SEARCH [4]	$\alpha_0 \in \{10^i : i \in \mathbb{Z}, -5 \leq i \leq 3\}$
GD	$\eta \in \{10^i : i \in \{10^i : i \in \mathbb{Z}, -4 \leq i \leq 1\}\}$
SAFERATE[ADAGRAD] (OURS)	$\delta = 0$
SAFERATE[ADAM] (OURS)	$\beta_1 = 0.9$, $\beta_2 = 0.999$, $\epsilon = 10^{-8}$
SAFERATE[GD] (OURS)	—
SAFECOMBINATION[PER-LAYER ADAGRAD] (OURS)	$\delta = 0$
SAFECOMBINATION[PER-LAYER ADAM] (OURS)	$\beta_1 = 0.9$, $\beta_2 = 0.999$, $\epsilon = 10^{-8}$
SAFECOMBINATION[PER-LAYER GD] (OURS)	—

In addition, we evaluate the performance of *SafeRate* using three choices for the directional oracle: *SafeRate[GD]* uses the negative gradient direction, *SafeRate[AdaGrad]* uses the AdaGrad direction (determined based on the observed history of gradient vectors), and *SafeRate[Adam]* uses the Adam direction. The *SafeRate[AdaGrad]* and *SafeRate[Adam]* update directions are based on a learning rate of .1 for the underlying AdaGrad/Adam algorithm, and the recommended default values for all other hyperparameters. Note that the learning rate affects only the scale of the update direction, and the behavior of *SafeRate* is largely invariant to this scale (it is not strictly invariant because of the way the scale interacts with the trust region size). For this reason we do not need to tune the learning rate.

Finally, we evaluate the performance of *SafeCombination*, using three choices for the matrix of update directions. For *SafeCombination[per-layer GD]*, there is an update direction for each tensor \mathbf{W} that appears in the loss, and the update direction for a tensor \mathbf{W} equals the negative gradient with entries for tensors other than \mathbf{W} zeroed out. Thus, when applied to a neural network optimization problem, *SafeCombination[per-layer GD]* computes a per-layer learning rate (hence its name). *SafeCombination[per-layer AdaGrad]* and

SafeCombination[per-layer Adam] are similar, except they use the per-layer update directions given by AdaGrad and Adam, respectively, rather than the negative gradient. The Adam/AdaGrad update directions are determined in the same way described in the previous paragraph.

When plotting an optimizer’s performance as a function of the number of steps, we consider each distinct point evaluated as a separate step (for backtracking line search, this includes points where the sufficient-loss-decrease condition is not satisfied).

5.3.2 One-Dimensional Problems

We begin by experimenting with synthetic one-dimensional problems. This will allow us to understand the behavior of SafeRate qualitatively, in a low-dimensional setting where the results can be easily visualized.

Losses

Table 5.2: One-dimensional loss functions used in our experiments.

PROBLEM NAME	LOSS FUNCTION
1-D LEAST SQUARES LINEAR REGRESSION	$x \mapsto (x - \frac{3}{2})^2$
1-D LINEAR REGRESSION WITH NON-NORMAL ERRORS	$x \mapsto (x - 3)^4$
1-D LOGISTIC REGRESSION	$x \mapsto \frac{2}{3} \log(1 + \exp(x)) + \frac{1}{3} \log(1 + \exp(-x))$
OPTIMIZING A SINGLE NEURAL NETWORK PARAMETER	$x \mapsto ((\text{sigmoid}(x - 10) - \frac{1}{2})^2$

Table 5.2 summarizes the loss functions used in these experiments. Each loss is a one-dimensional example of a widely-studied problem. For least squares linear regression, we consider a problem with a single feature, making the loss a quadratic polynomial. The specific choice of quadratic does not qualitatively change the results; we choose $(x - \frac{3}{2})^2$. We also consider linear regression with error terms drawn from a *generalized symmetric normal distribution* [61, 80]. Setting the β parameter of the generalized symmetric normal distribution to 4 results in a quartic polynomial loss, where again the specific choice of quartic does not qualitatively change the results. For logistic regression, we choose a one-dimensional problem where two thirds of the labels are negative, and there is a single feature whose value is always 1.

As a one-dimensional example of neural network training, we consider the loss $f(x) = ((\text{sigmoid}(x - 10) - \frac{1}{2})^2$. Minimizing this loss can be thought of as optimizing the bias parameter in the first layer of a single-hidden-layer neural network with sigmoid activation functions and squared error, with a training set of size 1 and appropriate initial values for parameters other than x . This loss is interesting because initially (when $x = 0$) the input to the sigmoid is very small, resulting in very small initial gradients that can pose a challenge for traditional optimizers.

Performance comparison

Figure 5.2 compares the performance of SafeRate to that of tuned versions of the baseline optimizers, on the four one-dimensional optimization problems given in Table 5.2. For optimizers other than SafeRate (which has no hyperparameters), each plot shows the best-performing¹ hyperparameter settings for each problem, considering all the settings in the grid defined by Table 5.1. For these one-dimensional problems, all optimizers require similar wall time per step.

We make the following observations:

- Despite not requiring hyperparameter tuning, SafeRate outperforms tuned version of all baseline optimizers on all four problems, with one exception (with a learning rate of 1, AdaGrad performs better on the neural network parameter optimization problem).

¹Performance is measured by the minimum loss reached on any step.

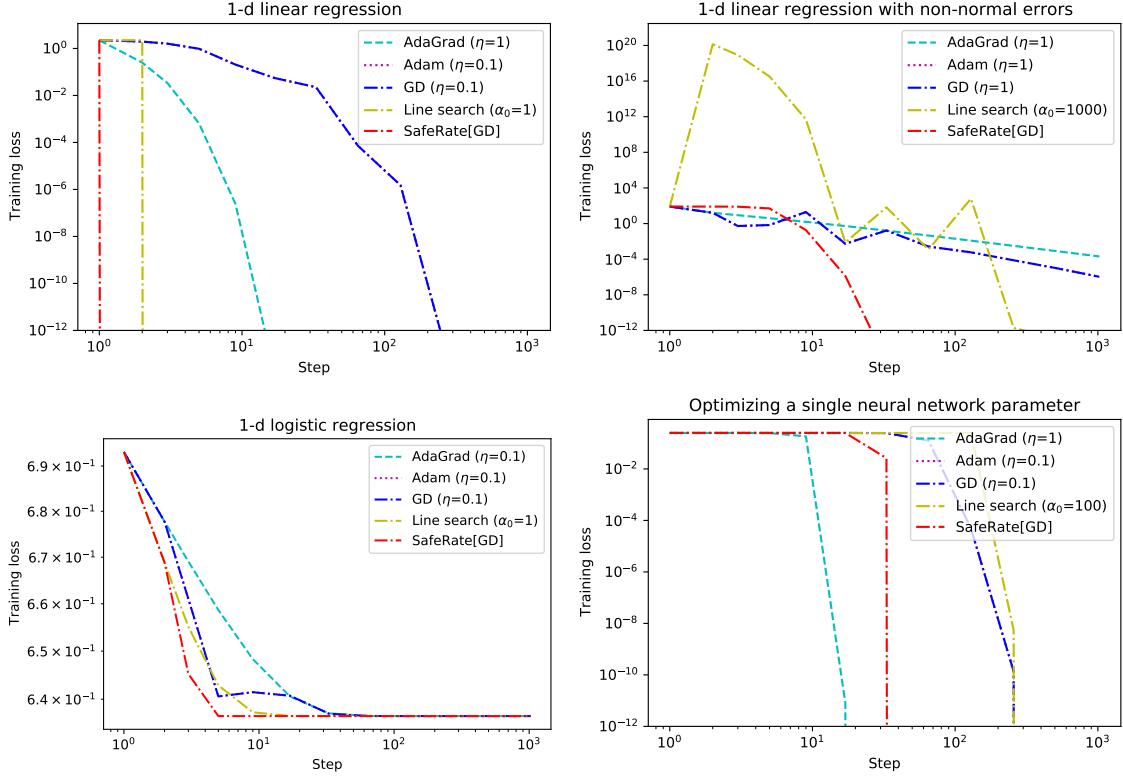


Figure 5.2: Comparison of optimizers on one-dimensional optimization problems. Each plot shows the loss as a function of the number of iterations (log scale). For optimizers other than SafeRate, the plot shows the best-performing hyperparameter from the grid defined in Table 5.1 (the best-performing hyperparameter is different for each plot). Despite not requiring hyperparameter tuning, SafeRate generally outperforms tuned versions of all baseline optimizers. For these one-dimensional problems, all optimizers require similar wall time per step.

- For 1-d least squares linear regression, the quadratic majorizer derived using AutoBound is exact, and thus SafeRate jumps to the global minimum on the first step.
- For 1-d linear regression with non-normal errors, SafeRate converges super-linearly², whereas gradient descent and AdaGrad appear to converge linearly.

Safe learning rates

We now examine in more detail how SafeRate behaves on these one-dimensional problems. Recall that the “safe” learning rate computed by SafeRate on step t depends on two things: the current iterate x_t , and the maximum learning rate $\bar{\eta}_t$ (which determines the trust region, $[0, \bar{\eta}_t]$). Figure 5.3 depicts the safe learning rate as a function of $x = x_t$, for various values of the trust region.

In examining Figure 5.3, several things are worth noting:

- In general, the learning rate depends in a non-trivial way on the current iterate x , and can be orders of magnitude larger for some x than for others.

²An optimizer is said to converge linearly if the log of the optimality gap decreases linearly as a function of the log of the number of steps.

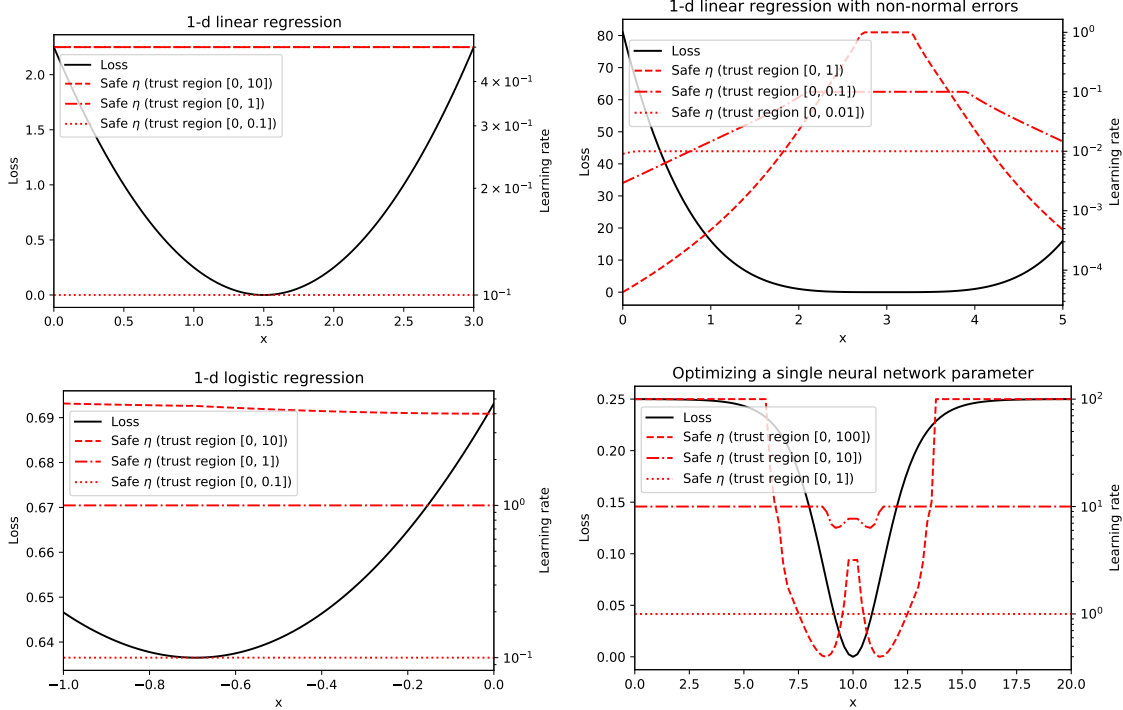


Figure 5.3: Safe gradient descent learning rates for various one-dimensional problems, as a function of the current iterate x and the trust region. For each x , each plotted learning rate η is computed using the symbolic expression for the loss f , and is guaranteed to reduce the loss: $f(x - \eta \nabla f(x)) \leq f(x)$.

- For some problems, the “safe” learning rate increases dramatically as one approaches the global minimum, while for other problems it decreases dramatically.
- The optimal trust region width (i.e., the one that lets us compute the largest “safe” learning rate) also depends on x . For example, for the linear regression problem with non-normal errors, at $x = 0$ the optimal trust region width is .01; at $x = 1$ it is 0.1, and at $x = 2.9$ it is 1.

These points illustrate the potential for SafeRate to non-trivially adapt the learning rate during the course of optimization, and make clear that the trust region must adapt over time if we wish to compute the largest possible safe learning rates.

SafeRate trust region adaptation

Figure 5.4 shows how the learning rate η_t and the maximum learning rate $\bar{\eta}_t$ (which determines the trust region) evolve when running SafeRate on each of the one-dimensional problems.

We summarize the results shown in Figure 5.4 as follows:

- For least squares linear regression, SafeRate converges in one step, and thus trust region adaptation plays no role.
- For linear regression with non-normal errors, the maximum learning rate $\bar{\eta}_t$ is initially too large, and hence $\eta_t \ll \bar{\eta}_t$, leading to slow progress. As a result, SafeRate decreases $\bar{\eta}_t$ exponentially, which causes η_t to increase exponentially. Then, once $\eta_t \approx \bar{\eta}_t$, both $\bar{\eta}_t$ and η_t increase exponentially for the remainder of the optimization process. We note that this learning rate schedule is very different

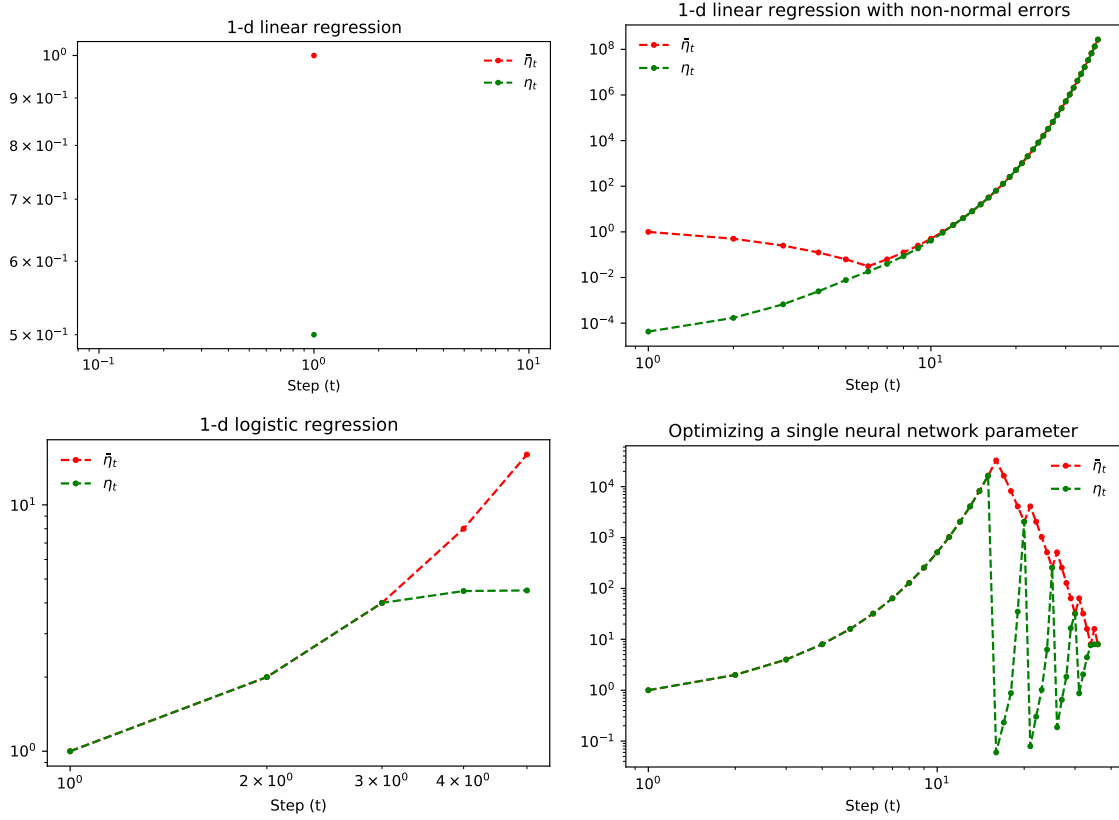


Figure 5.4: The evolution of η_t and $\bar{\eta}_t$ when using SafeRate to minimize various one-dimensional losses.

from the regret-bound-minimizing schedule used in algorithms such as AdaGrad [19] and FTPRL [60], which always decreases the learning rate and does so at a polynomial rate.

- For logistic regression, $\bar{\eta}_t$ is initially too small, causing η_t to be capped at its maximum value. This causes $\bar{\eta}_t$ to double until this is no longer the case, leading to convergence in a few steps.
- For the one-dimensional neural network problem, the gradients are initially very small, and a very large learning rate is necessary to make progress. As in the logistic regression problem, η_t is initially capped at its maximum value, causing $\bar{\eta}_t$ to double until this is no longer the case. Then, once the optimizer reaches the part of the sigmoid curve where the gradients are larger, η_t suddenly decreases by more than four orders of magnitude. This causes $\bar{\eta}_t$ to decrease, causing η_t to increase again, and η_t continues to oscillate up and down for the remainder of the optimization run, while at the same time the loss decreases rapidly (as shown in Figure 5.2).

Overall, the simple doubling/halving heuristic used by SafeRate is very effective on these problems, and leads to qualitatively different behaviors on each problem.

5.3.3 Random Regression Problems

For our next experiment, we evaluate SafeRate on randomly-generated linear and logistic regression problems. For linear regression, we consider both least-squares linear regression, as well as linear regression with non-normal error terms, described in more detail below.

We generate random, well-specified regression problems by sampling feature vectors from a normal distribution with a specified covariance matrix, and generating labels based on a known model. Letting d denote the number of features, the covariance matrix is $\mathbf{Z}^\top \mathbf{Z}$, where \mathbf{Z} is a d by d matrix whose elements are drawn from a standard normal distribution. The true model is $\beta^* \in \mathbb{R}^d$, where each coordinate of β^* is drawn independently from a standard normal distribution. The labels are generated as follows:

- For least-squares linear regression, the label for an example with feature vector \mathbf{a} is drawn from a normal distribution with mean $\mathbf{a}^\top \beta^*$ and standard deviation 0.1.
- For logistic regression, the label for an example with feature vector \mathbf{a} is drawn from a Bernoulli distribution with mean $\frac{1}{1 + \exp(-\mathbf{a}^\top \beta^*)}$.
- For linear regression with non-normal errors [61, 80], the label for an example with feature vector \mathbf{a} is drawn from a generalized symmetric normal distribution with parameters $\alpha = .1$ and $\beta = 4$.

For all three problems, the loss is the negative log-likelihood. We use $d = 100$ features and $n = 10000$ training examples.

For linear regression with non-normal errors, the loss is $f(\mathbf{x}) = \sum_{i=1}^n (\mathbf{A}_i^\top \mathbf{x} - \mathbf{b}_i)^\beta$, where \mathbf{A} is the feature matrix and \mathbf{b} is the label vector. Because we set $\beta = 4$, the loss grows as a quartic function of the estimation error (as in the one-dimensional example in §5.3.2).

It is worth noting that, for least squares linear regression, the quadratic upper bound that SafeRate uses to compute a safe learning rate is tight, and the SafeRate learning rate is therefore the rate that maximally reduces the loss on each step. Thus, applied to least squares linear regression, SafeRate[Adam] can be thought of as a variant of Adam that at each step moves as far as possible in the Adam direction, stopping at the point where further movement would increase the loss. In contrast, when applied to logistic regression or linear regression with non-normal errors, SafeRate will always choose a learning rate that reduces the loss, but this rate will be smaller than the one that reduces the loss maximally.

Figure 5.5 compares SafeRate[GD], SafeRate[AdaGrad], and SafeRate[Adam] to tuned versions of the baseline optimizers given in Table 5.1. As in our previous experiment, we show only the best-performing hyperparameter value for each baseline optimizer. The plots on the left use the number of steps as the horizontal axis, while the plots on the right use wall time.

Examining Figure 5.5, we note that:

- For all three problems, SafeRate[Adam] outperforms all other optimizers in terms of the loss reached after a given number of steps. For linear regression with non-normal errors, it is also better in terms of wall time, while for the other two problems it is slightly worse in terms of wall time.
- For the two linear regression problems, SafeRate[GD] outperforms the best fixed GD learning rate by a wide margin.
- SafeRate[AdaGrad] consistently outperforms all fixed AdaGrad learning rates early in optimization (see also Figure 5.6), but a well-tuned AdaGrad learning rate performs slightly better asymptotically. For linear regression, this implies that greedily choosing the learning rate that maximally reduces the loss (as SafeRate[AdaGrad] does) does not produce the best loss asymptotically (although it comes close).

For all three problems, SafeRate requires three matrix-vector products per step, whereas each step of GD, Adam, and AdaGrad requires only two. For this reason, we would expect SafeRate[Adam] to take about 1.5 times as long as Adam to complete a fixed number of steps. Empirically, however, it takes roughly twice as long, which may point to suboptimality of the generated computation graph for SafeRate (and an opportunity to improve the results).

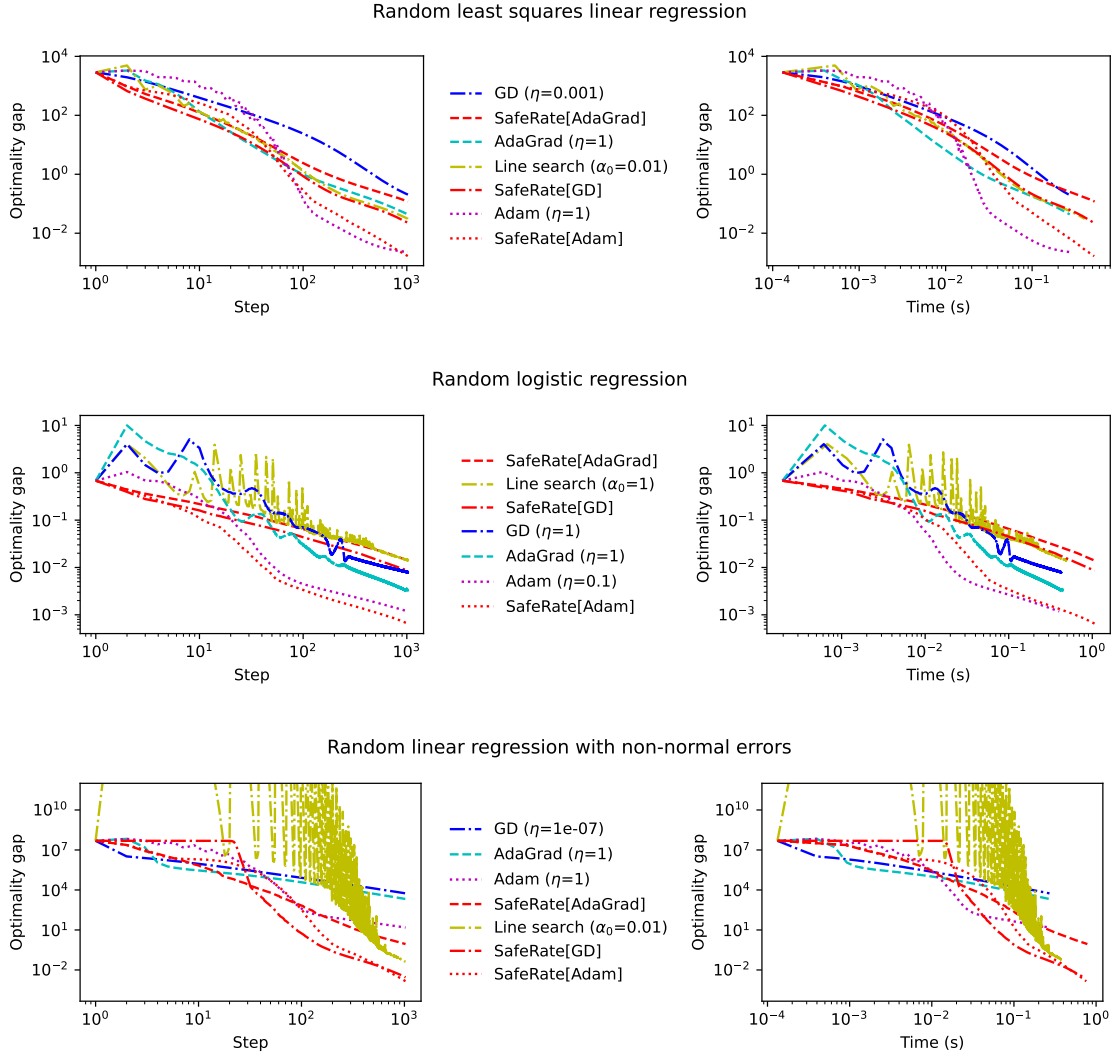


Figure 5.5: Comparison of optimizers on randomly-generated linear and logistic regression problems. Each plot shows the loss as a function of the number of iterations (left) or wall time (right), on a log scale. For optimizers other than SafeRate, the plot shows the best-performing hyperparameter from the grid defined in Table 5.1. Despite not requiring hyperparameter tuning, SafeRate typically performs about as well as the best learning rate in our grid, and sometimes outperforms it dramatically.

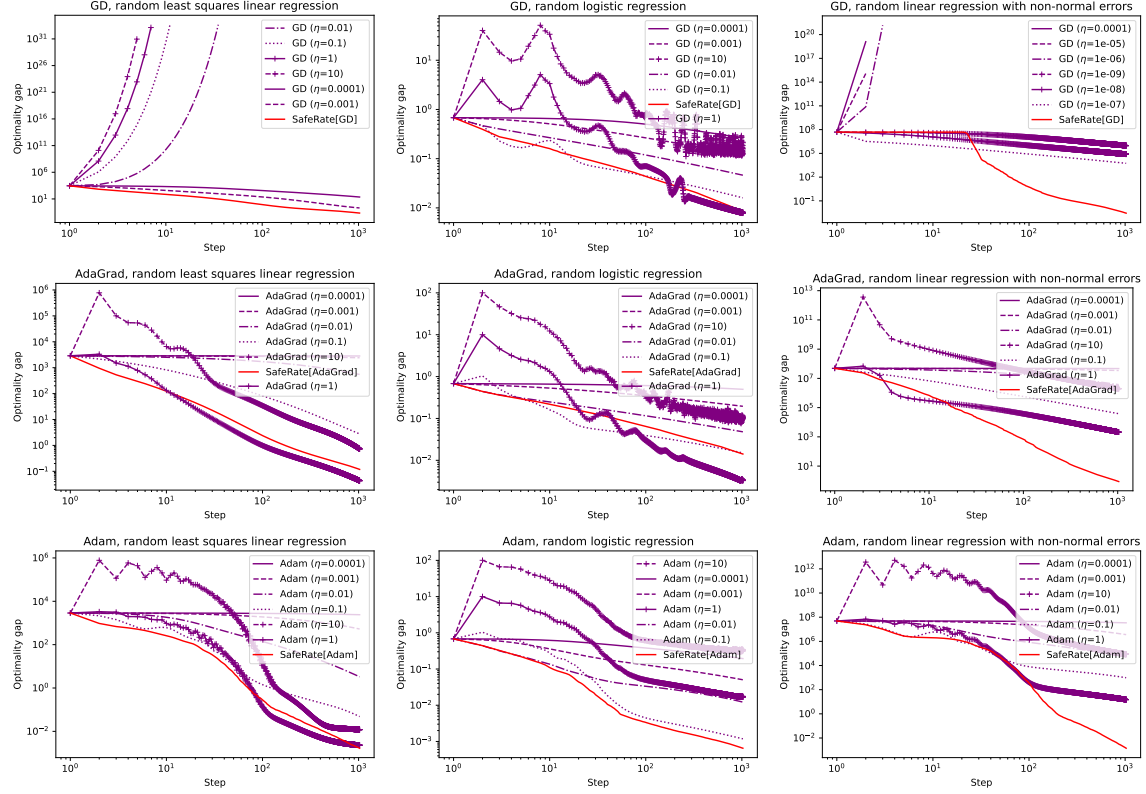


Figure 5.6: Comparison of SafeRate to optimizers with a learning rate hyperparameter, when used to solve randomly-generated linear and logistic regression problems. *On these problems, SafeRate takes roughly twice as much wall time per step as the other algorithms (see Figure 5.5).*

Figure 5.6 presents a more detailed view of these results. In this figure, there are separate plots for GD, AdaGrad, and Adam that include results for all learning rates in the grid, plus results for the corresponding SafeRate algorithm. Figure 5.6 makes it clear that, in addition to being competitive with the best learning rate in the grid, SafeRate dramatically outperforms suboptimal learning rates, some of which lead to divergence or very slow progress.

5.3.4 Multi-Layer Perceptrons

For our final set of experiments, we use SafeRate and SafeCombination to train deep networks to classify images.

Specifically, we train a fully connected network with one or two hidden layers to classify images from the MNIST dataset. We use 1000 hidden units, the softplus activation function, and the square loss. Following the recommendation of [35], we do *not* use a final softmax layer when computing the square loss. We train in the full-batch setting, using the first 1000 images as our training set. To work around numerical issues in the AutoBound algorithm, we use `float64` for the two-hidden-layer experiments with SafeRate and SafeCombination, and to keep the comparison fair we also use `float64` for the baseline optimizers.

As in our previous experiment, we evaluate SafeRate using three different choices of update direction, namely the directions given by GD, AdaGrad, and Adam (based on the observed sequence of gradients, as described in §5.3.1). Additionally, we evaluate SafeCombination[per-layer GD], SafeCombination[per-layer AdaGrad], and SafeCombination[per-layer Adam], which compute adaptive per-layer learning rates using the update directions given by GD, AdaGrad, and Adam, respectively.

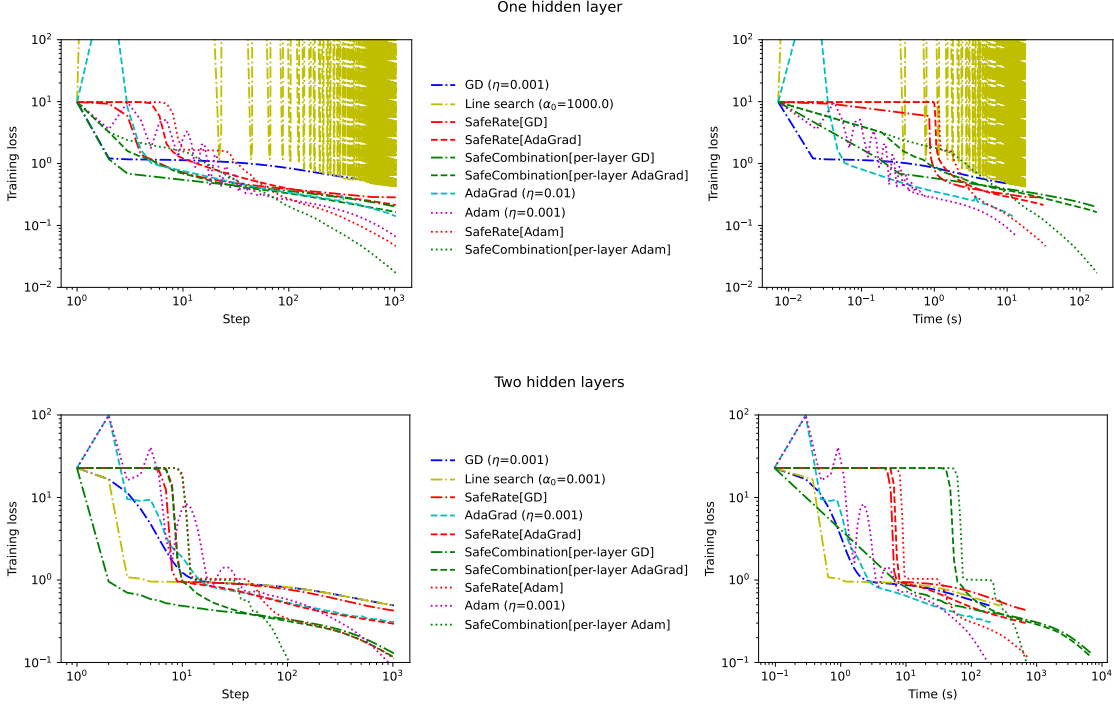


Figure 5.7: Comparison of optimizers, training a multi-layer perceptron on a subset of the MNIST dataset. Each plot shows the loss as a function of the number of iterations (left) or wall time (right), on a log scale. For optimizers other than SafeRate and SafeCombination, the plot shows the best-performing hyperparameter from the grid defined in Table 5.1.

Figure 5.7 shows the training loss reached by each optimizer as a function of the number of iterations, and as a function of wall time. We note that:

- For the one-hidden-layer problem, SafeRate[Adam] reaches lower training loss than all the baseline optimizers (after 1024 steps). However, it requires about 2.5x as much wall time per step as Adam, and thus is somewhat worse in terms of training loss vs. wall time.
- SafeCombination consistently makes more progress per step than SafeRate, at the cost of additional computation.
- Using our current implementation, SafeCombination is very slow, requiring roughly 13x as much wall time per step as Adam on the one-hidden-layer problem, and roughly 100x as much time per step on the two-hidden-layer problem.³ Thus, SafeCombination is not currently competitive with the baseline optimizers in terms of wall time. These wall time numbers should be taken with a grain of salt, however, as we suspect they could be significantly reduced by optimizing our implementation.⁴

Figure 5.8 presents a more detailed view of the same results, with separate plots for GD, Adam, and AdaGrad, showing the performance of various learning rates along with that of the corresponding SafeRate and SafeCombination algorithms. To reduce clutter, only learning rates between 10^{-4} and 0.1 are shown; learning rates outside this range performed poorly on both problems. For the one-hidden-layer network, SafeRate is generally able to offer performance comparable to the best learning rate in our grid on a per-step

³Applied to a neural network with H hidden layers, SafeCombination requires $O(d^3 H)$ time per step, where d is the number of update directions. For SafeCombination[per-layer-Adam], we have $d = H + 1$, and thus the time per step is $O(H^4)$.

⁴In particular, the wall time can likely be improved by taking advantage of the sparsity of the update directions.

basis. The results are best for gradient descent, where SafeRate[GD] takes an order of magnitude fewer steps to reach the loss that GD reaches after 1024 steps with a tuned learning rate.

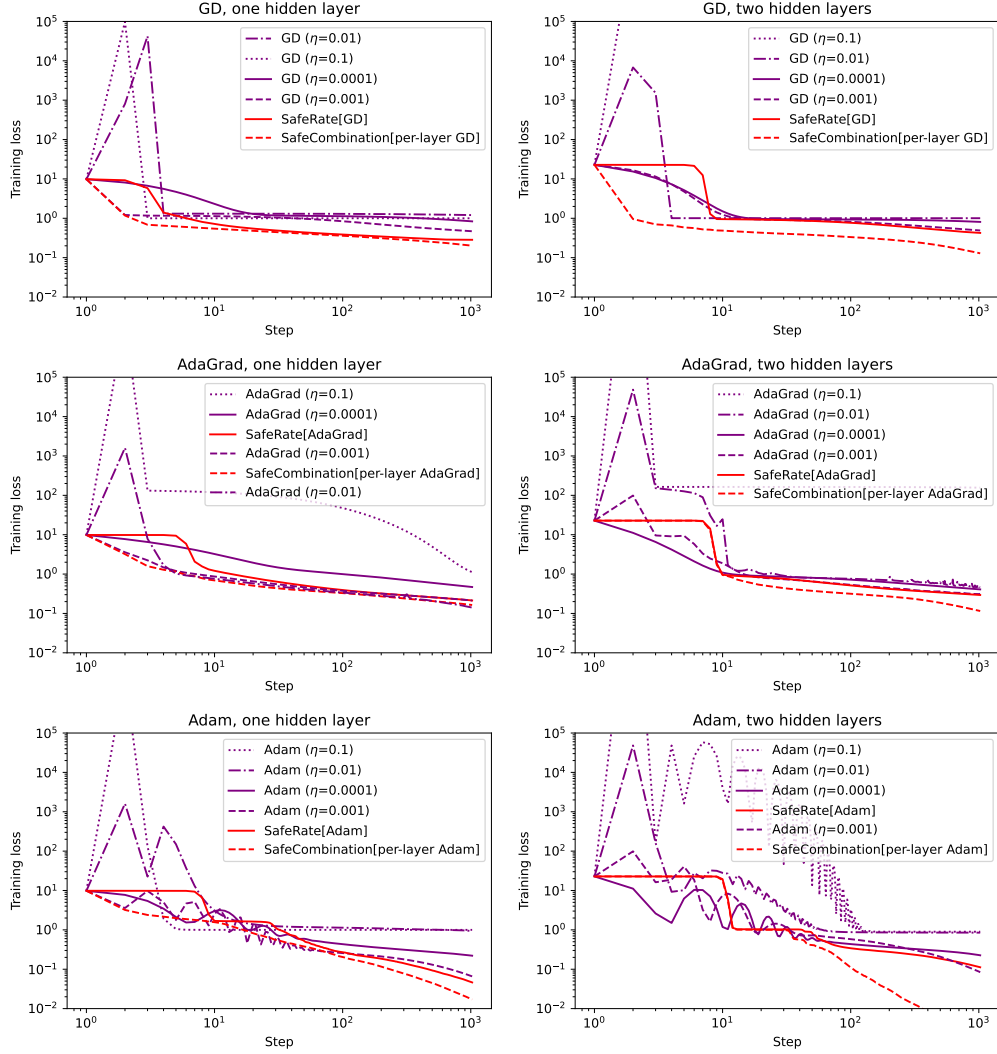


Figure 5.8: Comparison of SafeRate and SafeCombination to optimizers with a learning rate hyperparameter, when used to optimize a multi-layer perceptron on a subset of the MNIST dataset. SafeCombination makes more progress per step than SafeRate, but also requires significantly more computation per step. *Using our current implementation, SafeCombination[per-layer Adam] requires 13x more wall time per step than Adam for the one-hidden-layer problem, and 103x more wall time per step for the two-hidden-layer problem (see Figure 5.7).*

Remarkably, we will see in §5.3.5 that for these neural networks, the quadratic bounds used by SafeRate[GD] are nearly tight. Thus, on these problems, SafeRate[GD] greedily chooses a learning rate that is very close to the one that maximally reduces the loss on each step (similar to its behavior in the linear regression experiment).

Training an Overparameterized Neural Network in One Step

In §5.3.5, we will see that the quadratic bounds used by SafeRate[GD] are *empirically tight* for single-hidden-layer networks with squared error loss: the upper and lower bounds are nearly identical, with the actual loss sandwiched in between them. Though we have not yet analyzed this phenomenon formally, we would expect the bounds to be tight when the trust region is small enough that the activations are near-affine as a function of the learning rate, for all learning rates in the trust region. At the same time, theory suggests that gradient descent can train sufficiently wide neural networks without ever departing from a small region of parameter space where the activations are near-affine [51]. Taken together, these observations suggest that SafeRate may become very efficient as the width of the network increases.

As a partial confirmation of this conjecture, we now show that there exist (contrived) neural network optimization problems that require hundreds of steps to solve using the Adam optimizer, but that SafeCombination is able to solve after just *one step*. To show this, we consider the same setup as in the previous experiment, but with the size of the training set reduced from 1000 examples to just *one example*, and the number of hidden units increased from 1000 to 10^5 (and a single hidden layer). Figure 5.9 compares the performance of SafeRate and SafeCombination to various baseline optimizers, again considering the best hyperparameter value for each baseline optimizer.⁵

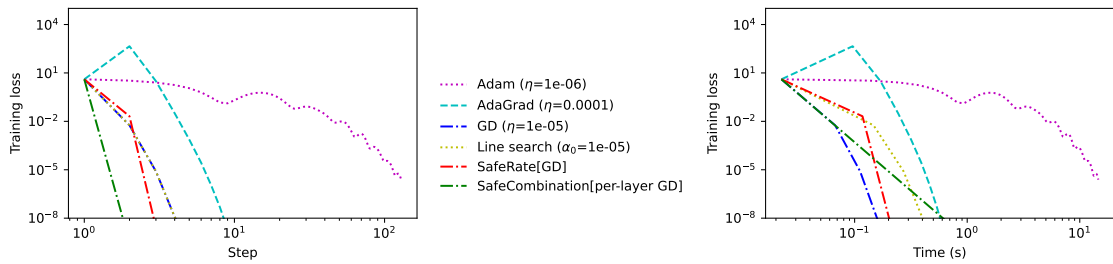


Figure 5.9: Comparison of optimizers on a highly overparameterized problem with only a single training example. SafeCombination is able to solve the problem in just one step, whereas Adam requires hundreds of steps, even using the best learning rate from a coarse grid.

We note that, with a single training example, the optimization problem becomes trivial, and one could imagine other methods that would reach a global minimum in one step. Nevertheless, the fact that our universal MM optimizers recover good performance in this extreme case is encouraging, and suggests theoretical analysis of their behavior in the infinite-width limit as an interesting area of future work.

5.3.5 Tightness of Automatically-Derived Majorizers

The effectiveness of any MM optimization algorithm depends on the tightness of the majorizers (i.e., how close the upper bound is to the actual loss). For least-squares linear regression, it can be shown that the upper bounds used by SafeRate are exact. For more complex losses, the tightness of the upper bounds must be measured empirically.

Figure 5.11 plot the majorizers used by the first iteration of SafeRate for the MNIST classification problem discussed in §5.3.4, for multi-layer perceptrons with 1, 4, 16, or 64 hidden layers. Each plot shows quadratic, cubic, and quartic majorizers.

With a single hidden layer (top plot), even the quadratic upper bounds are empirically tight. This is perhaps surprising considering that the loss itself is not quadratic, due to the softplus hidden layer. However, the function $h_t(\eta) = f(\mathbf{x}_t - \eta \nabla f(\mathbf{x}_t))$ is empirically very close to quadratic for relevant values of η (those that are small enough to reduce the loss).

⁵For this experiment, the baseline optimizers benefit from lower learning rates, so we used a larger grid than the one given in Table 5.1.

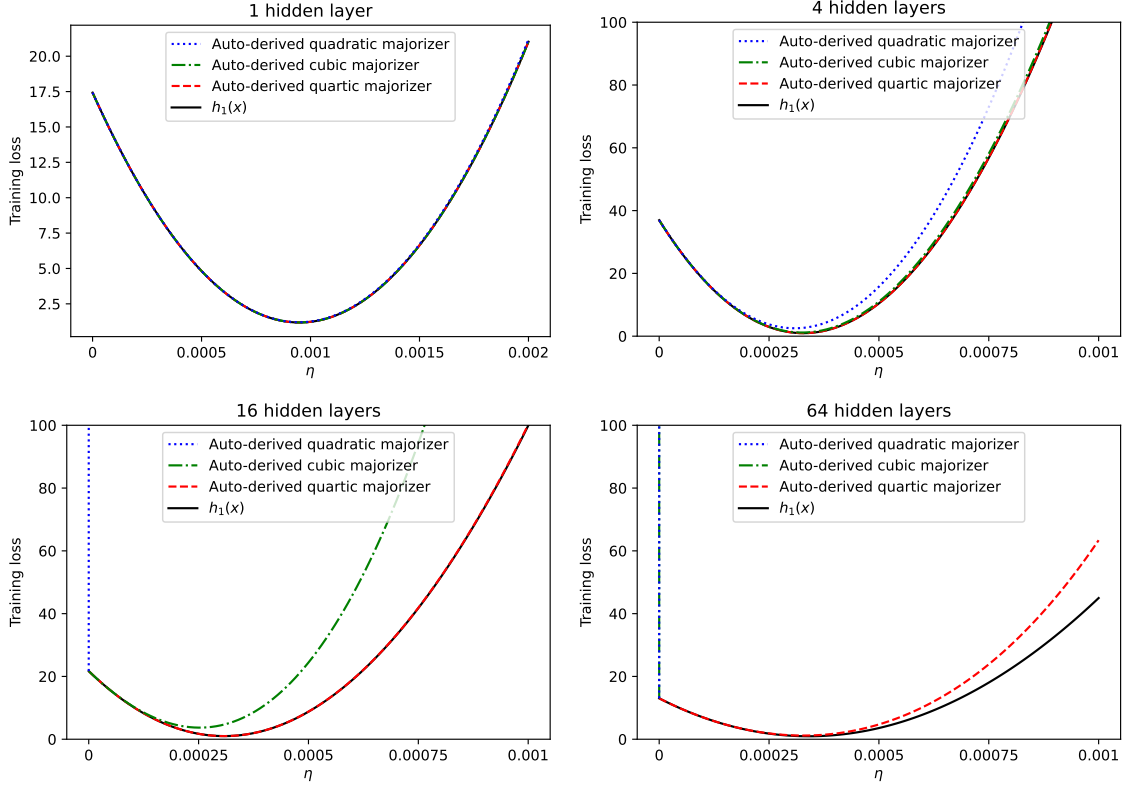


Figure 5.10: Automatically-derived majorizers for the function $h_1(\eta) = f(\mathbf{x}_1 - \eta \nabla f(\mathbf{x}_1))$, where f is the training loss for a multi-layer perceptron on a subset of the MNIST dataset.

As the number of hidden layers increases, the quadratic bounds become looser, but this can be compensated for by increasing the polynomial degree. Even with 64 hidden layers, the quartic polynomial majorizer is nearly tight. Thus, even for very deep networks, SafeRate is able to compute a learning rate that near-maximally reduces the loss, at the cost of only a single additional forward pass.

Figure 5.10 compares the quadratic majorizers derived by AutoBound to quadratic majorizers derived from a bound on the range of the second derivative. Recall from §2.2 that by bounding the range of the second derivative of a function over a given trust region, we can obtain quadratic bounds on the function which hold over the trust region, and recall that the range of the derivative can be bounded by evaluating the derivative using interval arithmetic. We consider a variant of this baseline method that handles bilinear operations efficiently using the tensor interval extension described in Theorem 8 (which AutoBound also uses).

With one hidden layer, both methods produce nearly tight majorizers. However, as the number of hidden layers increases, the majorizers produced by the baseline method quickly become much looser than those produced by AutoBound. With three hidden layers, the majorizer produced by the baseline method yields a learning rate that is over 11 times smaller than the one obtained using the majorizer produced by AutoBound. With four hidden layers, the learning rate produced by the baseline method is over 2500 times smaller than the one obtained using AutoBound.

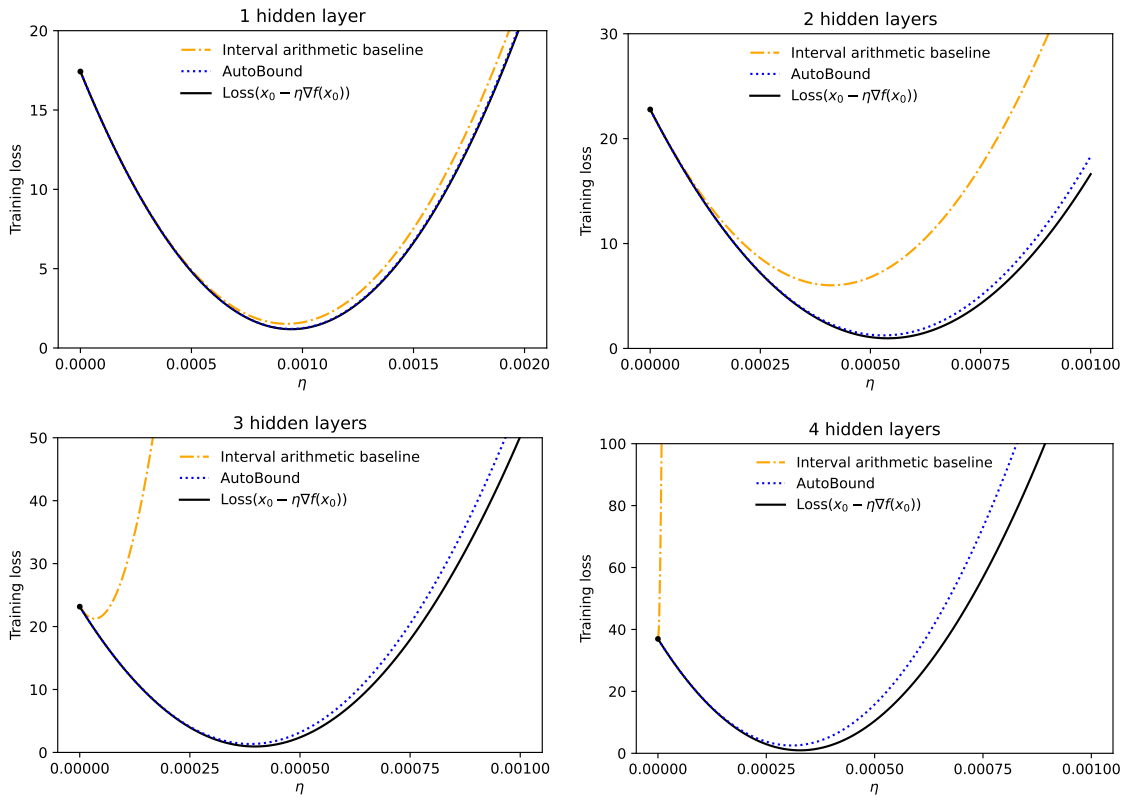


Figure 5.11: Comparison of quadratic majorizers derived by AutoBound to those derived using a baseline method based on range-bounding the second derivative. Each plot shows majorizers for the function $h_1(\eta) = f(\mathbf{x}_1 - \eta \nabla f(\mathbf{x}_1))$, where f is the training loss for a multi-layer perceptron on a subset of the MNIST dataset.

5.3.6 Summary

In this section, we evaluated SafeRate and SafeCombination on a variety of full-batch optimization problems. Some of our most significant observations are:

- Applied to random linear and logistic regression problems, SafeRate is able to boost the performance of gradient descent and Adam while simultaneously eliminating the need to tune a learning rate hyperparameter. For linear regression with non-normal errors, SafeRate can *dramatically* outperform tuned versions of the baseline optimizers.
- There exist optimization problems where SafeRate converges at a faster rate than gradient descent, Adam, or AdaGrad (in particular, applied to a one-dimensional quartic, SafeRate converges at a super-linear rate, whereas gradient descent, Adam, and AdaGrad appear to converge linearly). It would be very interesting to characterize the space of such problems theoretically.
- For multi-layer perceptrons with squared error loss, the bounds computed by SafeRate are *empirically tight* (for up to 64 hidden layers, when using quartic bounds), and thus SafeRate uses the learning rate that maximally reduces the loss at each step. As a result, SafeRate can boost the performance of gradient descent while eliminating the learning rate hyperparameter, as was the case with linear regression.

We also saw that SafeCombination can dramatically outperform SafeRate on a per-step basis, at the cost of significant additional computation per step. In the extreme case of a wide single-hidden-layer network and a single training example, SafeCombination was able to reach a global minimum in *one step*. Our evaluation of SafeCombination considered only a few possible choices for the matrix of update directions, and further exploration of this space remains a promising area of future work.

5.4 Related Work

At a high level, this chapter considers the problem of minimizing a scalar-valued function $f : \mathbb{R}^n \rightarrow \mathbb{R}$, where the function f is available in symbolic form, and is composed of sub-differentiable atomic functions. This problem has been studied in the applied mathematics community for at least 80 years and is the subject of a vast literature; see the textbook by Nocedal and Wright [67] for an introduction.

Most relevant to our work is the literature on majorization-minimization (MM) optimizers, which iteratively reduce the loss by minimizing a locally-tight upper bound (called a majorizer). MM is itself the subject of a large literature; see [38] for a tutorial, and see the textbooks by Lange [50] and de Leeuw [16] for a through introduction. Majorizers have been derived by hand for many specific problems of interest, including logistic regression [8], quantile regression [37], multidimensional scaling [15, 18, 29] generalized Bradley-Terry models [36], and support vector machines [30].

However, there seems to be almost no work on deriving the majorizer automatically via symbolic computation, as we have done. The closest thing we are aware of is [76], which derives a quadratic majorizer using a recursive procedure that can be applied to neural networks of any depth. However, the approach taken by [76] differs from ours in several critical ways:

1. The algorithm of [76] seeks a quadratic majorizer that is valid everywhere (not just over a specified trust region), and hence is not applicable to losses such as $f(x) = (x - 3)^4$, which grow faster than any quadratic. As a consequence, the algorithm of [76] can only derive a quadratic majorizer for a neural network loss when the weights in all but one layer are held constant.
2. The algorithm of [76] propagates bounds from the output of the network toward the input, analogous to reverse-mode automatic differentiation. Such an algorithm has the virtue of efficiently computing majorizers that depend on a large number of input variables. In contrast, AutoBound uses memory linear in the number of input variables, making it only practical for majorizers that are a function

of some lower-dimensional quantity such as the learning rate. However, the efficiency of the reverse-mode algorithm comes at a price, as the backward propagation of quadratic bounds requires the use of inequalities that can become very loose as the network grows wide.

3. As presented, the algorithm of [76] is specific to training a neural network with squared error loss and hyperbolic tangent activation functions, although we believe it could be generalized to other activation functions.

As mentioned in §4.4, we plan to develop a reverse-mode variant of AutoBound in the future, which could be used to derive majorizers that are more directly comparable to the ones derived by [76].

5.5 Future Work

In this chapter, we have presented universal MM optimization algorithms built on top of AutoBound. Though we believe our experiments have shown that these algorithms exhibit qualitatively new (and desirable) behavior, we have not done all we can to turn them into practical general-purpose optimizers.

Promising areas of future work include:

- *Mini-batch optimization.* Both the theory and experiments in this chapter have been limited to full-batch optimization. However, the MM paradigm can be extended to mini-batch optimization (e.g., [54]). A universal mini-batch MM optimization algorithm may outperform Adam and AdaGrad on certain large-scale machine learning problems.
- *Higher-order majorizers.* Our experiments with SafeRate considered only quadratic majorizers. Though preliminary experiments showed that higher-order majorizers (such as cubic or quartic majorizers) are not beneficial for the shallow neural networks considered in our experiments, they may be beneficial for deeper networks.
- *Approximate majorizers.* Currently, both SafeRate and SafeCombination require more wall time per step than Adam or AdaGrad. However, the wall time can be made comparable to Adam or AdaGrad by computing the majorizer approximately, using a random subset of the training data. Preliminary experiments show that this can yield better tradeoffs between loss and wall time early in optimization, but some care is required to ensure convergence to the same loss asymptotically.

Additionally, the universal MM optimization algorithms presented in this chapter have been limited to majorizing the loss as a function of a small number of learning rates. This was necessary because AutoBound, like forward-mode automatic differentiation, requires memory linear in the number of inputs. However, as discussed in §4.4, we plan to develop a reverse-mode variant of AutoBound that would allow us to efficiently compute quadratic majorizers for a function $f : \mathbb{R}^n \rightarrow \mathbb{R}$ as a function of the n -dimensional input. This would allow us to define universal MM optimization algorithms that determine the update direction on their own, rather than taking it as a given (as SafeRate does).

Chapter 6

Additional Applications

In this chapter, we outline three additional applications of the AutoBound algorithm: verified global optimization, verified numerical integration, and automatically deriving sharper versions of Jensen’s inequality.

6.1 Verified Global Optimization

Global optimization is the subject of a vast literature. A large subset of this literature assumes the loss function being minimized is deterministic and available in symbolic form (as opposed to being accessible only via queries, for example if the loss is the result of a physical experiment).

Verified global optimization (e.g., [5, 11, 31, 32, 39, 45, 59, 72]) seeks to find a *provable* global minimum of an arbitrary (possibly non-convex) loss, provided in symbolic form. This goal differs from that of MM optimization (discussed in Chapter 5), which only seeks to converge to a local minimum.

Verified global optimization algorithms are typically instances of *branch and bound*, a procedure that finds a global minimum by iteratively partitioning the parameter space into disjoint subsets, and proving lower bounds on the minimum value of the loss within each subset. A global lower bound can be obtained by taking the minimum lower bound across all subsets in the partition. As the partition is refined to contain smaller and smaller subsets, the difference between the best known upper bound on the minimum loss (obtained by evaluating the loss at some point) and the global lower bound can be made arbitrarily small, allowing the algorithm to guarantee that it has found a point whose loss is within ϵ of the global minimum, for arbitrarily small $\epsilon > 0$.

Bounds on the Taylor remainder series of the form given by *Taylor models* have previously been used for verified global optimization [59]. The Taylor remainder series bounds provided in this work have the potential to improve these results by providing both tighter upper bounds and tighter lower bounds.

To explain how, suppose we wish to globally minimize a function $f : \mathbb{R}^n \rightarrow \mathbb{R}$. As discussed in Chapter 5, for any point \mathbf{x}_t in parameter space, and any trust region (specified by a tensor interval), we can compute an upper bound $\bar{f}(\mathbf{x}, \mathbf{x}_t)$ that is tight at \mathbf{x}_t and valid over the trust region. We can similarly derive a function $\underline{f}(\mathbf{x}_t, \mathbf{x})$ that lower bounds f , where the bound is tight at \mathbf{x}_t . The minimum values of \bar{f} and \underline{f} over the trust region, which can be computed in closed form in the case where they are quadratic, can then be used as the basis of a branch-and-bound algorithm. These bounds can be tighter than the ones that would be obtained using Taylor models, and hence can let us find an approximate global minimum more efficiently.

6.1.1 Experiment

Figure 6.1 depicts the results of globally minimizing the non-convex function $f(x) = 2(x - 1)^2 + (x - 1)^3$ over the interval $[-2, 2]$, using a branch and bound algorithm based on quadratic upper and lower bounds returned by AutoBound. The plot on the left shows the loss function, as well as the points at which f was evaluated by the branch and bound algorithm during the search. The plot on the right shows the upper and

lower bounds on the global minimum as a function of the number of steps (each step involves computing upper and lower bounds that are valid over some trust region that is a subset of $[-2, 2]$). After 17 steps, the algorithm is able to find the global minimum (which in this case is simply the left end point of the interval, -2) up to machine precision.

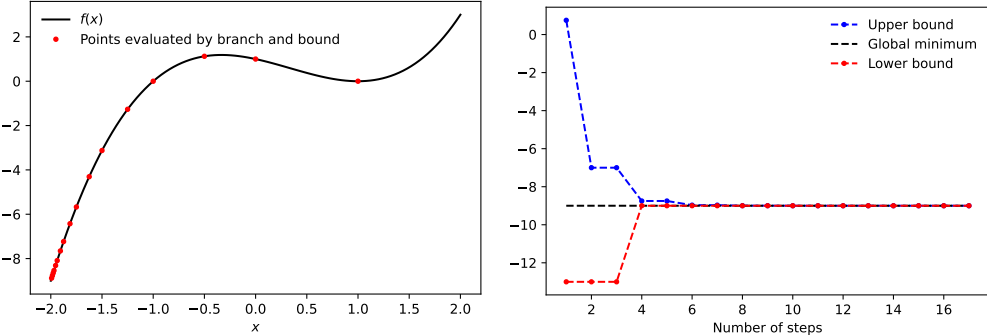


Figure 6.1: Globally minimizing the non-convex function $f(x) = 2(x-1)^2 + (x-1)^3$, using a branch and bound algorithm based on quadratic upper and lower bounds computed by AutoBound. The left plot shows the points evaluated on each step, and the right plot shows the upper and lower bounds on the minimum loss as a function of the number of steps.

6.2 Verified Numerical Integration

We now consider the problem of verified numerical integration (e.g., [6, 12, 23, 34, 46, 49, 69]). In this problem, we wish to compute upper and lower bounds on an integral,

$$\int_{\mathcal{X}} f(x) dx \quad (6.1)$$

where \mathcal{X} is typically some set over which polynomials can be integrated in closed form, such as a hyperrectangle. As was the case with verified global optimization, verified numerical integration is a problem to which Taylor models have been successfully applied [6], and which can potentially be solved more effectively using the bounds computed by AutoBound.

Using the AutoBound algorithm, we can obtain polynomial upper and lower bounds on f , which we can then integrate over \mathcal{X} in order to obtain upper and lower bounds on the integral. These upper and lower bounds may be loose, but can be made tighter by partitioning \mathcal{X} into disjoint subsets, applying the same method to each subset, and summing the upper and lower bounds over all subsets. The partitioning of \mathcal{X} into subsets can be done adaptively, by greedily subdividing the subsets where the difference between the upper and lower bounds is largest.

6.2.1 Algorithm Description

To illustrate this idea, suppose we wish to compute $\int_{x=a}^b f(x) dx$, for some function $f : \mathbb{R} \rightarrow \mathbb{R}$ provided in symbolic form. Given a point $x_0 \in [a, b]$, we can obtain upper and lower bounds on the integral as follows. First, we use AutoBound to compute an interval I such that

$$f(x) \in T_{k-1}(x; f, x_0) + I(x - x_0)^k \quad (6.2)$$

where $T_{k-1}(\cdot; f, x_0)$ is the degree $k-1$ Taylor polynomial of f at x_0 (see §2.1). We then have

$$\int_{x=a}^b f(x)dx \in \int_{x=a}^b T_{k-1}(x; f, x_0) + I(x - x_0)^k dx. \quad (6.3)$$

The integral on the right hand side can be computed in closed form, yielding an interval whose end points provide lower and upper bounds on $\int_{x=a}^b f(x)dx$.

To obtain tighter upper and lower bounds, we may partition the interval $[a, b]$ into intervals $[x_i, x_{i+1}]$ for $i = 1, 2, \dots, n$, and for each interval $[x_i, x_{i+1}]$, use AutoBound to compute an interval I_i such that $f(x) \in T_{k-1}(x; f, \bar{x}_i) + I_i(x - x_0)^k$ for $x \in [x_i, x_{i+1}]$, where $\bar{x}_i \triangleq \frac{x_i + x_{i+1}}{2}$ denotes the midpoint of the i th interval. We then have

$$\int_{x=a}^b f(x)dx = \sum_{i=1}^n \int_{x=x_i}^{x_{i+1}} f(x)dx \in \sum_{i=1}^n \int_{x=x_i}^{x_{i+1}} T_{k-1}(x; f, \bar{x}_i) + I_i(x - \bar{x}_i)^k dx. \quad (6.4)$$

This approach generalizes the approach of bounding the integral in each cell using interval arithmetic (e.g., see Chapter 9 of [62]), which can be recovered by computing Taylor enclosures of degree 0. The approach can be easily generalized to integration over higher-dimensional sets.

There are many ways we might partition the interval into subintervals. A natural approach is to adaptively subdivide the intervals where the gap between the upper and lower bounds on the integral is largest. We leave investigation of such strategies to future work, adopting a simple non-adaptive strategy in the experiments that follow.

6.2.2 Experiment

Figure 6.2 summarizes the performance of the algorithm just described, when used to bound the value of $\int_{x=0}^1 \exp(x)dx$, by partitioning the interval $[0, 1]$ into a uniform grid of n cells. In this simple case, the exact value of the integral can be computed in closed form, and is $e - 1$. The figure plots the width of the computed interval (whose end points are the upper and lower bounds on the integral) as a function of n , as well as the distance from the midpoint of the interval to the exact value (which is $e - 1$). Note that the latter quantity is orders of magnitude smaller than the former – in this case, the midpoint of the lower and upper bounds provides an estimate of the integral that is much more accurate than the worst-case approximation error bound given by the interval width.

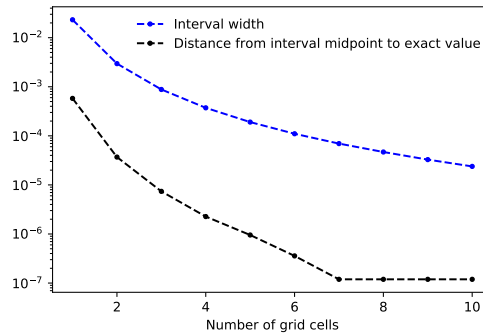


Figure 6.2: Width of an interval that encloses the integral $\int_{x=0}^1 \exp(x)dx$, computed via equation (6.4) using AutoBound, as a function of the number of grid cells n into which the interval $[0, 1]$ is divided.

As mentioned previously, these results can likely be improved by using an adaptively-refined grid instead of a uniform grid.

6.3 Automatically Sharpening Jensen's Inequality

Jensen's inequality is among the most widely used inequalities in applied mathematics. Among other things, it is used to show non-negativity of the Kullback-Liebler divergence in information theory [13], and in the derivation of MM optimization algorithms for various functions [50].

Applied to a one-dimensional convex function $\varphi : \mathbb{R} \rightarrow \mathbb{R}$, Jensen's inequality states that for any scalar random variable X ,

$$\mathbb{E}[\varphi(X)] - \varphi(\mathbb{E}[X]) \geq 0. \quad (6.5)$$

The left hand side of (6.5) is called the *Jensen gap*. Jensen's inequality says that if φ is convex, the Jensen gap belongs to the interval $[0, \infty]$. If all we know is that φ is convex, it can be shown that this interval cannot be tightened. However, a series of recent works [25, 52, 53, 75, 77] have shown that by exploiting additional knowledge about φ , one can compute tighter bounds on the Jensen gap.

Most relevant to our work, [52, 53] showed that tighter bounds on the Jensen gap can be obtained by computing a Taylor enclosure of φ (though neither work uses this terminology). Liao and Berg [53] showed how to take advantage of quadratic Taylor enclosures, and Lee *et al.* [52] extended their result to Taylor enclosures of arbitrary even degree. We further extend this result to Taylor enclosures of arbitrary degree (odd or even), to obtain the following theorem.

Theorem 12 (Extending Theorem 2.1 of [52]). *Let $\varphi : \mathbb{R} \rightarrow \mathbb{R}$ be a $(k-1)$ -times differentiable function, and let X be a scalar random variable that lies in the interval $[a, b]$ with probability 1. Let the interval $I \in \mathbb{IR}$ define a degree k Taylor enclosure of φ , centered at $\mu \triangleq \mathbb{E}[X]$, and valid over $[a, b]$, so that we have*

$$\varphi(x) \in \left(\sum_{i=0}^{k-1} \frac{1}{i!} \varphi^{(i)}(\mu) (x - \mu)^i \right) + I \cdot (x - \mu)^k \quad \forall x \in [a, b].$$

Then,

$$\mathbb{E}[\varphi(X)] \in \varphi(\mu) + \left(\sum_{i=2}^{k-1} \frac{1}{i!} \varphi^{(i)}(\mu) \mathbb{E}[(X - \mu)^i] \right) + I \cdot \mathbb{E}[\min \{0, (X - \mu)^k\}] + I \cdot \mathbb{E}[\max \{0, (X - \mu)^k\}].$$

If k is even,¹ this simplifies to:

$$\mathbb{E}[\varphi(X)] \in \varphi(\mu) + \left(\sum_{i=2}^{k-1} \frac{1}{i!} \varphi^{(i)}(\mu) \mathbb{E}[(X - \mu)^i] \right) + I \cdot \mathbb{E}[(X - \mu)^k].$$

In the special case $k = 2$, Theorem 12 says that if I defines a quadratic Taylor enclosure of φ at $\mathbb{E}[X]$ over $[a, b]$, then

$$\mathbb{E}[\varphi(X)] - \varphi(\mathbb{E}[X]) \in I \cdot \text{Var}[X]. \quad (6.6)$$

If φ is convex, we can set $I = 0$ to recover Jensen's inequality. If $I > 0$, we obtain an inequality that is tighter than Jensen's. Furthermore, if φ is an analytic function over $[a, b]$, and if $\mathbb{E}[(X - \mu)^k]$ is finite for all k , then Theorem 12 gives upper and lower bounds on the Jensen gap that become arbitrarily tight as $k \rightarrow \infty$ [52].

One limitation of previous work is that it did not have a general-purpose mechanism for computing an interval I that defines a Taylor enclosure suitable for use in Theorem 12, limiting the applicability of the theorem to cases where φ can be analyzed by hand. Our work provides such a mechanism, thus greatly extending the reach of Theorem 12.

¹Note that the same simplification is not possible if k is odd. For example, if $k = 1$, X is uniform over $[-2, 2]$, and $I = [-1, 1]$, then $I \cdot \mathbb{E}[\min \{0, (X - \mu)^k\}] + I \cdot \mathbb{E}[\max \{0, (X - \mu)^k\}] = [-1, 1] \cdot -\frac{1}{2} + [-1, 1] \cdot \frac{1}{2} = [-1, 1]$, whereas $I \cdot \mathbb{E}[(X - \mu)^k] = [-1, 1] \cdot 0 = 0$.

6.3.1 Experiment

As an example, we now compute upper and lower bounds on the Jensen gap for the function $\varphi(x) = \exp(x)$, for X drawn from a uniform distribution over $[-1, 1]$. In this simple example, the Jensen gap can be computed exactly in closed form, and is

$$\mathbb{E}[\varphi(X)] - \varphi(\mathbb{E}[X]) = \frac{e - e^{-1}}{2} - 1 \approx 0.175201. \quad (6.7)$$

Figure 6.3 plots the upper and lower bounds on the Jensen gap that we obtain using Theorem 12, computing the interval I using AutoBound, as a function of the degree of the Taylor enclosure (i.e., the value of $k + 1$ in the theorem statement). As can be seen in the figure, the upper and lower bounds rapidly converge to the true value, with the gap between the upper and lower bounds decreasing exponentially as a function of degree. Note that even the degree 2 Taylor enclosure gives a much sharper bound than Jensen's inequality, which shows only that the Jensen gap is in $[0, \infty]$.

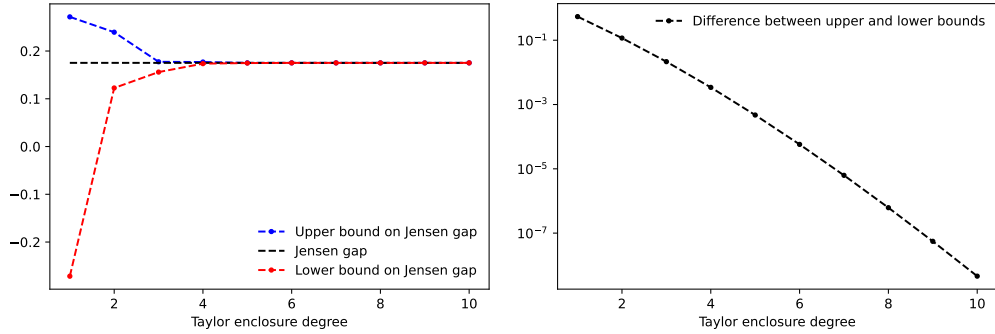


Figure 6.3: Upper and lower bounds on the Jensen gap, $\mathbb{E}[\varphi(X)] - \varphi(\mathbb{E}[X])$, for $\varphi(x) = \exp(x)$ and $X \sim \text{Uniform}(-1, 1)$, as a function of the degree of the Taylor enclosure used to compute the bound. The left plot shows the upper and lower bounds, and the right plot shows the difference between them. For degree 2 or larger, each bound provides a sharper version of Jensen's inequality, which only guarantees that the Jensen gap lies in the interval $[0, \infty]$.

Chapter 7

Summary and Conclusions

In this work, we have presented a generalization of Taylor-mode automatic differentiation that, in addition to computing a Taylor polynomial approximation of a function, computes polynomial upper and lower bounds that are guaranteed to hold over a user-specified *trust region*.

To develop our algorithm, we began by deriving *sharp* Taylor enclosures for functions whose derivatives are monotonically increasing or decreasing (such as \exp or \log), and for functions with an even-symmetric Hessian (such as ReLU, Softplus, and other neural network activation functions). These results generalized earlier work on sharp quadratic majorizers for one-dimensional functions [17] in three ways: by considering a wider variety of functions, by deriving polynomial bounds of arbitrary degree, and by taking into account a trust region (which tightens the bounds). This theory, developed in Chapter 2, also yields a large number of mathematical inequalities of the type that are often derived by hand for use in proofs. For example, for $x \in [-1, 1]$, it implies $1 + x + \frac{1}{2}x^2 \leq \exp(1 + x) \leq 1 + x + \frac{e^2 - 3}{4}x^2$.

In Chapter 3, we considered the problem of deriving a Taylor enclosure of an arbitrary function composed of known atomic functions. To this end, we developed an interval arithmetic variant of Taylor mode automatic differentiation which we call AutoBound. AutoBound is similar in spirit to the algorithm used in previous work to compute *Taylor models* [55, 56, 57, 58], but produces bounds of a different functional form that allows for additional applications, and contains several technical innovations that make the bounds tighter.

In Chapter 4, we extended the results of Chapter 3 to tensor-valued and tensor-variate functions. This required us to introduce additional notation, and to pay special attention to handling bilinear operations in a way that allows our algorithm to be implemented efficiently using modern automatic differentiation frameworks (such as TensorFlow, PyTorch, or JAX). In the process of doing so, we generalized previous results for Interval Bound Propagation [27], and developed an alternative that produces tighter bounds at the cost of additional computation.

We then turned our attention to applications of AutoBound. Most notably, in Chapter 5 we showed that the bounds computed by AutoBound can be used to create *universal* majorization-minimization (MM) optimization algorithms. MM optimization algorithms are very appealing because, unlike gradient descent and variants thereof, they *never diverge* and *do not require hyperparameter tuning*. However, the reach of MM has until now been limited to specific losses for which majorizers have been derived by hand (e.g., [8, 15, 18, 29, 30, 36, 37]). By instead deriving the majorizer *automatically* from the symbolic expression for the loss, we have vastly enlarged the set of problems to which the MM paradigm can be applied.

Empirically, our universal MM optimization algorithms were shown to exhibit a number of desirable properties. For certain problems, such as training a wide and shallow neural network on a training set with just one example, the algorithms jump to the global optimum in one step. For other problems, such as linear regression with non-normal errors, they converge at a faster rate than AdaGrad or Adam. When used to train a single hidden layer perceptron on a subset of the MNIST dataset, our algorithms make more progress per step than tuned versions of Adam and AdaGrad, despite not requiring hyperparameter tuning.

Finally, in Chapter 6 we showed, via simple demonstrations on toy problems, that AutoBound can be used for verified global optimization, verified numerical integration, and deriving sharper versions of Jensen's

inequality.

Our work suggests many possible extensions, some of which we have discussed in our chapter-specific future work sections (§2.7, §4.4 and §5.5). Perhaps the most important of these is the development of a reverse-mode algorithm (discussed in §4.4), which would allow us to efficiently compute Taylor enclosures for functions of a large number of scalar variables. In addition, we believe there are many applications of Taylor enclosures which remain to be explored.

Bibliography

- [1] Martín Abadi, Paul Barham, Jianmin Chen, Zhifeng Chen, Andy Davis, Jeffrey Dean, Matthieu Devin, Sanjay Ghemawat, Geoffrey Irving, Michael Isard, et al. TensorFlow: a system for large-scale machine learning. In *Proceedings of OSDI '16: 12th USENIX Symposium on Operating Systems Design and Implementation*, pages 265–283, 2016.
- [2] Josh Alman and Virginia Vassilevska Williams. A refined laser method and faster matrix multiplication. In *Proceedings of the 2021 ACM-SIAM Symposium on Discrete Algorithms (SODA)*, pages 522–539. SIAM, 2021.
- [3] Tom M Apostol. *Calculus, Volume 1*. John Wiley & Sons, 1991.
- [4] Larry Armijo. Minimization of functions having Lipschitz continuous first partial derivatives. *Pacific Journal of Mathematics*, 16(1):1–3, 1966.
- [5] S Berner. New results on verified global optimization. *Computing*, 57(4):323–343, 1996.
- [6] Martin Berz and Kyoko Makino. New methods for high-dimensional verified quadrature. *Reliable Computing*, 5(1):13–22, 1999.
- [7] Jesse Bettencourt, Matthew J Johnson, and David Duvenaud. Taylor-mode automatic differentiation for higher-order derivatives in JAX. 2019. URL <https://openreview.net/pdf?id=SkxEF3FNPH>.
- [8] Dankmar Böhning and Bruce G Lindsay. Monotonicity of quadratic-approximation algorithms. *Annals of the Institute of Statistical Mathematics*, 40(4):641–663, 1988.
- [9] James Bradbury, Roy Frostig, Peter Hawkins, Matthew James Johnson, Chris Leary, Dougal Maclaurin, George Necula, Adam Paszke, Jake VanderPlas, Skye Wanderman-Milne, and Qiao Zhang. JAX: composable transformations of Python+NumPy programs, 2018. URL <http://github.com/google/jax>.
- [10] Ryan P Browne and Paul D McNicholas. Multivariate sharp quadratic bounds via σ -strong convexity and the Fenchel connection. *Electronic Journal of Statistics*, 9(2):1913–1938, 2015.
- [11] Ole Caprani, Brian Godthaab, and Kaj Madsen. Use of a real-valued local minimum in parallel interval global optimization. *Interval Computations*, 2:71–82, 1993.
- [12] George F Corliss and Louis B Rall. Adaptive, self-validating numerical quadrature. *SIAM Journal on Scientific and Statistical Computing*, 8(5):831–847, 1987.
- [13] Thomas M Cover. *Elements of Information Theory*. John Wiley & Sons, 1999.
- [14] Etienne De Klerk. The complexity of optimizing over a simplex, hypercube or sphere: a short survey. *Central European Journal of Operations Research*, 16(2):111–125, 2008.
- [15] Jan De Leeuw. Convergence of the majorization method for multidimensional scaling. *Journal of Classification*, 5(2):163–180, 1988.

[16] Jan de Leeuw. *Block Relaxation Methods in Statistics*. 2016. URL <https://bookdown.org/jandeleeuw6/bras/>.

[17] Jan de Leeuw and Kenneth Lange. Sharp quadratic majorization in one dimension. *Computational Statistics & Data Analysis*, 53(7):2471–2484, 2009.

[18] Jan De Leeuw and Patrick Mair. Multidimensional scaling using majorization: SMACOF in R. *Journal of Statistical Software*, 31:1–30, 2009.

[19] John Duchi, Elad Hazan, and Yoram Singer. Adaptive subgradient methods for online learning and stochastic optimization. *Journal of Machine Learning Research*, 12(7), 2011.

[20] Jan Andrzej Duracz and Michał Konecný. Polynomial function enclosures and floating point software verification. *Proceedings of CFV*, pages 56–67, 2008.

[21] Jean-Pierre Eckmann and Peter Wittwer. A complete proof of the Feigenbaum conjectures. *Journal of Statistical Physics*, 46(3):455–475, 1987.

[22] Jean Pierre Eckmann, Hans Koch, and Peter Wittwer. *A computer-assisted proof of universality for area-preserving maps*. American Mathematical Society, 1984.

[23] Martin C Eiermann. Automatic, guaranteed integration of analytic functions. *BIT Numerical Mathematics*, 29(2):270–282, 1989.

[24] Stefan Elfwing, Eiji Uchibe, and Kenji Doya. Sigmoid-weighted linear units for neural network function approximation in reinforcement learning. *Neural Networks*, 107:3–11, 2018.

[25] Xiang Gao, Meera Sitharam, and Adrian E Roitberg. Bounds on the Jensen gap, and implications for mean-concentrated distributions. *arXiv preprint arXiv:1712.05267*, 2017.

[26] Saeed Ghadimi and Guanghui Lan. Stochastic first-and zeroth-order methods for nonconvex stochastic programming. *SIAM Journal on Optimization*, 23(4):2341–2368, 2013.

[27] Sven Gowal, Krishnamurthy Dvijotham, Robert Stanforth, Rudy Bunel, Chongli Qin, Jonathan Uesato, Relja Arandjelovic, Timothy Mann, and Pushmeet Kohli. On the effectiveness of interval bound propagation for training verifiably robust models. In *International Conference on Computer Vision*, 2018.

[28] Andreas Griewank and Andrea Walther. *Evaluating Derivatives: Principles and Techniques of Algorithmic Differentiation*. SIAM, 2008.

[29] Patrick JF Groenen, Rudolf Mathar, and Willem J Heiser. The majorization approach to multidimensional scaling for Minkowski distances. *Journal of Classification*, 12(1):3–19, 1995.

[30] Patrick JF Groenen, Georgi Nalbantov, and Jan C Bioch. SVM-Maj: a majorization approach to linear support vector machines with different hinge errors. *Advances in Data Analysis and Classification*, 2(1):17–43, 2008.

[31] Eldon Hansen and G William Walster. *Global Optimization Using Interval Analysis: Revised and Expanded*, volume 264. CRC Press, 2003.

[32] Eldon R Hansen. Global optimization using interval analysis: the one-dimensional case. *Journal of Optimization Theory and Applications*, 29(3):331–344, 1979.

[33] Dan Hendrycks and Kevin Gimpel. Gaussian error linear units (GELUs). *arXiv preprint arXiv:1606.08415*, 2016.

[34] Oliver Holzmann, Bruno Lang, and Holger Schütt. Newton’s constant of gravitation and verified numerical quadrature. *Reliable Computing*, 2(3):229–239, 1996.

[35] Like Hui and Mikhail Belkin. Evaluation of neural architectures trained with square loss vs cross-entropy in classification tasks. In *International Conference on Learning Representations*, 2021.

[36] David R Hunter. MM algorithms for generalized Bradley-Terry models. *The Annals of Statistics*, 32(1):384–406, 2004.

[37] David R Hunter and Kenneth Lange. Quantile regression via an MM algorithm. *Journal of Computational and Graphical Statistics*, 9(1):60–77, 2000.

[38] David R Hunter and Kenneth Lange. A tutorial on MM algorithms. *The American Statistician*, 58(1):30–37, 2004.

[39] Kozo Ichida and Yasuo Fujii. An interval arithmetic method for global optimization. *Computing*, 23(1):85–97, 1979.

[40] Luc Jaulin, Michel Kieffer, Olivier Didrit, and Éric Walter. *Applied Interval Analysis*. Springer, 2001.

[41] E Kaucher and WL Miranker. Residual correction and validation in functoids. In *Defect Correction Methods*, pages 169–192. Springer, 1984.

[42] Edgar Kaucher. Solving function space problems with guaranteed close bounds. In *A New Approach to Scientific Computation*, pages 139–164. Elsevier, 1983.

[43] Edgar Kaucher and Willard L Miranker. Validating computation in a function space. In *Reliability in Computing*, pages 403–425. Elsevier, 1988.

[44] Edgar W Kaucher and Willard L Miranker. *Self-validating numerics for function space problems: Computation with guarantees for differential and integral equations*. Elsevier, 1984.

[45] R Baker Kearfott. A review of techniques in the verified solution of constrained global optimization problems. *Applications of Interval Computations*, pages 23–59, 1996.

[46] Rainer Kelch. Numerical quadrature by extrapolation with automatic result verification. In *Mathematics in science and engineering*, volume 189, pages 143–185. Elsevier, 1993.

[47] Diederik P Kingma and Jimmy Ba. Adam: A method for stochastic optimization. In *International Conference on Learning Representations*, 2015.

[48] Oscar E Lanford. A computer-assisted proof of the Feigenbaum conjectures. *American Mathematical Society*, 6(3), 1982.

[49] Bruno Lang. Derivative-based subdivision in multi-dimensional verified gaussian quadrature. In *Symbolic Algebraic Methods and Verification Methods*, pages 145–152. Springer, 2001.

[50] Kenneth Lange. *MM optimization algorithms*. SIAM, 2016.

[51] Jaehoon Lee, Lechao Xiao, Samuel Schoenholz, Yasaman Bahri, Roman Novak, Jascha Sohl-Dickstein, and Jeffrey Pennington. Wide neural networks of any depth evolve as linear models under gradient descent. *Advances in Neural Information Processing Systems*, 32, 2019.

[52] Sang Kyu Lee, Jae Ho Chang, and Hyoung-Moon Kim. Further sharpening of Jensen’s inequality. *Statistics*, 55(5):1154–1168, 2021.

[53] JG Liao and Arthur Berg. Sharpening Jensen’s inequality. *The American Statistician*, 2018.

[54] Julien Mairal. Stochastic majorization-minimization algorithms for large-scale optimization. *Advances in Neural Information Processing Systems*, 26, 2013.

[55] K Makino and M Berz. Higher order verified inclusions of multidimensional systems by Taylor models. *Nonlinear Analysis: Theory, Methods & Applications*, 47(5):3503–3514, 2001.

[56] Kyoko Makino and Martin Berz. Remainder differential algebras and their applications. *Computational Differentiation: Techniques, Applications, and Tools*, pages 63–74, 1996.

[57] Kyoko Makino and Martin Berz. Efficient control of the dependency problem based on Taylor model methods. *Reliable Computing*, 5(1):3–12, 1999.

[58] Kyoko Makino and Martin Berz. Taylor models and other validated functional inclusion methods. *International Journal of Pure and Applied Mathematics*, 6:239–316, 2003.

[59] Kyoko Makino and Martin Berz. Verified global optimization with Taylor model-based range bounders. *Transactions on Computers*, 11(4):1611–1618, 2005.

[60] H Brendan McMahan and Matthew Streeter. Adaptive bound optimization for online convex optimization. In *Proceedings of the Twenty Third Annual Conference on Learning Theory*, pages 244–256, 2010.

[61] Angelo Mineo and Mariantonietta Ruggieri. A software tool for the exponential power distribution: The normalp package. *Journal of Statistical Software*, 12:1–24, 2005.

[62] Ramon E Moore. *Interval Analysis*, volume 4. Prentice-Hall Englewood Cliffs, 1966.

[63] Vinod Nair and Geoffrey E Hinton. Rectified linear units improve restricted Boltzmann machines. In *Proceedings of the 27th International Conference on Machine Learning*, pages 807–814, 2010.

[64] Markus Neher. Improved validated bounds for Taylor coefficients and for Taylor remainder series. *Journal of Computational and Applied Mathematics*, 152(1-2):393–404, 2003.

[65] Yurii Nesterov. *Introductory Lectures on Convex Optimization: A Basic Course*, volume 87. Springer Science & Business Media, 2003.

[66] Arnold Neumaier. Taylor forms – use and limits. *Reliable Computing*, 9(1):43–79, 2003.

[67] Jorge Nocedal and Stephen J Wright. *Numerical Optimization*. Springer, 1999.

[68] Adam Paszke, Sam Gross, Francisco Massa, Adam Lerer, James Bradbury, Gregory Chanan, Trevor Killeen, Zeming Lin, Natalia Gimelshein, Luca Antiga, et al. Pytorch: An imperative style, high-performance deep learning library. *Advances in neural information processing systems*, 32, 2019.

[69] Knut Petras. Principles of verified numerical integration. *Journal of Computational and Applied Mathematics*, 199(2):317–328, 2007.

[70] William H Press, Saul A Teukolsky, William T Vetterling, and Brian P Flannery. *Numerical recipes 3rd edition: The art of scientific computing*. Cambridge University Press, 2007.

[71] Prajit Ramachandran, Barret Zoph, and Quoc V Le. Searching for activation functions. *arXiv preprint arXiv:1710.05941*, 2017.

[72] Helmut Ratschek and Jon Rokne. *New Computer Methods for Global Optimization*. Wiley, 1988.

[73] Jon Rokne. Reducing the degree of an interval polynomial. *Computing*, 14(1):5–14, 1975.

[74] Jon Rokne. Bounds for an interval polynomial. *Computing*, 18(3):225–240, 1977.

- [75] Slavko Simic. Best possible global bounds for Jensen’s inequality. *Applied Mathematics and Computation*, 215(6):2224–2228, 2009.
- [76] Dung T Tran, Nobutaka Ono, and Emmanuel Vincent. Fast DNN training based on auxiliary function technique. In *2015 IEEE International Conference on Acoustics, Speech and Signal Processing (ICASSP)*, pages 2160–2164. IEEE, 2015.
- [77] Stephen G Walker. On a lower bound for the Jensen inequality. *SIAM Journal on Mathematical Analysis*, 46(5):3151–3157, 2014.
- [78] James B. Walters and George F. Corliss. *Automatic Differentiation: Point and Interval Taylor Operators*, pages 170–176. Springer, 2009.
- [79] Mu Wang. *High Order Reverse Mode of Automatic Differentiation*. PhD thesis, Purdue University, 2017.
- [80] Richard Zeckhauser and Mark Thompson. Linear regression with non-normal error terms. *The Review of Economics and Statistics*, pages 280–286, 1970.
- [81] Martin Zinkevich. Online convex programming and generalized infinitesimal gradient ascent. In *Proceedings of the 20th International Conference on Machine Learning*, pages 928–936, 2003.

Appendix A

Proofs

A.1 Sharp Taylor Enclosures in One Dimension

We first prove Proposition 1. To do so, we will make use of the fact the product of a scalar and an interval satisfies an associative property. Recall that for an interval $I \in \mathbb{IR}$ and scalar $\alpha \in \mathbb{R}$, we defined $I\alpha \triangleq \{\alpha x : x \in I\}$. It follows that for any interval $I \in \mathbb{IR}$ and scalars $\alpha, \beta \in \mathbb{R}$,

$$(I\alpha)\beta = I(\alpha\beta). \quad (\text{A.1})$$

Proposition 1. *For a $(k-1)$ -times differentiable function $f : \mathbb{R} \rightarrow \mathbb{R}$, scalar $x_0 \in \mathbb{R}$, and trust region $[a, b]$, an interval $I \in \mathbb{IR}$ defines a degree k Taylor enclosure of f at x_0 over $[a, b]$ if any only if*

$$\underline{I} \leq \inf_{x \in [a, b] \setminus \{x_0\}} \left\{ \frac{R_{k-1}(x; f, x_0)}{(x - x_0)^k} \right\}$$

and

$$\bar{I} \geq \sup_{x \in [a, b] \setminus \{x_0\}} \left\{ \frac{R_{k-1}(x; f, x_0)}{(x - x_0)^k} \right\}.$$

Proof. By Definition 1, I defines a Taylor enclosure of f at x_0 over $[a, b]$ iff. for all $x \in [a, b]$,

$$R_{k-1}(x; f, x_0) \in I(x - x_0)^k. \quad (\text{A.2})$$

Because $R_{k-1}(x_0; f, x_0) = 0$, (A.2) holds trivially for $x = x_0$. For $x \neq x_0$, multiplying both sides by $\frac{1}{(x - x_0)^k}$ and using (A.1) shows that (A.2) is equivalent to $\frac{R_{k-1}(x; f, x_0)}{(x - x_0)^k} \in I$. Thus, I defines a Taylor enclosure of f at x_0 iff. $\frac{R_{k-1}(x; f, x_0)}{(x - x_0)^k} \in I$ for all $x \in [a, b] \setminus \{x_0\}$, which is equivalent to the two inequalities listed in the proposition. \square

A.1.1 Proof of Theorem 1

The idea of the proof will be to identify conditions under which the ratio $\frac{R_{k-1}(x; f, x_0)}{(x - x_0)^k}$ is increasing or decreasing. To do so, we first derive an expression for the derivative of this ratio with respect to x . In doing so we will make use of the following proposition, which provides an expression for the derivative of the numerator of the ratio.

Proposition 2. *For any j -times differentiable function $f : \mathbb{R} \rightarrow \mathbb{R}$,*

$$\frac{d}{dx} R_j(x; f, x_0) = R_{j-1}(x; f', x_0).$$

Proof.

$$\begin{aligned}
\frac{d}{dx} R_j(x; f, x_0) &= \frac{d}{dx} \left(f(x) - \sum_{i=0}^j \frac{1}{i!} f^{(i)}(x_0) (x - x_0)^i \right) \\
&= f'(x) - \sum_{i=1}^j \frac{1}{(i-1)!} f^{(i)}(x_0) (x - x_0)^{i-1} \\
&= f'(x) - \sum_{i=1}^j \frac{1}{(i-1)!} (f')^{(i-1)}(x_0) (x - x_0)^{i-1} \\
&= f'(x) - \sum_{h=0}^{j-1} \frac{1}{h!} (f')^{(h)}(x_0) (x - x_0)^h \\
&= R_{j-1}(x; f', x_0).
\end{aligned}$$

□

With this proposition in hand, we can now derive an expression for $\frac{d}{dx} \frac{R_{k-1}(x; f, x_0)}{(x - x_0)^k}$.

Lemma 1. *For any function $f : \mathbb{R} \rightarrow \mathbb{R}$, and any integer $k \geq 2$, where $f^{(k-1)}$ is absolutely continuous over the closed interval between x_0 and x ,*

$$\frac{d}{dx} \frac{R_{k-1}(x; f, x_0)}{(x - x_0)^k} = \frac{1}{(x - x_0)^{k+1}} \int_{t=x_0}^x f^{(k)}(t) \left((x - x_0) \frac{1}{(k-2)!} (x - t)^{k-2} - \frac{k}{(k-1)!} (x - t)^{k-1} \right) dt.$$

Proof. Using the rule for the derivative of a ratio, then applying Proposition 2, we have

$$\begin{aligned}
\frac{d}{dx} \frac{R_{k-1}(x; f, x_0)}{(x - x_0)^k} &= \frac{\frac{d}{dx} R_{k-1}(x; f, x_0)}{(x - x_0)^k} - k \frac{R_{k-1}(x; f, x_0)}{(x - x_0)^{k+1}} \\
&= \frac{R_{k-2}(x; f', x_0)}{(x - x_0)^k} - k \frac{R_{k-1}(x; f, x_0)}{(x - x_0)^{k+1}} \\
&= \frac{1}{(x - x_0)^{k+1}} ((x - x_0) R_{k-2}(x; f', x_0) - k R_{k-1}(x; f, x_0)). \tag{A.3}
\end{aligned}$$

Using the integral form of the Taylor remainder series (Proposition 3) to rewrite $R_{k-2}(x; f', x_0)$ and $R_{k-1}(x; f, x_0)$, we have

$$\begin{aligned}
&(x - x_0) R_{k-2}(x; f', x_0) - k R_{k-1}(x; f, x_0) \\
&= (x - x_0) \int_{t=x_0}^x (f')^{(k-1)}(t) \frac{1}{(k-2)!} (x - t)^{k-2} dt - k \int_{t=x_0}^x f^{(k)}(t) \frac{1}{(k-1)!} (x - t)^{k-1} dt \\
&= \int_{t=x_0}^x f^{(k)}(t) \left((x - x_0) \frac{1}{(k-2)!} (x - t)^{k-2} - \frac{k}{(k-1)!} (x - t)^{k-1} \right) dt. \tag{A.4}
\end{aligned}$$

Plugging the expression on the right hand side of (A.4) into (A.3) completes the proof. □

Lastly, we prove Lemma 2, from which Theorem 1 immediately follows.

Lemma 2. *Let $f : \mathbb{R} \rightarrow \mathbb{R}$ be a function that is k times differentiable over the interval $[a, b]$, for $k \geq 0$. If $f^{(k)}$ is monotonically increasing (decreasing) over $[a, b]$, then for $x_0 \in (a, b)$, $\frac{R_{k-1}(x; f, x_0)}{(x - x_0)^k}$ is monotonically increasing (decreasing) over $[a, b]$.*

Proof. For $k = 0$, we have $f^{(k)}(x) = f(x) = \frac{R_{k-1}(x; f, x_0)}{(x-x_0)^k}$, and the theorem is trivially true. For $k = 1$, the proof was given in the main text. We now consider the general case, $k \geq 2$.

Suppose that $f^{(k)}$ is either monotonically increasing or monotonically decreasing, and define

$$S = \begin{cases} 1 & \text{if } f^{(k)} \text{ is monotonically increasing} \\ -1 & \text{otherwise.} \end{cases} \quad (\text{A.5})$$

To simplify the proof, we will assume that $f^{(k)}$ is differentiable, and that $\frac{d}{dt}f^{(k)}(t)$ is never exactly 0. This assumption, together with the assumption that $f^{(k)}$ is either monotonically increasing or decreasing over $[a, b]$, implies that $\text{sign}(\frac{d}{dt}f^{(k)}(t))$ is the same for all $t \in [a, b]$, and we have

$$S = \text{sign}\left(\frac{d}{dt}f^{(k)}(t)\right) \quad \forall t \in [a, b]. \quad (\text{A.6})$$

To prove the lemma, it suffices to show that $\text{sign}\left(\frac{d}{dx}\frac{R_{k-1}(x; f, x_0)}{(x-x_0)^k}\right) = S$. To do so, we first rewrite $\frac{d}{dx}\frac{R_{k-1}(x; f, x_0)}{(x-x_0)^k}$ in terms of $f^{(k)}$. By Lemma 1,

$$\frac{d}{dx}\frac{R_{k-1}(x; f, x_0)}{(x-x_0)^k} = \frac{1}{(x-x_0)^{k+1}} \int_{t=x_0}^x f^{(k)}(t)w(t)dt \quad (\text{A.7})$$

where

$$w(t) \triangleq (x-x_0) \frac{1}{(k-2)!} (x-t)^{k-2} - \frac{k}{(k-1)!} (x-t)^{k-1}. \quad (\text{A.8})$$

The bulk of the proof is contained in the following claim.

Claim 1.

$$\text{sign}\left(\int_{t=x_0}^x f^{(k)}(t)w(t)dt\right) = \text{sign}((x-x_0)^{k-1}) \cdot S.$$

Proof of Claim 1. To prove the claim, we first express the sign of $w(t)$ in terms of the sign of $t - t^*$, where

$$t^* \triangleq x - \frac{k-1}{k}(x-x_0). \quad (\text{A.9})$$

Using the definition of $w(t)$, and the fact that $\text{sign}(ab) = \text{sign}(a)\text{sign}(b)$ for any $a, b \in \mathbb{R}$, we have

$$\begin{aligned} \text{sign}(w(t)) &= \text{sign}((x-t)^{k-2})\text{sign}\left((x-x_0)\frac{1}{(k-2)!} - \frac{k}{(k-1)!}(x-t)\right) \\ &= \text{sign}((x-t)^{k-2})\text{sign}\left((x-x_0)\frac{k-1}{k} - (x-t)\right) \\ &= \text{sign}((x-t)^{k-2})\text{sign}\left(t - \left(x - \frac{k-1}{k}(x-x_0)\right)\right) \\ &= \text{sign}((x-t)^{k-2})\text{sign}(t - t^*). \end{aligned} \quad (\text{A.10})$$

Next, we show that $\int_{t=x_0}^x f^{(k+1)}(t)w(t)dt$ is equivalent to a different integral whose sign is easier to analyze. To do so, first note that

$$\int_{t=x_0}^x w(t)dt = \left((x-x_0) \frac{1}{(k-1)!} (x-t)^{k-1} - \frac{1}{(k-1)!} (x-t)^k \right) \Big|_{x_0}^x = 0. \quad (\text{A.11})$$

Therefore,

$$\int_{t=x_0}^x f^{(k)}(t)w(t)dt = \int_{t=x_0}^x \left(f^{(k)}(t) - f^{(k)}(t^*) \right) w(t)dt. \quad (\text{A.12})$$

We now compute the sign of the integrand on the right hand side of (A.12). To do so, first note that because $f^{(k)}$ is either monotonically increasing or monotonically decreasing,

$$\text{sign}\left(f^{(k)}(t) - f^{(k)}(t^*)\right) = \text{sign}(t - t^*) \cdot S. \quad (\text{A.13})$$

It follows that, for any t in the closed interval between x_0 and x ,

$$\begin{aligned} & \text{sign}\left((f^{(k)}(t) - f^{(k)}(t^*))w(t)\right) \\ &= \text{sign}\left(f^{(k)}(t) - f^{(k)}(t^*)\right) \text{sign}(w(t)) \\ &= \text{sign}(t - t^*) \cdot S \cdot \text{sign}((x - t)^{k-2}) \text{sign}(t - t^*) \quad \text{by (A.10) and (A.13)} \\ &= \text{sign}((x - t)^{k-2}) \cdot S \\ &= \text{sign}((x - x_0)^{k-2}) \cdot S \end{aligned} \quad (\text{A.14})$$

where the last step uses the fact that if t is between x_0 and x , then $x - t$ has the same sign as $x - x_0$.

To complete the proof, note that for any function $h : \mathbb{R} \rightarrow \mathbb{R}$, if $\text{sign}(h(t)) = C$ for all t in the closed interval between x_0 and x , then $\text{sign}(\int_{t=x_0}^x h(t)dt) = C \cdot \text{sign}(x - x_0)$. Thus, using (A.14),

$$\begin{aligned} \text{sign}\left(\int_{t=x_0}^x (f^{(k)}(t) - f^{(k)}(t^*))w(t)dt\right) &= \text{sign}((x - x_0)^{k-2}) \cdot S \cdot \text{sign}(x - x_0) \\ &= \text{sign}((x - x_0)^{k-1}) \cdot S. \end{aligned} \quad (\text{A.15})$$

Taking the sign of both sides of (A.12), and using (A.15) completes the proof of Claim 1. ■

To complete the proof, we take the sign of both sides of (A.7) and apply Claim 1:

$$\begin{aligned} \text{sign}\left(\frac{d}{dx} \frac{R_{k-1}(x; f, x_0)}{(x - x_0)^{k+1}}\right) &= \text{sign}\left(\frac{1}{(x - x_0)^{k+1}} \int_{t=x_0}^x f^{(k)}(t)w(t)dt\right) \quad \text{by (A.7)} \\ &= \text{sign}\left(\frac{1}{(x - x_0)^{k+1}}\right) \text{sign}\left(\int_{t=x_0}^x f^{(k)}(t)w(t)dt\right) \\ &= \text{sign}\left(\frac{1}{(x - x_0)^{k+1}}\right) \text{sign}((x - x_0)^{k-1}) \cdot S \quad \text{by Claim 1} \\ &= \text{sign}((x - x_0)^{-2}) \cdot S \\ &= S. \end{aligned} \quad (\text{A.16})$$

□

A.1.2 Proof of Theorem 2

We now prove Theorem 2. We will need the following technical lemma.

Lemma 4. *Let $\alpha > 0$ be a positive real number, and let $I = [-\alpha, \alpha]$ be an interval. Let $h : \mathbb{R} \rightarrow \mathbb{R}$ be a function that is even-symmetric over I (meaning $h(x) = h(-x) \forall x \in I$), and decreasing over $[0, \alpha]$. Then, for any $t, \delta \in \mathbb{R}$ such that $t + \delta \in I$ and $t - \delta \in I$,*

$$\text{sign}(h(t + \delta)) - \text{sign}(h(t - \delta)) = -\text{sign}(t)\text{sign}(\delta).$$

Proof. Because h is even symmetric over I ,

$$h(y) = h(|y|) \quad \forall y \in I. \quad (\text{A.17})$$

Because h is decreasing over $[0, \alpha]$,

$$\text{sign}(h(|y|) - h(|z|)) = -\text{sign}(|y| - |z|) \quad \forall y, z \in I. \quad (\text{A.18})$$

Thus,

$$\begin{aligned} \text{sign}(h(t + \delta)) - \text{sign}(h(t - \delta)) &= \text{sign}(h(|t + \delta|)) - \text{sign}(h(|t - \delta|)) && \text{by (A.17)} \\ &= -\text{sign}(|t + \delta| - |t - \delta|). && \text{by (A.18)} \end{aligned} \quad (\text{A.19})$$

To complete the proof, it suffices to show

$$\text{sign}(|t + \delta| - |t - \delta|) = \text{sign}(t)\text{sign}(\delta). \quad (\text{A.20})$$

We prove (A.20) by considering three cases. If either t or δ is 0, then both sides of (A.20) are 0. Otherwise, if t and δ have the same sign, then $|t + \delta| > |t - \delta|$, and both sides of (A.20) are 1. Finally, if t and δ have opposite sign, then $|t + \delta| < |t - \delta|$, and both sides of (A.20) are -1. \square

Theorem 2. *Let $f : \mathbb{R} \rightarrow \mathbb{R}$ be a twice-differentiable function, and suppose for some $\alpha > 0$, f'' is even symmetric over $[-\alpha, \alpha]$ (meaning $f''(x) = f''(-x) \forall x \in [-\alpha, \alpha]$), and f'' is decreasing over $[0, \alpha]$. Then, the sharp quadratic Taylor enclosure of f over $[a, b] \subseteq [-\alpha, \alpha]$ at $x_0 \in (a, b)$ is given by:*

$$I_2^*(f, x_0, [a, b]) = \left[\min \left\{ \frac{R_1(a; f, x_0)}{(a - x_0)^2}, \frac{R_1(b; f, x_0)}{(b - x_0)^2} \right\}, \frac{R_1(c; f, x_0)}{(c - x_0)^2} \right]$$

where $c \triangleq \min \{b, \max \{-x_0, a\}\}$.

Proof. Consider some fixed $x \in [a, b] \setminus \{x_0\}$, and define

$$w(t) \triangleq 2t - x - x_0. \quad (\text{A.21})$$

By Lemma 1,

$$\frac{d}{dx} \frac{R_1(x; f, x_0)}{(x - x_0)^2} = \frac{1}{(x - x_0)^3} \int_{t=x_0}^x f''(t)w(t)dt. \quad (\text{A.22})$$

The bulk of the proof is contained in the following claim.

Claim 1.

$$\text{sign} \left(\int_{t=x_0}^x f''(t)w(t)dt \right) = -\text{sign}(x + x_0)\text{sign}(x - x_0).$$

Proof of Claim 1. First, observe that for

$$t^* \triangleq \frac{x + x_0}{2} \quad (\text{A.23})$$

we have

$$w(t^* + \delta) = 2\delta = -w(t^* - \delta) \quad \forall \delta \in \mathbb{R}. \quad (\text{A.24})$$

We now use (A.24) to rewrite the integral on the right hand side of (A.22):

$$\begin{aligned}
& \int_{t=x_0}^x f''(t)w(t)dt \\
&= \int_{t=x_0}^{t^*} f''(t)w(t)dt + \int_{t=t^*}^x f''(t)w(t)dt \\
&= \int_{t=x_0}^{t^*} f''(t)w(t)dt + \int_{\delta=0}^{x-t^*} f''(t^*+\delta)w(t^*+\delta)d\delta & \text{letting } \delta = t - t^* \\
&= \int_{\delta'=0}^{t^*-x_0} f''(t^*-\delta')w(t^*-\delta')d\delta' + \int_{\delta=0}^{x-t^*} f''(t^*+\delta)w(t^*+\delta)d\delta & \text{letting } \delta' = t^* - t \\
&= \int_{\delta'=0}^{t^*-x_0} -f''(t^*-\delta')w(t^*+\delta')d\delta' + \int_{\delta=0}^{x-t^*} f''(t^*+\delta)w(t^*+\delta)d\delta & \text{by (A.24)} \\
&= \int_{\delta=0}^{t^*-x_0} -f''(t^*-\delta)w(t^*+\delta)d\delta + \int_{\delta=0}^{t^*-x_0} f''(t^*+\delta)w(t^*+\delta)d\delta \\
&= \int_{\delta=0}^{t^*-x_0} w(t^*+\delta)(f''(t^*+\delta) - f''(t^*-\delta))d\delta. & \text{(A.25)}
\end{aligned}$$

It is easy to verify that $t^* + \delta \in [a, b]$ and $t^* - \delta \in [a, b]$. Therefore, by Lemma 4,

$$\text{sign}(f''(t^* + \delta) - f''(t^* - \delta)) = -\text{sign}(t^*)\text{sign}(\delta). \quad (\text{A.26})$$

We are now ready to analyze the sign of the integral on the right hand side of (A.25). First, we show that the integrand has a constant sign (independent of δ):

$$\begin{aligned}
& \text{sign}(w(t^* + \delta)(f''(t^* + \delta) - f''(t^* - \delta))) \\
&= \text{sign}(w(t^* + \delta))\text{sign}(f''(t^* + \delta) - f''(t^* - \delta)) \\
&= \text{sign}(2\delta)\text{sign}(f''(t^* + \delta) - f''(t^* - \delta)) \\
&= -\text{sign}(2\delta)\text{sign}(t^*)\text{sign}(\delta) & \text{by (A.26)} \\
&= -\text{sign}(t^*) \\
&= -\text{sign}(x + x_0). & \text{(A.27)}
\end{aligned}$$

To complete the proof, note that for any function $h : \mathbb{R} \rightarrow \mathbb{R}$, if $\text{sign}(h(t)) = C$ for all t in the closed interval between 0 and $t^* - x_0$, then $\text{sign}(\int_{t=x_0}^x h(t)dt) = C \cdot \text{sign}(t^* - x_0)$. Thus, using (A.27), we have

$$\begin{aligned}
\text{sign}\left(\int_{\delta=0}^{t^*-x_0} w(t^*+\delta)(f''(t^*+\delta) - f''(t^*-\delta))d\delta\right) &= -\text{sign}(x+x_0)\text{sign}(t^*-x_0) \\
&= -\text{sign}(x+x_0)\text{sign}(x-x_0). & \text{(A.28)}
\end{aligned}$$

Combining (A.25) and (A.28) completes the proof of Claim 1. ■

To complete the proof, we use (A.22) and Claim 1 to show that for any $x \in [a, b] \setminus \{x_0\}$:

$$\begin{aligned}
\text{sign}\left(\frac{d}{dx} \frac{R_1(x; f, x_0)}{(x-x_0)^2}\right) &= \text{sign}\left(\frac{1}{(x-x_0)^3} \int_{t=x_0}^x f''(t)w(t)dt\right) & \text{by (A.22)} \\
&= \text{sign}\left(\frac{1}{(x-x_0)^3}\right) \text{sign}\left(\int_{t=x_0}^x f''(t)w(t)dt\right) \\
&= -\text{sign}\left(\frac{1}{(x-x_0)^3}\right) \text{sign}(x+x_0)\text{sign}(x-x_0) & \text{by Claim 1} \\
&= -\text{sign}(x+x_0). & \text{(A.29)}
\end{aligned}$$

It follows from (A.29) that the function $r(x) \triangleq \frac{R_1(x; f, x_0)}{(x-x_0)^2}$ is increasing for $x < -x_0$, decreasing for $x > -x_0$, and locally maximized at $x = x_0$. Thus, over the interval $[a, b]$, $r(x)$ is maximized at the point $x = \min\{b, \max\{-x_0, a\}\}$, and minimized at either $x = a$ or $x = b$. Using the definition of $I_2^*(f, x_0, [a, b])$ then proves the lemma. \square

A.1.3 Proof of Theorem 3

To prove Theorem 3, we will need the following corollary of Theorem 1.

Corollary 1. *Let $f : \mathbb{R} \rightarrow \mathbb{R}$ be an analytic function. If $f^{(k)}$ is monotonically increasing over an interval $[a, b]$ with $b > a$, then the degree k sharp Taylor enclosure of f at a over $[a, b]$ is given by $I_k^*(f, a, [a, b]) = \left[\frac{1}{k!} f^{(k)}(a), \frac{R_{k-1}(b; f, a)}{(b-a)^k} \right]$.*

Proof. By Theorem 1, for any $\epsilon \in (0, b-a)$ we have

$$\underline{I}_k^*(f, a + \epsilon, [a, b]) = \frac{R_{k-1}(a; f, a + \epsilon)}{(-\epsilon)^k}. \quad (\text{A.30})$$

Because f is analytic, $\underline{I}_k^*(f, x_0, [a, b])$ is continuous as a function of x_0 . Therefore,

$$\begin{aligned} \underline{I}_k^*(f, a, [a, b]) &= \lim_{\epsilon \rightarrow 0} \underline{I}_k^*(f, a + \epsilon, [a, b]) \\ &= \lim_{\epsilon \rightarrow 0} \frac{R_{k-1}(a; f, a + \epsilon)}{(-\epsilon)^k} \\ &= \lim_{\epsilon \rightarrow 0} \frac{\sum_{i=k}^{\infty} \frac{1}{i!} f^{(i)}(x_0) (-\epsilon)^i}{(-\epsilon)^k} \\ &= \frac{1}{k!} f^{(k)}(x_0). \end{aligned}$$

A similar argument shows $\overline{I}_k^*(f, a, [a, b]) = \frac{R_{k-1}(b; f, a)}{(b-a)^k}$, completing the proof. \square

Theorem 3. *For any analytic function $f : \mathbb{R} \rightarrow \mathbb{R}$, any integer $k > 0$, and any $x_0 \in \mathbb{R}$,*

$$\lim_{\epsilon \rightarrow 0} \frac{\text{width}(I_k^{\text{Lagrange}}(f, [x_0, x_0 + \epsilon]))}{\text{width}(I_k^*(f, x_0, [x_0, x_0 + \epsilon]))} = \binom{k+\ell}{\ell}$$

where $I_k^{\text{Lagrange}}(f, [a, b]) \triangleq \frac{1}{k!} \left[\inf_{y \in [a, b]} \{f^{(k)}(y)\}, \sup_{y \in [a, b]} \{f^{(k)}(y)\} \right]$, ℓ is the smallest positive integer such that $f^{(k+\ell)}(x_0) \neq 0$, and for any interval $I = [\underline{I}, \overline{I}]$, we define $\text{width}(I) \triangleq \overline{I} - \underline{I}$. Furthermore, both $I_k^{\text{Lagrange}}(f, [x_0, x_0 + \epsilon])$ and $I_k^*(f, x_0, [x_0, x_0 + \epsilon])$ have width $O(\epsilon^\ell)$ (as $\epsilon \rightarrow 0$).

Proof. Because f is analytic,

$$f(x) = \sum_{i=0}^{\infty} \frac{1}{i!} f^{(i)}(x_0) (x - x_0)^i. \quad (\text{A.31})$$

Therefore,

$$f^{(k)}(x) = \sum_{i=k}^{\infty} \frac{1}{(i-k)!} f^{(i)}(x_0) (x - x_0)^{i-k}. \quad (\text{A.32})$$

For sufficiently small ϵ , $f^{(k)}$ must be either monotonically increasing or monotonically decreasing over the interval $[x_0, x_0 + \epsilon]$. Assume without loss of generality that $f^{(k)}$ is monotonically increasing over $[x_0, x_0 + \epsilon]$. Under this assumption,

$$\inf_{y \in [a, b]} \{f^{(k)}(y)\} = f^{(k)}(x_0) \quad (\text{A.33})$$

and

$$\begin{aligned}
\sup_{y \in [a, b]} \{f^{(k)}(y)\} &= f^{(k)}(x_0 + \epsilon) \\
&= f^{(k)}(x_0) + \sum_{i=k+1}^{\infty} \frac{1}{(i-k)!} f^{(i)}(x_0) \epsilon^{i-k} && \text{by (A.32)} \\
&= f^{(k)}(x_0) + \sum_{i=k+\ell}^{\infty} \frac{1}{(i-k)!} f^{(i)}(x_0) \epsilon^{i-k} && \text{by definition of } \ell.
\end{aligned} \tag{A.34}$$

Therefore,

$$\text{width}(I_k^{\text{Lagrange}}(f, [x_0, x_0 + \epsilon])) = \frac{1}{k!} \sum_{i=k+\ell}^{\infty} \frac{1}{(i-k)!} f^{(i)}(x_0) \epsilon^{i-k}. \tag{A.35}$$

Dividing both sides of (A.35) by ϵ^ℓ , and taking the limit as $\epsilon \rightarrow 0$, we have

$$\lim_{\epsilon \rightarrow 0} \frac{\text{width}(I_k^{\text{Lagrange}}(f, [x_0, x_0 + \epsilon]))}{\epsilon^\ell} = \frac{1}{k! \ell!} f^{(k+\ell)}(x_0). \tag{A.36}$$

At the same time, by Corollary 1,

$$I_k^*(f, x_0, [x_0, x_0 + \epsilon]) = \left[\frac{1}{k!} f^{(k)}(x_0), \frac{R_{k-1}(x_0 + \epsilon; f, x_0)}{\epsilon^k} \right]. \tag{A.37}$$

Therefore,

$$\begin{aligned}
\text{width}(I_k^*(f, x_0, [x_0, x_0 + \epsilon])) &= \frac{R_{k-1}(x_0 + \epsilon; f, x_0)}{\epsilon^k} - \frac{1}{k!} f^{(k)}(x_0) \\
&= \left(\sum_{i=k}^{\infty} \frac{1}{i!} f^{(i)}(x_0) \epsilon^{i-k} \right) - \frac{1}{k!} f^{(k)}(x_0) \\
&= \sum_{i=k+1}^{\infty} \frac{1}{i!} f^{(i)}(x_0) \epsilon^{i-k} \\
&= \sum_{i=k+\ell}^{\infty} \frac{1}{i!} f^{(i)}(x_0) \epsilon^{i-k}.
\end{aligned} \tag{A.38}$$

(A.39)

Dividing both sides of (A.38) by ϵ^ℓ , and taking the limit as $\epsilon \rightarrow 0$, we have

$$\lim_{\epsilon \rightarrow 0} \frac{\text{width}(I_k^*(f, x_0, [x_0, x_0 + \epsilon]))}{\epsilon^\ell} = \frac{1}{(k+\ell)!} f^{(k+\ell)}(x_0). \tag{A.40}$$

By definition of ℓ , the right hand side of (A.40) is nonzero. Dividing (A.36) by (A.40) then proves the first part of the theorem.

The second part of the theorem (that both intervals have width $O(\epsilon^\ell)$ as $\epsilon \rightarrow 0$) follows immediately from (A.36) and (A.40). \square

A.2 Taylor Enclosures for Arbitrary Univariate Functions

We now prove Theorem 4. We will need the following lemma, which shows that if F is an interval polynomial enclosure in which only the final coefficient is an interval (rather than a scalar), then F is a Taylor enclosure.

Lemma 5. Let $F(z) = \sum_{i=0}^k F_{[i]} z^i$ be a degree k interval polynomial enclosure of a k times differentiable function $f : \mathbb{R} \rightarrow \mathbb{R}$ over $Z \in \mathbb{IR}$. Suppose that, for $j < k$, $F_{[j]}$ is a scalar (rather than an interval). Then $F_{[j]} = \frac{1}{j!} f^{(j)}(0)$, and F is therefore a Taylor enclosure of f at 0 over Z . (Accordingly, if $g(x) = f(x - x_0)$, then F is a Taylor enclosure of g at x_0 over $x_0 + Z$.)

Proof. Suppose for contradiction that the lemma does not hold, and let j be the smallest index such that $F_j \neq \frac{1}{j!} f^{(j)}(0)$. Let T_j and R_j denote the Taylor polynomial and the corresponding remainder term, as defined in §2.1. Then,

$$\lim_{z \rightarrow 0} \frac{R_{j-1}(z; f, 0)}{z^j} = \frac{1}{j!} f^{(j)}(0) \neq F_{[j]}. \quad (\text{A.41})$$

At the same time, letting $\underline{F}(z) \triangleq \underline{F}(z)$ and $\overline{F}(z) \triangleq \overline{F}(z)$, we have

$$F_{[j]} = \lim_{z \rightarrow 0} \frac{R_{j-1}(z; \underline{F}, 0)}{z^j} = \lim_{z \rightarrow 0} \frac{R_{j-1}(z; \overline{F}, 0)}{z^j}. \quad (\text{A.42})$$

Thus, for some sufficiently small $z > 0$, we must have

$$\frac{R_{j-1}(z; f, 0)}{z^j} \notin \left[\frac{R_{j-1}(z; \underline{F}, 0)}{z^j}, \frac{R_{j-1}(z; \overline{F}, 0)}{z^j} \right]. \quad (\text{A.43})$$

At the same time, because $F_{[i]} = \frac{1}{i!} f^{(i)}(0)$ for $i < j$ (by definition of j),

$$T_{j-1}(z; f, 0) = T_{j-1}(z; \underline{F}, 0) = T_{j-1}(z; \overline{F}, 0). \quad (\text{A.44})$$

Thus, multiplying both sides by of (A.43) by z^j , adding $T_{j-1}(z; f, 0)$ to both sides, and using (A.44),

$$f(z) \notin [\underline{F}(z), \overline{F}(z)] = F(z) \quad (\text{A.45})$$

contradicting the assumption that F is an interval polynomial enclosure of f . \square

Theorem 4. Assume that the table Σ provided as a hyperparameter to *AutoBound1D* contains interval polynomial extensions of each primitive function in \mathbb{O} . (That is, for any primitive function $\sigma : \mathbb{R}^m \rightarrow \mathbb{R} \in \mathbb{O}$, integer $k > 0$, and intervals $Y_1, Y_2, \dots, Y_m, Z \in \mathbb{IR}$, the function $F(z) = \Sigma[\sigma, k](z; Y_1, Y_2, \dots, Y_m, Z)$ is an interval polynomial extension of σ over Y_1, Y_2, \dots, Y_m and Z .)

Then, when given as input a symbolic expression $(\mathcal{V}, \mathcal{E})$, an interval $[a, b] \in \mathbb{IR}$, a scalar $x_0 \in [a, b]$, and a target degree $k > 0$, *AutoBound1D* returns a tuple containing the coefficients of a degree k interval polynomial P_n that satisfies:

$$f(x) \in P_n(x - x_0) \quad \forall x \in [a, b]$$

where $f : \mathbb{R} \rightarrow \mathbb{R}$ is the function represented by the symbolic expression $(\mathcal{V}, \mathcal{E})$. Furthermore, if the first $k - 1$ coefficients of P_n are scalars (which is the case when Σ is set to its default value), then P_n is a Taylor enclosure of f at x_0 over $[a, b]$.

Proof. Let Y_i and P_i , and be defined as in the pseudocode for *AutoBound1D*, and let $v_i(x)$ denote the value of intermediate variable v_i as a function of x . We will show by induction that, for $i = 0, 1, \dots, n$, the following two invariants hold:

1. $v_i(x) \in Y_i \quad \forall x \in [a, b]$.
2. P_i is an interval polynomial enclosure of $a_i(z) \triangleq v_i(x_0 + z)$ over $Z \triangleq [a - x_0, b - x_0]$.

For the base case $i = 0$, we have $v_0(x) = x$ and $Y_0 = (a, b)$, so invariant (1) holds trivially. Because $P_0(z) = x_0 + z = v_0(x_0 + z) = a_0(z)$, invariant (2) holds trivially as well.

Now consider some arbitrary $i > 0$, and assume that invariants (1) and (2) hold for all smaller i . Letting $L_i = (v_{j_1}, v_{j_2}, \dots, v_{j_m})$ (as in the pseudocode), we have:

$$\begin{aligned}
Y_i &\subseteq Y_i^{(0)} \\
&= \sigma_i(Y_{j_1}, Y_{j_2}, \dots, Y_{j_m}) \\
&\triangleq \{\sigma_i(y_{j_1}, y_{j_2}, \dots, y_{j_m}) : y_{j_l} \in Y_{j_l} \ \forall l \in \{1, 2, \dots, m\}\} \\
&\ni \sigma_i(v_{j_1}(x), v_{j_2}(x), \dots, v_{j_m}(x)) \\
&= v_i(x)
\end{aligned} \tag{A.46}$$

where the fourth line uses the induction hypothesis. Thus, invariant (1) holds. To show that invariant (2) also holds, first observe that

$$a_i(z) = \sigma_i(a_{j_1}(z), a_{j_2}(z), \dots, a_{j_m}(z)). \tag{A.47}$$

By the induction hypothesis, P_{j_l} is an interval polynomial enclosure of a_{j_l} over Z for all $l \in \{1, 2, \dots, m\}$, and $a_{j_l}(z) \in Y_{j_l}$ for all $z \in Z$. Furthermore, by the assumptions about Σ made in the theorem statement, the code sets $P_i = F(P_{j_1}, P_{j_2}, \dots, P_{j_m})$, where F is an interval polynomial extension of σ_i over $Y_{j_1}, Y_{j_2}, \dots, Y_{j_m}$ and Z . It follows by Proposition 4 that invariant (2) holds.

We have thus shown that invariants (1) and (2) hold for all i . Taking $i = n$, invariant (2) says that P_n is an interval polynomial enclosure of $a_n(z) = v_n(x_0 + z) = f(x_0 + z)$ over $Z = [a - x_0, b - x_0]$. Making the change of variable $x = z + x_0$ completes the first part of the proof.

The second claim (that P_n is a Taylor enclosure if its first $k - 1$ coefficients are scalars) follows from Lemma 5. \square

To prove Theorem 5, we will use the following lemma.

Lemma 6. *Let k and ℓ be positive integers, and let $f(x) = x^{k+\ell}$. For any interval $[a, b]$ with $0 \in [a, b]$,*

$$I_{\text{IntervalArithmetic}}(f, k, [a, b]) = \binom{k+\ell}{\ell} [a, b]^\ell$$

and

$$I_{\text{AutoBound}}(f, k, [a, b], 0) = [a, b]^\ell$$

where $I_{\text{IntervalArithmetic}}$ and $I_{\text{AutoBound}}$ are defined as in Theorem 5.

Proof. The k th derivative is $f^{(k)}(x) = \frac{(k+\ell)!}{\ell!} x^\ell$. Plugging in $x = [a, b]$, and evaluating the resulting expression according to the rules of interval arithmetic, gives

$$f^{(k)}([a, b]) = \frac{(k+\ell)!}{\ell!} [a, b]^\ell. \tag{A.48}$$

Therefore,

$$I_{\text{IntervalArithmetic}}(f, k, [a, b]) = \frac{1}{k!} f^{(k)}([a, b]) = \binom{k+\ell}{\ell} [a, b]^\ell. \tag{A.49}$$

Applied to f , AutoBound1D returns a polynomial P_1 , obtained by applying the interval polynomial extension of non-negative integer exponentiation (defined in §3.3.1) to the polynomial $P_0(z) = x_0 + z$. The interval polynomial extension expands $P_0(z)^{k+\ell} = (x_0 + z)^{k+\ell}$ using the binomial theorem, factors terms of degree $> k$ into the product of z^k and a single polynomial, and invokes the RangeBound function to obtain

$$\begin{aligned}
P_1(z) &= \left(\sum_{i=0}^{k-1} \binom{k+\ell}{i} x_0^{k+\ell-i} z^i \right) + z^k \cdot \text{RangeBound} \left(z \mapsto \sum_{i=k}^{k+\ell} \binom{k+\ell}{i} x_0^{k+\ell-i} z^{i-k}, Z \right) \\
&= z^k \cdot \text{RangeBound} (z \mapsto z^\ell, Z)
\end{aligned} \tag{A.50}$$

where on the second line we have used the fact that $x_0 = 0$ (defining $0^0 \triangleq 1$). Assuming the RangeBound function uses interval arithmetic evaluation, we have $\text{RangeBound}(z \mapsto z^\ell, Z) = Z^\ell = [a, b]^\ell$ (for $x_0 = 0$). Therefore,

$$I_{\text{AutoBound}}(f, k, [a, b], 0) = [a, b]^\ell. \quad (\text{A.51})$$

□

Theorem 5. Let $f(x) = \sum_{i=0}^n \alpha_i x^i$, and let k be a positive integer such that for some $l > 0$, $\alpha_{k+l} \neq 0$. Let ℓ be the smallest positive integer such that $\alpha^{k+\ell} \neq 0$. Then,

$$\lim_{\epsilon \rightarrow 0} \frac{\text{width}(I_{\text{IntervalArithmetic}}(f, k, [-\epsilon, \epsilon]))}{\text{width}(I_{\text{AutoBound}}(f, k, [-\epsilon, \epsilon], 0))} = \binom{k+\ell}{\ell}$$

where $I_{\text{IntervalArithmetic}}(f, k, [a, b])$ is the interval obtained by evaluating $\frac{1}{k!} f^{(k)}$ over the interval $[a, b]$ according to the rules of interval arithmetic, and $I_{\text{AutoBound}}(f, k, [a, b], 0)$ is the degree k coefficient of the polynomial returned by AutoBound1D given the same arguments.

Proof. By the rules of interval arithmetic,

$$\begin{aligned} & I_{\text{IntervalArithmetic}}(f, k, [-\epsilon, \epsilon]) \\ &= \sum_{i=0}^n \alpha_i I_{\text{IntervalArithmetic}}(x \mapsto x^i, k, [-\epsilon, \epsilon]) \\ &= \alpha_k + \sum_{i=k+1}^n \alpha_i I_{\text{IntervalArithmetic}}(x \mapsto x^i, k, [-\epsilon, \epsilon]) \\ &= \alpha_k + \sum_{j=1}^{n-k} \alpha_{k+j} I_{\text{IntervalArithmetic}}(x \mapsto x^{k+j}, k, [-\epsilon, \epsilon]) \\ &= \alpha_k + \sum_{j=1}^{n-k} \alpha_{k+j} \binom{k+j}{j} [-\epsilon, \epsilon]^j \quad \text{by Lemma 6.} \end{aligned} \quad (\text{A.52})$$

For any intervals $I, J \in \mathbb{IR}$,

$$\text{width}(I + J) = \text{width}(I) + \text{width}(J). \quad (\text{A.53})$$

Thus, taking the width of both sides of (A.52), we have

$$\text{width}(I_{\text{IntervalArithmetic}}(f, k, [-\epsilon, \epsilon])) = \sum_{j=1}^{n-k} \alpha_{k+j} \binom{k+j}{j} \text{width}([-\epsilon, \epsilon]^j). \quad (\text{A.54})$$

By a similar argument,

$$\text{width}(I_{\text{AutoBound}}(f, k, [-\epsilon, \epsilon], 0)) = \sum_{j=1}^{n-k} \alpha_{k+j} \text{width}([-\epsilon, \epsilon]^j). \quad (\text{A.55})$$

Dividing (A.54) by (A.55), and taking the limit as $\epsilon \rightarrow 0$ completes the proof. □

A.3 Generalization to Multivariate Functions

We first prove Proposition 5. To do so, we will use the following proposition.

Proposition 9. For any interval vector $X \in \mathbb{IR}^n$ and vector $\mathbf{y} \in \mathbb{R}^n$,

$$X \cdot \mathbf{y} = \{\mathbf{x} \cdot \mathbf{y} : \mathbf{x} \in X\}.$$

Proposition 9 is a special case of a more general result for interval expressions in which each interval is used exactly once; see [62, Chapter 5].

Proposition 5. *The tensor interval inner product defined by (4.1) extends the tensor inner product defined by (4.1). That is, for any tensor intervals \mathcal{A} and \mathcal{B} of appropriate shapes,*

$$\{\langle \mathbf{A}, \mathbf{B} \rangle : \mathbf{A} \in \mathcal{A}, \mathbf{B} \in \mathcal{B}\} \subseteq \langle \mathcal{A}, \mathcal{B} \rangle.$$

Furthermore, when the second argument is a tensor (or a singleton tensor interval) this extension is exact: for any tensor interval \mathcal{A} and tensor \mathbf{B} of appropriate shapes,

$$\{\langle \mathbf{A}, \mathbf{B} \rangle : \mathbf{A} \in \mathcal{A}\} = \langle \mathcal{A}, \mathbf{B} \rangle.$$

Proof. The first equation follows immediately from the properties of interval addition and multiplication.

We now prove the second equation. By definition, if \mathcal{A} has rank r and \mathbf{B} has rank $q \leq r$,

$$\langle \mathcal{A}, \mathbf{B} \rangle_{i_1, i_2, \dots, i_{r-q}} \triangleq \sum_{(j_1, j_2, \dots, j_q) \in \text{indices}(\mathbf{B})} \mathcal{A}_{i_1, i_2, \dots, i_{r-q}, j_1, j_2, \dots, j_q} \mathbf{B}_{j_1, j_2, \dots, j_q} \quad (\text{A.56})$$

Viewing the right hand side as a dot product of appropriately-defined vectors, it follows from Lemma 1 that

$$\langle \mathcal{A}, \mathbf{B} \rangle_{i_1, i_2, \dots, i_{r-q}} = \{\langle \mathbf{X}, \mathbf{B} \rangle : \mathbf{X} \in \mathcal{A}_{i_1, i_2, \dots, i_{r-q}}\}.$$

Because the choice of $\mathbf{X} \in \mathcal{A}_{i_1, i_2, \dots, i_{r-q}}$ can be made independently for each element of $\langle \mathcal{A}, \mathbf{B} \rangle$, it follows that $\langle \mathcal{A}, \mathbf{B} \rangle = \{\langle \mathbf{A}, \mathbf{B} \rangle : \mathbf{A} \in \mathcal{A}\}$. \square

A.3.1 Bilinear Operations on Tensor Intervals

We now provide proofs of the rules given in §4.2.1 for applying bilinear operations to tensor intervals. We first prove Proposition 6, which provides a simple rule that generalizes previous work on Interval Bound Propagation [27].

Proposition 6. *Let $\mathbf{b}(\mathbf{X}, \mathbf{Y}) = \langle \langle \mathbf{W}, \mathbf{X} \rangle, \mathbf{Y} \rangle$ be a bilinear operation, where $\mathbf{W} \geq \mathbf{0}$ (elementwise). Then, for any tensor intervals \mathcal{A} and \mathcal{B} , and any tensors $\mathbf{A} \in \mathcal{A}$, $\mathbf{B} \in \mathcal{B}$,*

$$\mathbf{b}(\mathbf{A}, \mathbf{B}) \in \mathbf{b}(m(\mathcal{A}), m(\mathcal{B})) + [-1, 1](\mathbf{b}(r(\mathcal{A}), |m(\mathcal{B})|) + \mathbf{b}(|m(\mathcal{A})|, r(\mathcal{B})) + \mathbf{b}(r(\mathcal{A}), r(\mathcal{B})))$$

where the functions m and r were defined in §4.1, and return the midpoint and radius of a tensor interval, respectively.

If $\underline{\mathcal{A}} = \overline{\mathcal{A}}$, this can be simplified to:

$$\mathbf{b}(\underline{\mathcal{A}}, \mathbf{B}) \in \mathbf{b}(m(\mathcal{A}), m(\mathcal{B})) + [-1, 1]\mathbf{b}(|m(\mathcal{A})|, r(\mathcal{B})) \quad \forall \mathbf{B} \in \mathcal{B}$$

while if $\underline{\mathcal{B}} = \overline{\mathcal{B}}$, it can be simplified to

$$\mathbf{b}(\mathbf{A}, \underline{\mathcal{B}}) \in \mathbf{b}(m(\mathcal{A}), m(\mathcal{B})) + [-1, 1]\mathbf{b}(r(\mathcal{A}), |m(\mathcal{B})|) \quad \forall \mathbf{A} \in \mathcal{A}.$$

Proof. Consider two arbitrary tensors $\mathbf{A} \in \mathcal{A}$ and $\mathbf{B} \in \mathcal{B}$. Because \mathbf{b} is bilinear,

$$\begin{aligned} \mathbf{b}(\mathbf{A}, \mathbf{B}) &= \mathbf{b}(\mathbf{A}, m(\mathcal{B}) + \mathbf{B} - m(\mathcal{B})) \\ &= \mathbf{b}(\mathbf{A}, m(\mathcal{B})) + \mathbf{b}(\mathbf{A}, \mathbf{B} - m(\mathcal{B})) \\ &= \mathbf{b}(m(\mathcal{A}), m(\mathcal{B})) + \mathbf{b}(\mathbf{A} - m(\mathcal{A}), m(\mathcal{B})) + \mathbf{b}(m(\mathcal{A}), \mathbf{B} - m(\mathcal{B})) + \mathbf{b}(m(\mathcal{A}) - m(\mathcal{B}), \mathbf{B} - m(\mathcal{B})). \end{aligned} \quad (\text{A.57})$$

Because $\mathbf{W} \geq 0$ (elementwise),

$$\mathbf{b}(\mathbf{A} - m(\mathcal{A}), m(\mathcal{B})) \leq \mathbf{b}(|\mathbf{A} - m(\mathcal{A})|, |m(\mathcal{B})|) \leq \mathbf{b}(r(\mathcal{A}), |m(\mathcal{B})|) \quad (\text{A.58})$$

and similarly,

$$\mathbf{b}(m(\mathcal{A}), \mathbf{B} - m(\mathcal{B})) \leq \mathbf{b}(|m(\mathcal{A})|, r(\mathcal{B})). \quad (\text{A.59})$$

Combining (A.57), (A.58) and (A.59), we have

$$\mathbf{b}(\mathbf{A}, \mathbf{B}) \leq \mathbf{b}(m(\mathcal{A}), m(\mathcal{B})) + \mathbf{b}(r(\mathcal{A}), |m(\mathcal{B})|) + \mathbf{b}(|m(\mathcal{A})|, r(\mathcal{B})) + \mathbf{b}(r(\mathcal{A}), r(\mathcal{B})). \quad (\text{A.60})$$

We can similarly prove the lower bound

$$\mathbf{b}(\mathbf{A}, \mathbf{B}) \geq \mathbf{b}(m(\mathcal{A}), m(\mathcal{B})) - \mathbf{b}(r(\mathcal{A}), |m(\mathcal{B})|) - \mathbf{b}(|m(\mathcal{A})|, r(\mathcal{B})) - \mathbf{b}(r(\mathcal{A}), r(\mathcal{B})). \quad (\text{A.61})$$

Combining (A.60) and (A.61) proves the first inequality stated in the proposition. The simplification in the special case $\underline{\mathcal{A}} = \bar{\mathcal{A}}$ follows from noting that this implies $r(\mathcal{A}) = \mathbf{0}$, and therefore $\mathbf{b}(r(\mathcal{A}), |m(\mathcal{B})|) = \mathbf{0}$. The simplification in the special case $\underline{\mathcal{B}} = \bar{\mathcal{B}}$ follows similarly. \square

We next prove Theorem 6, which provides an alternative rule that yields a potentially narrower interval at the cost of additional computation. To do so, we first prove Lemma 3.

Lemma 3. *For intervals $[\underline{x}, \bar{x}]$ and $[\underline{y}, \bar{y}]$,*

$$[\underline{x}, \bar{x}] \cdot [\underline{y}, \bar{y}] \subseteq [\underline{x}^+ \underline{y}^+ + \bar{x}^+ \underline{y}^- + \underline{x}^- \bar{y}^+ + \bar{x}^- \bar{y}^-, \bar{x}^+ \bar{y}^+ + \underline{x}^+ \bar{y}^- + \bar{x}^- \underline{y}^+ + \underline{x}^- \underline{y}^-]$$

where for $z \in \mathbb{R}$, we define $z^+ \triangleq \max\{z, 0\}$ and $z^- \triangleq \min\{z, 0\}$.

Proof. First note that for any $z \in \mathbb{R}$, $z = z^+ + z^-$. Therefore,

$$\begin{aligned} [\underline{x}, \bar{x}] \cdot [\underline{y}, \bar{y}] &= ([\underline{x}^+, \bar{x}^+] + [\underline{x}^-, \bar{x}^-]) \cdot ([\underline{y}^+, \bar{y}^+] + [\underline{y}^-, \bar{y}^-]) \\ &\subseteq [\underline{x}^+, \bar{x}^+] \cdot [\underline{y}^+, \bar{y}^+] + [\underline{x}^+, \bar{x}^+] \cdot [\underline{y}^-, \bar{y}^-] + [\underline{x}^-, \bar{x}^-] \cdot [\underline{y}^+, \bar{y}^+] + [\underline{x}^-, \bar{x}^-] \cdot [\underline{y}^-, \bar{y}^-] \\ &= [\underline{x}^+ \underline{y}^+, \bar{x}^+ \bar{y}^+] + [\bar{x}^+ \underline{y}^-, \underline{x}^+ \bar{y}^-] + [\underline{x}^- \bar{y}^+, \bar{x}^- \underline{y}^+] + [\bar{x}^- \bar{y}^-, \underline{x}^- \underline{y}^-] \\ &= [\underline{x}^+ \underline{y}^+ + \bar{x}^+ \underline{y}^- + \underline{x}^- \bar{y}^+ + \bar{x}^- \bar{y}^-, \bar{x}^+ \bar{y}^+ + \underline{x}^+ \bar{y}^- + \bar{x}^- \underline{y}^+ + \underline{x}^- \underline{y}^-]. \end{aligned}$$

\square

We are now ready to prove Theorem 6.

Theorem 6. *Let \mathbf{b} be a bilinear function. For tensor intervals \mathcal{A}, \mathcal{B} , and tensors $\mathbf{A} \in \mathcal{A}, \mathbf{B} \in \mathcal{B}$,*

$$\begin{aligned} \mathbf{b}(\mathbf{A}, \mathbf{B}) &\in \left[\mathbf{b}(\underline{\mathcal{A}}^+, \underline{\mathcal{B}}^+) + \mathbf{b}(\bar{\mathcal{A}}^+, \underline{\mathcal{B}}^-) + \mathbf{b}(\underline{\mathcal{A}}^-, \bar{\mathcal{B}}^+) + \mathbf{b}(\bar{\mathcal{A}}^-, \bar{\mathcal{B}}^-), \right. \\ &\quad \left. \mathbf{b}(\bar{\mathcal{A}}^+, \bar{\mathcal{B}}^+) + \mathbf{b}(\underline{\mathcal{A}}^+, \bar{\mathcal{B}}^-) + \mathbf{b}(\bar{\mathcal{A}}^-, \underline{\mathcal{B}}^+) + \mathbf{b}(\underline{\mathcal{A}}^-, \underline{\mathcal{B}}^-) \right] \end{aligned}$$

where for any tensor \mathbf{Z} we define $\mathbf{Z}^+ \triangleq \max\{\mathbf{Z}, \mathbf{0}\}$ and $\mathbf{Z}^- \triangleq \min\{\mathbf{Z}, \mathbf{0}\}$ (and the minimum and maximum are elementwise).

Proof. Without loss of generality, consider a scalar-valued and vector-variate bilinear operation $\mathbf{b} : \mathbb{R}^n \times \mathbb{R}^m \rightarrow \mathbb{R}$. Because \mathbf{b} is bilinear, there exists a matrix $\mathbf{W} \in \mathbb{R}^{n \times m}$ such that, for any $\mathbf{a} \in \mathbb{R}^n$ and $\mathbf{b} \in \mathbb{R}^m$,

$$\mathbf{b}(\mathbf{a}, \mathbf{b}) = \sum_{i=1}^n \sum_{j=1}^m \mathbf{a}_i \mathbf{W}_{ij} \mathbf{b}_j.$$

It then follows from the properties of interval arithmetic that, for tensor intervals $\mathcal{A} \in (\mathbb{R}^n)^2$ and $\mathcal{B} \in (\mathbb{R}^m)^2$,

$$\mathbf{b}(\mathcal{A}, \mathcal{B}) \subseteq \sum_{i=1}^n \sum_{j=1}^m \mathcal{A}_i \mathbf{W}_{ij} \mathcal{B}_j.$$

Applying Lemma 3 to each term on the right hand side, then rewriting the result in terms of applications of \mathbf{b} to the end points of \mathcal{A} and \mathcal{B} , completes the proof. \square

A.3.2 Proof of Theorem 7

In order to prove Theorem 7, we first prove Proposition 7.

Proposition 7. *For a tensor \mathbf{Z} , non-negative integers p and q , length s non-negative integer tuple S , tensor \mathbf{U} of shape $S + p * \text{shape}(\mathbf{Z})$, and tensor \mathbf{V} of shape $S + q * \text{shape}(\mathbf{Z})$,*

$$\langle \mathbf{U}, \mathbf{Z}^{\otimes p} \rangle \odot \langle \mathbf{V}, \mathbf{Z}^{\otimes q} \rangle = \langle \mathbf{U} \otimes_s \mathbf{V}, \mathbf{Z}^{\otimes(p+q)} \rangle.$$

Furthermore, for tensor intervals \mathcal{U} and \mathcal{V} , of the same shape as \mathbf{U} and \mathbf{V} respectively,

$$\langle \mathcal{U}, \mathbf{Z}^{\otimes p} \rangle \odot \langle \mathcal{V}, \mathbf{Z}^{\otimes q} \rangle \subseteq \langle \mathcal{U} \otimes_s \mathcal{V}, \mathbf{Z}^{\otimes(p+q)} \rangle.$$

Proof. Assume without loss of generality that \mathbf{Z} is a vector, and that $s = 1$, so that both $\langle \mathbf{U}, \mathbf{Z}^{\otimes p} \rangle$ and $\langle \mathbf{B}, \mathbf{Z}^{\otimes q} \rangle$ are vectors. Then, for any valid index i ,

$$\begin{aligned} (\langle \mathbf{U}, \mathbf{Z}^{\otimes p} \rangle \odot \langle \mathbf{V}, \mathbf{Z}^{\otimes q} \rangle)_i &= \left(\sum_{j_1, j_2, \dots, j_p} \mathbf{U}_{i, j_1, j_2, \dots, j_p} \prod_{l=1}^p \mathbf{Z}_{j_l} \right) \left(\sum_{k_1, k_2, \dots, k_q} \mathbf{V}_{i, k_1, k_2, \dots, k_q} \prod_{m=1}^q \mathbf{Z}_{k_m} \right) \\ &= \sum_{j_1, j_2, \dots, j_p, k_1, k_2, \dots, k_q} \mathbf{U}_{i, j_1, j_2, \dots, j_p} \mathbf{V}_{i, k_1, k_2, \dots, k_q} \prod_{l=1}^p \prod_{m=1}^q \mathbf{Z}_{j_l} \mathbf{Z}_{k_m} \\ &= \langle \mathbf{U} \otimes_s \mathbf{V}, \mathbf{Z}^{\otimes(p+q)} \rangle_i \end{aligned} \tag{A.62}$$

where the last equality follows from the definitions of inner and outer products ((4.1) and (4.5)).

For the second part of the theorem, we have:

$$\begin{aligned} \langle \mathcal{U}, \mathbf{Z}^{\otimes p} \rangle \odot \langle \mathcal{V}, \mathbf{Z}^{\otimes q} \rangle &= \{ \langle \mathbf{U}, \mathbf{Z}^{\otimes p} \rangle \odot \langle \mathbf{V}, \mathbf{Z}^{\otimes q} \rangle : \mathbf{U} \in \mathcal{U}, \mathbf{V} \in \mathcal{V} \} && \text{by Proposition 5} \\ &= \{ \langle \mathbf{U} \otimes_s \mathbf{V}, \mathbf{Z}^{\otimes(p+q)} \rangle : \mathbf{U} \in \mathcal{U}, \mathbf{V} \in \mathcal{V} \} && \text{by (A.62)} \\ &\subseteq \langle \mathcal{U} \otimes_s \mathcal{V}, \mathbf{Z}^{\otimes(p+q)} \rangle \end{aligned} \tag{A.63}$$

where the last line follows because the tensor interval inner and outer product operations are tensor interval extensions of the corresponding operations on tensors. \square

To prove Theorem 7, we will also need the following proposition.

Proposition 10. *For any tensors \mathbf{A} , \mathbf{B} and \mathbf{C} , of shapes such that $\langle \mathbf{A}, \mathbf{B} \otimes \mathbf{C} \rangle$ is well-defined,*

$$\langle \mathbf{A}, \mathbf{B} \otimes \mathbf{C} \rangle = \langle \langle \mathbf{A}, \mathbf{C} \rangle, \mathbf{B} \rangle.$$

Proof. To simplify indexing, assume without loss of generality that \mathbf{A} is a matrix, and that both \mathbf{B} and \mathbf{C} are vectors (which implies $\langle \mathbf{A}, \mathbf{B} \otimes \mathbf{C} \rangle$ is a scalar). We have

$$\begin{aligned} \langle \mathbf{A}, \mathbf{B} \otimes \mathbf{C} \rangle &= \sum_{ij} \mathbf{A}_{ij} (\mathbf{B} \otimes \mathbf{C})_{ij} \\ &= \sum_{ij} \mathbf{A}_{ij} \mathbf{B}_i \mathbf{C}_j \\ &= \sum_i \left(\sum_j \mathbf{A}_{ij} \mathbf{C}_j \right) \mathbf{B}_i \\ &= \langle \langle \mathbf{A}, \mathbf{C} \rangle, \mathbf{B} \rangle. \end{aligned} \tag{A.64}$$

\square

We are now ready to prove Theorem 7.

Theorem 7. *For a tensor \mathbf{Z} , non-negative integers p and q , length s non-negative integer tuple S , tensor \mathbf{A} of shape $S + p * \text{shape}(\mathbf{Z})$, tensor \mathbf{B} of shape $S + q * \text{shape}(\mathbf{Z})$, and non-negative integer $k \leq p + q$,*

$$\langle \mathbf{A}, \mathbf{Z}^{\otimes p} \rangle \odot \langle \mathbf{B}, \mathbf{Z}^{\otimes q} \rangle = \left\langle \left\langle \mathbf{A} \otimes_s \mathbf{B}, \mathbf{Z}^{\otimes(p+q-k)} \right\rangle, \mathbf{Z}^{\otimes k} \right\rangle.$$

Proof. First observe that the outer product defined in (4.2) is associative, and therefore

$$\mathbf{Z}^{\otimes(p+q)} = \mathbf{Z}^{\otimes k} \otimes \mathbf{Z}^{\otimes(p+q-k)}. \quad (\text{A.65})$$

The theorem then follows from Propositions 7 and 10:

$$\begin{aligned} \langle \mathbf{A}, \mathbf{Z}^{\otimes p} \rangle \odot \langle \mathbf{B}, \mathbf{Z}^{\otimes q} \rangle &= \left\langle \mathbf{A} \otimes_s \mathbf{B}, \mathbf{Z}^{\otimes(p+q)} \right\rangle && \text{by Proposition 7} \\ &= \left\langle \mathbf{A} \otimes_s \mathbf{B}, \mathbf{Z}^{\otimes k} \otimes \mathbf{Z}^{\otimes(p+q-k)} \right\rangle && \text{by (A.65)} \\ &= \left\langle \left\langle \mathbf{A} \otimes_s \mathbf{B}, \mathbf{Z}^{\otimes(p+q-k)} \right\rangle, \mathbf{Z}^{\otimes k} \right\rangle && \text{by Proposition 10.} \end{aligned} \quad (\text{A.66})$$

□

A.3.3 Proof of Theorem 8

To prove Theorem 8, we will need the following lemma.

Lemma 7. *Let $\mathcal{A}(\mathbf{Z}) = \sum_{i=0}^k \langle \mathcal{A}_{[i]}, \mathbf{Z}^{\otimes i} \rangle$ be a degree k interval polynomial. Then, for any tensor \mathbf{Z} ,*

$$\sum_{i=0}^k \langle \mathcal{A}_{[i]}, \mathbf{Z}^{\otimes i} \rangle = \left\{ \sum_{i=0}^k \langle \mathbf{A}_i, \mathbf{Z}^{\otimes i} \rangle : \mathbf{A}_i \in \mathcal{A}_{[i]} \ \forall i \in \{0, 1, \dots, k\} \right\}.$$

Lemma 7 follows from Proposition 5, and the fact that $\mathcal{X} + \mathcal{Y} = \{\mathbf{X} + \mathbf{Y} : \mathbf{X} \in \mathcal{X}, \mathbf{Y} \in \mathcal{Y}\}$.

Theorem 8. *Let $\mathbf{b} : \mathbb{R}^n \times \mathbb{R}^m \rightarrow \mathbb{R}$ be a scalar-valued, vector-variate bilinear operation, and let $\mathbf{W} \in \mathbb{R}^{n \times m}$ be its transformation matrix, so that $\mathbf{b}(\mathbf{x}, \mathbf{y}) = \mathbf{x}^\top \mathbf{W} \mathbf{y}$. For any tensor \mathbf{U} whose first dimension has length n , and any tensor \mathbf{V} whose first dimension has length m , define*

$$\text{batched}(\mathbf{U}, \mathbf{V}) \triangleq \sum_{p=1}^n \sum_{q=1}^m \mathbf{W}_{pq} (\mathbf{U}_p \otimes \mathbf{V}_q).$$

Let *Batched* be a tensor interval extension of *batched*.

For any degree k tensor interval polynomials \mathcal{A} and \mathcal{B} , let the degree k interval polynomial $\mathcal{Q}(\mathcal{A}, \mathcal{B})$ be defined by:

$$\mathcal{Q}(\mathcal{A}, \mathcal{B})_{[i]} \triangleq \begin{cases} \sum_{l, m \in \mathbb{Z}_{0:k}: l+m=i} \text{Batched}(\mathcal{A}_{[l]}, \mathcal{B}_{[m]}) & i < k \\ \text{RangeBound} \left(\sum_{\substack{l, m \in \mathbb{Z}_{0:k}: \\ l+m \geq k}} \langle \text{Batched}(\mathcal{A}_{[l]}, \mathcal{B}_{[m]}), \mathbf{Z}^{\otimes(l+m-k)} \rangle, \mathcal{Z} \right) & i = k \end{cases}$$

where $\mathbb{Z}_{0:k} \triangleq \{0, 1, \dots, k\}$.

Then, for any degree k tensor interval polynomials \mathcal{A} and \mathcal{B} , and any tensor interval \mathcal{Z} ,

$$\{\mathbf{b}(\mathbf{X}, \mathbf{Y}) : \mathbf{X} \in \mathcal{A}(\mathbf{Z}), \mathbf{Y} \in \mathcal{B}(\mathbf{Z})\} \subseteq \sum_{i=0}^k \langle \mathcal{Q}(\mathcal{A}, \mathcal{B})_{[i]}, \mathbf{Z}^{\otimes i} \rangle \quad \forall \mathbf{Z} \in \mathcal{Z}.$$

Accordingly, for any tensor intervals \mathcal{Y}_1 , \mathcal{Y}_2 , and \mathcal{Z} , \mathcal{Q} is a degree k tensor interval polynomial extension of \mathbf{b} over trust regions $(\mathcal{Y}_1, \mathcal{Y}_2)$ and \mathcal{Z} (where \mathcal{Y}_1 and \mathcal{Y}_2 play no role).

Proof. Let \mathcal{A} and \mathcal{B} be tensor interval polynomials of degree k . Consider some fixed $\mathbf{Z} \in \mathcal{Z}$, and fixed tensors $\mathbf{X} \in \mathcal{A}(\mathbf{Z})$ and $\mathbf{Y} \in \mathcal{B}(\mathbf{Z})$. By Lemma 7, there exist tensors $\mathbf{A}_0, \mathbf{A}_1, \dots, \mathbf{A}_k$, with $\mathbf{A}_l \in \mathcal{A}_{[l]}$ for all l , such that

$$\mathbf{X} = \sum_{l=0}^k \langle \mathbf{A}_l, \mathbf{Z}^{\otimes l} \rangle. \quad (\text{A.67})$$

Similarly, there exist tensors $\mathbf{B}_0, \mathbf{B}_1, \dots, \mathbf{B}_k$, with $\mathbf{B}_m \in \mathcal{B}_{[m]}$ for all m , such that

$$\mathbf{Y} = \sum_{m=0}^k \langle \mathbf{B}_m, \mathbf{Z}^{\otimes m} \rangle. \quad (\text{A.68})$$

Thus, because \mathbf{b} is bilinear,

$$\mathbf{b}(\mathbf{X}, \mathbf{Y}) = \sum_{l=0}^k \sum_{m=0}^k \mathbf{b}(\langle \mathbf{A}_l, \mathbf{Z}^{\otimes l} \rangle, \langle \mathbf{B}_m, \mathbf{Z}^{\otimes m} \rangle). \quad (\text{A.69})$$

To complete the proof, we will show that for all l and m ,

$$\mathbf{b}(\langle \mathbf{A}_l, \mathbf{Z}^{\otimes l} \rangle, \langle \mathbf{B}_m, \mathbf{Z}^{\otimes m} \rangle) \in \left\langle \left\langle \text{Batched}(\mathcal{A}_l, \mathcal{B}_m), \mathbf{Z}^{\otimes \max\{0, l+m-k\}} \right\rangle, \mathbf{Z}^{\otimes \min\{k, l+m\}} \right\rangle. \quad (\text{A.70})$$

This suffices to prove the theorem because, combining (A.69) and (A.70), we have:

$$\begin{aligned} \mathbf{b}(\mathbf{X}, \mathbf{Y}) &\subseteq \sum_{l=0}^k \sum_{m=0}^k \left\langle \left\langle \text{Batched}(\mathcal{A}_l, \mathcal{B}_m), \mathbf{Z}^{\otimes \max\{0, l+m-k\}} \right\rangle, \mathbf{Z}^{\otimes \min\{k, l+m\}} \right\rangle \\ &\subseteq \mathcal{Q}(\mathbf{Z}) \end{aligned} \quad (\text{A.71})$$

where the second line follows from the definition of \mathcal{Q} (and the assumed behavior of the RangeBound function).

To see that (A.70) holds, observe that for any tensor intervals \mathcal{U} and \mathcal{V} , and tensors $\mathbf{U} \in \mathcal{U}$, $\mathbf{V} \in \mathcal{V}$,

$$\begin{aligned} \mathbf{b}(\langle \mathbf{U}, \mathbf{Z}^{\otimes l} \rangle, \langle \mathbf{V}, \mathbf{Z}^{\otimes m} \rangle) &= \sum_{p,q} \mathbf{W}_{pq} \langle \mathbf{U}, \mathbf{Z}^{\otimes l} \rangle_p \langle \mathbf{V}, \mathbf{Z}^{\otimes m} \rangle_q \\ &= \sum_{p,q} \mathbf{W}_{pq} \langle \mathbf{U}_p, \mathbf{Z}^{\otimes l} \rangle \langle \mathbf{V}_q, \mathbf{Z}^{\otimes m} \rangle && \text{by inner product def.} \\ &= \sum_{p,q} \mathbf{W}_{pq} \langle \mathbf{U}_p \otimes \mathbf{V}_q, \mathbf{Z}^{\otimes(l+m)} \rangle && \text{by Proposition 7} \\ &= \left\langle \sum_{p,q} \mathbf{W}_{pq} (\mathbf{U}_p \otimes \mathbf{V}_q), \mathbf{Z}^{\otimes(l+m)} \right\rangle && \text{by inner product def.} \\ &= \left\langle \text{batched}(\mathbf{U}, \mathbf{V}), \mathbf{Z}^{\otimes(l+m)} \right\rangle && \text{by def. of batched} \\ &\in \left\langle \text{Batched}(\mathcal{U}, \mathcal{V}), \mathbf{Z}^{\otimes(l+m)} \right\rangle && \text{by def. of Batched} \\ &\subseteq \left\langle \left\langle \text{Batched}(\mathcal{U}, \mathcal{V}), \mathbf{Z}^{\otimes \max\{0, l+m-k\}} \right\rangle, \mathbf{Z}^{\otimes \min\{k, l+m\}} \right\rangle && \text{by Theorem 7.} \end{aligned} \quad (\text{A.72})$$

Plugging $\mathbf{U} = \mathbf{A}_l$, $\mathcal{U} = \mathcal{A}_{[l]}$, $\mathbf{V} = \mathbf{B}_m$, and $\mathcal{V} = \mathcal{B}_{[m]}$ into (A.72) proves (A.70), which proves the theorem. \square

A.3.4 Proof of Theorem 9

Theorem 9. Assume that the AutoBound hyperparameter Σ has the properties stated in the pseudocode. Then, given as input a symbolic expression $(\mathcal{V}, \mathcal{E})$ defining a function $f : \mathbb{R}^d \rightarrow \mathbb{R}^s$, a vector $\mathbf{x}_0 \in \mathbb{R}^d$, and a target degree k , AutoBound returns the coefficients of a tensor interval polynomial \mathcal{P}_n such that

$$f(\mathbf{x}) \in \mathcal{P}_n(\mathbf{x} - \mathbf{x}_0) \quad \forall \mathbf{x} \in [\mathbf{a}, \mathbf{b}].$$

Proof. We will show inductively that, for $i = 0, 1, \dots, n$, the algorithm maintains the following invariants:

1. $v_i(\mathbf{x}) \in \mathcal{Y}_i$ for all $\mathbf{x} \in [\mathbf{a}, \mathbf{b}]$.
2. $v_i(\mathbf{x}) \in \mathcal{P}_i(\mathbf{x} - \mathbf{x}_0)$ for all $\mathbf{x} \in [\mathbf{a}, \mathbf{b}]$.

For the base case $i = 0$, we have $\mathcal{Y}_0 = [\mathbf{a}, \mathbf{b}]$, and invariant (1) holds trivially. Similarly, because $\mathcal{P}_0(\mathbf{x}) = \mathbf{x}_0 + \langle \mathbb{I}_{d \times d}, \mathbf{x} - \mathbf{x}_0 \rangle = \mathbf{x}$, invariant (2) holds trivially.

Now consider some arbitrary $i > 0$, and assume the two invariants hold for all smaller i . Consider iteration i of the for loop, let Σ_0 and Σ_k be defined as in the pseudocode, and let $L_i = (v_{j_1}, v_{j_2}, \dots, v_{j_m})$ (as in the pseudocode). By assumption, Σ_0 is a tensor interval extension of σ_i . By the induction hypothesis, $v_{j_l}(\mathbf{x}) \in \mathcal{Y}_{j_l}$ for $l \in \{1, 2, \dots, m\}$ for all $\mathbf{x} \in [\mathbf{a}, \mathbf{b}]$. Thus, for any $\mathbf{x} \in [\mathbf{a}, \mathbf{b}]$,

$$v_i(\mathbf{x}) = \sigma_i(v_{j_1}(\mathbf{x}), v_{j_2}(\mathbf{x}), \dots, v_{j_l}(\mathbf{x})) \in \Sigma_0(\mathcal{Y}_{j_1}, \mathcal{Y}_{j_2}, \dots, \mathcal{Y}_{j_l}) \subseteq \mathcal{Y}_j \quad (\text{A.73})$$

and invariant (1) is satisfied.

Similarly, using the assumption that Σ_k is a degree k tensor interval polynomial extension of σ_i over $(\mathcal{Y}_{j_1}, \mathcal{Y}_{j_2}, \dots, \mathcal{Y}_{j_m})$ and \mathcal{Z} , for any $\mathbf{x} \in \mathbf{x}_0 + \mathcal{Z} = [\mathbf{a}, \mathbf{b}]$, we have:

$$v_j(\mathbf{x}) = \sigma_i(v_{j_1}(\mathbf{x}), v_{j_2}(\mathbf{x}), \dots, v_{j_m}(\mathbf{x})) \in \Sigma_k(\mathcal{P}_{j_1}, \mathcal{P}_{j_2}, \dots, \mathcal{P}_{j_m})(\mathbf{x} - \mathbf{x}_0) = \mathcal{P}_j(\mathbf{x} - \mathbf{x}_0) \quad (\text{A.74})$$

and invariant (2) is satisfied.

Both invariants therefore hold for all i . The theorem then follows from invariant (2), taking $i = n$. \square

A.4 Proof of Theorems 10 and 11

We now provide proofs for the theorems stated in §5.2.4.

We first prove Theorem 10, which shows that as $T \rightarrow \infty$, SafeRate and SafeCombination are guaranteed to find a point with vanishingly small gradient norm.

Theorem 10. Let f , \mathbf{v}_t , and P_t be defined as in the pseudocode for SafeRate. Suppose, for some $\beta \geq 1$, f is β -smooth over the level set $\{\mathbf{y} : f(\mathbf{y}) \leq f(\mathbf{x}_1)\}$, and suppose that the PolynomialUpperBound function returns

$$P_t(\eta) = f(\mathbf{x}_t) + \eta \nabla f(\mathbf{x}_t)^\top \mathbf{v}_t + \frac{\beta}{2} \eta^2 (f(\mathbf{x}_t)^\top \mathbf{v}_t)^2.$$

Further suppose $\mathbf{v}_t = -\nabla f(\mathbf{x}_t)$. Then,

$$\min_{1 \leq t \leq T} \left\{ \|\nabla f(\mathbf{x}_t)\|^2 \right\} \leq \frac{2\beta(f(\mathbf{x}_1) - f(\mathbf{x}_{T+1}))}{T}.$$

The same guarantee holds for SafeCombination, provided the negative gradient is one of the d update directions.

Proof. By our β -smoothness assumption, for any \mathbf{z} with $f(\mathbf{z}) \leq f(\mathbf{x}_1)$, and for any t , we have the quadratic upper bound

$$f(\mathbf{z}) \leq f(\mathbf{x}_t) + \nabla f(\mathbf{x}_t)^\top (\mathbf{z} - \mathbf{x}_t) + \frac{\beta}{2} \|\mathbf{z} - \mathbf{x}_t\|^2. \quad (\text{A.75})$$

By Proposition 8, $f(\mathbf{x}_{t+1}) \leq f(\mathbf{x}_t)$. Therefore, taking $\mathbf{z} = \mathbf{x}_{t+1}$, and letting $\mathbf{g}_t = \nabla f(\mathbf{x}_t)$ for compactness, we have

$$\begin{aligned} f(\mathbf{x}_{t+1}) &\leq f(\mathbf{x}_t) + \mathbf{g}_t^\top (-\eta_t \mathbf{g}_t) + \frac{\beta}{2} \|\eta_t \mathbf{g}_t\|^2 \\ &= f(\mathbf{x}_t) - \|\mathbf{g}_t\|^2 \left(\eta_t - \frac{\beta}{2} \eta_t^2 \right). \end{aligned} \quad (\text{A.76})$$

We will show below that for all t ,

$$\eta_t = \frac{1}{\beta}. \quad (\text{A.77})$$

We therefore have

$$f(\mathbf{x}_{t+1}) \leq f(\mathbf{x}_t) - \frac{1}{2\beta} \|\mathbf{g}_t\|^2. \quad (\text{A.78})$$

Summing this inequality over all t then proves

$$f(\mathbf{x}_{T+1}) - f(\mathbf{x}_1) \leq -\frac{1}{2\beta} \sum_{t=1}^T \|\mathbf{g}_t\|^2. \quad (\text{A.79})$$

Rearranging (A.79), and using $\min_{1 \leq t \leq T} \{\|\mathbf{g}_t\|^2\} \leq \frac{1}{T} \sum_{t=1}^T \|\mathbf{g}_t\|^2$ completes the proof.

We now prove (A.77) by induction. First note that the unconstrained minimizer of P_t is

$$\operatorname{argmin}_{\eta \in \mathbb{R}} \{P_t(\eta)\} = \frac{1}{\beta}. \quad (\text{A.80})$$

Therefore, $\eta_t = \frac{1}{\beta}$ so long as $\bar{\eta}_t \geq \frac{1}{\beta}$. For $t = 1$, we have $\bar{\eta}_1 = 1$, and because $\beta \geq 1$ by assumption, $\frac{1}{\beta} \leq \bar{\eta}_1$ and therefore $\eta_1 = \frac{1}{\beta}$.

Now assume that for some arbitrary t , we have $\eta_t = \frac{1}{\beta}$. Because $\eta_t \in [0, \bar{\eta}_t]$, this implies $\bar{\eta}_t \geq \frac{1}{\beta}$. Considering the two cases $\eta_t \geq \frac{1}{2} \bar{\eta}_t$ and $\eta_t < \frac{1}{2} \bar{\eta}_t$, we see that in either case,

$$\bar{\eta}_{t+1} \geq \frac{1}{\beta}. \quad (\text{A.81})$$

Therefore, by (A.80), $\eta_{t+1} = \frac{1}{\beta}$. □

We now prove Theorem 11.

Theorem 11. *Let $f : \mathbb{R}^n \rightarrow \mathbb{R}$ be a function such that for any $\mathbf{x} \in \mathbb{R}^n$, computing $f(\mathbf{x})$ requires M_0 multiplications, and calling DirectionOracle requires M_1 multiplications. Then, using AutoBound as the PolynomialUpperBound function, each iteration of SafeRate requires $O(M_1 + M_0 k \log(k))$ multiplications, where k is the polynomial degree, and each iteration of SafeCombination requires $O(M_1 + M_0 d^\omega)$ multiplications, where $\omega < 2.37286$.*

Proof. On each iteration, SafeRate must call DirectionOracle (using M_1 multiplications), and then must call AutoBound. For each multiplication required to compute $f(\mathbf{x}_t)$, AutoBound needs to multiply two degree k interval polynomials, each of which has the property that only the final coefficient is an interval (and all other coefficients are scalars). Using the Fast Fourier Transform, the product of two such interval polynomials can be computed using $O(k \log(k))$ multiplications. Therefore, each iteration takes $O(M_1 + M_0 k \log(k))$ multiplications.

For SafeCombination, the proof is similar, except that for each multiplication needed to compute $f(\mathbf{x}_t)$ we must now multiply two multivariate quadratic interval polynomials. Up to a constant factor, this has the same time complexity as multiplying two d by d matrices. This can be done in time $O(d^\omega)$, where ω is the matrix multiplication exponent. Thus the total time complexity is $O(M_1 + M_0 d^\omega)$. At the time of writing, the best bound on the matrix multiplication exponent is $\omega < 2.37286$ [2]. □

A.5 Proof of Theorem 12

Theorem 12. Let $\varphi : \mathbb{R} \rightarrow \mathbb{R}$ be a k times differentiable function, and let X be a scalar random variable that lies in the interval $[a, b]$ with probability 1. Let the interval $I \in \mathbb{IR}$ define a degree $k+1$ Taylor enclosure of φ , centered at $\mu \triangleq \mathbb{E}[X]$, and valid over $[a, b]$, so that we have

$$\varphi(x) \in \left(\sum_{i=0}^k \frac{\varphi^{(i)}(\mu)}{i!} (x - \mu)^i \right) + I \cdot (x - \mu)^{k+1} \quad \forall x \in [a, b].$$

Then,

$$\mathbb{E}[\varphi(X)] \in \varphi(\mu) + \left(\sum_{i=2}^k \frac{\varphi^{(i)}(\mu)}{i!} \mathbb{E}[(X - \mu)^i] \right) + I \cdot \mathbb{E}[\min\{0, (X - \mu)^{k+1}\}] + I \cdot \mathbb{E}[\max\{0, (X - \mu)^{k+1}\}].$$

If $k+1$ is even, this simplifies to:

$$\mathbb{E}[\varphi(X)] \in \varphi(\mu) + \left(\sum_{i=2}^k \frac{\varphi^{(i)}(\mu)}{i!} \mathbb{E}[(X - \mu)^i] \right) + I \cdot \mathbb{E}[(X - \mu)^{k+1}].$$

Proof. Letting F be the cumulative distribution function of X ,

$$\begin{aligned} \mathbb{E}[\varphi(X)] &= \int_a^b \varphi(x) dF(x) \\ &\in \int_a^b \left(\sum_{i=0}^{k-1} \frac{\varphi^{(i)}(\mu)}{i!} (x - \mu)^i \right) + I(x - \mu)^k dF(x) \\ &= \left(\sum_{i=0}^{k-1} \frac{\varphi^{(i)}(\mu)}{i!} \mathbb{E}[(X - \mu)^i] \right) + \int_a^b I(x - \mu)^k dF(x) \\ &= \varphi(\mu) + \left(\sum_{i=2}^{k-1} \frac{\varphi^{(i)}(\mu)}{i!} \mathbb{E}[(X - \mu)^i] \right) + \int_a^b I(x - \mu)^k dF(x). \end{aligned} \tag{A.82}$$

To complete the proof, we use the identity $z = \min\{0, z\} + \max\{0, z\}$ to write:

$$\begin{aligned} \int_a^b I(x - \mu)^k dF(x) &= \int_a^b I \cdot (\min\{0, (x - \mu)^k\} + \max\{0, (x - \mu)^k\}) dF(x) \\ &= \int_a^b I \cdot \min\{0, (x - \mu)^k\} dF(x) + \int_a^b I \cdot \max\{0, (x - \mu)^k\} dF(x) \\ &= I \cdot \int_a^b \min\{0, (x - \mu)^k\} dF(x) + I \cdot \int_a^b \max\{0, (x - \mu)^k\} dF(x) \\ &= I \cdot \mathbb{E}[\min\{0, (X - \mu)^k\}] + I \cdot \mathbb{E}[\max\{0, (X - \mu)^k\}] \end{aligned} \tag{A.83}$$

where on the third line, the fact that the integrand has the same sign for all $x \in [a, b]$ allowed us to bring the interval I outside the integral. Plugging (A.83) into (A.82) completes the proof. \square

Appendix B

Implementation Details

We now provide details about the SafeRate and SafeCombination algorithms that were omitted from the main text.

B.1 Computing the SafeRate Learning Rate

As described in §5.2.2, the SafeRate algorithm computes a learning rate η_t using the formula

$$\eta_t = \operatorname{argmin}_{\eta \in [0, \bar{\eta}_t]} \{P_t(\eta)\} \quad (\text{B.1})$$

where P_t is a degree k polynomial.

In the special case $k = 2$, letting \bar{I}_t denote the quadratic coefficient of P_t , we have

$$\eta_t = \begin{cases} \max \left\{ 0, \min \left\{ -\frac{\nabla f(\mathbf{x}_t)^\top \mathbf{v}_t}{2\bar{I}_t}, \bar{\eta}_t \right\} \right\} & \bar{I}_t > 0 \\ \operatorname{argmin}_{\eta \in \{0, \bar{\eta}_t\}} \{ \eta \nabla f(\mathbf{x}_t)^\top \mathbf{v}_t + \bar{I}_t \eta^2 \} & \bar{I}_t \leq 0. \end{cases} \quad (\text{B.2})$$

The solution in (B.2) for the case $\bar{I}_t > 0$ is obtained by minimizing the quadratic (by setting the derivative to 0) and projecting the minimizer onto the interval $[0, \bar{\eta}_t]$. The solution for $\bar{I}_t \leq 0$ holds because the minimizer of a concave quadratic over an interval is always one of the two endpoints.

More generally, the minimum value of a polynomial over a closed interval must either be one of the end points, or a point at which the derivative is zero. To find the points at which the derivative is zero, we must find the roots of a degree $k - 1$ polynomial, which can be done by computing the eigenvalues of the companion matrix [70]. We then obtain the argmin by minimizing P_t over this finite set of points (the roots of the derivative, plus the two endpoints of the interval, namely 0 and $\bar{\eta}_t$).

B.2 Optimizing a Non-Convex Quadratic Over a Hyperrectangle

In §5.2.3 we presented the SafeCombination algorithm, each step of which requires optimizing a possibly non-convex quadratic function over a hyperrectangle. Although this is in general NP-hard (as discussed below), we provide an efficient algorithm that maintains good performance in the case where the quadratic function is convex, while still offering a desirable performance guarantee in the general case.

For a vector $\mathbf{b} \in \mathbb{R}^d$, and a symmetric matrix $\mathbf{A} \in \mathbb{R}^{d \times d}$, let $f : \mathbb{R}^d \rightarrow \mathbb{R}$ be defined by

$$f(\mathbf{x}) \triangleq \frac{1}{2} \mathbf{x}^\top \mathbf{A} \mathbf{x} - \mathbf{b}^\top \mathbf{x}. \quad (\text{B.3})$$

For vectors $\underline{\mathbf{x}}, \bar{\mathbf{x}} \in \mathbb{R}^d$, with $\underline{\mathbf{x}} \leq \bar{\mathbf{x}}$ (elementwise), we wish to minimize f over the hyperrectangle $[\underline{\mathbf{x}}, \bar{\mathbf{x}}]$. That is, we wish to find

$$\mathbf{x}^* \triangleq \operatorname{argmin}_{\mathbf{x} \in [\underline{\mathbf{x}}, \bar{\mathbf{x}}]} \{f(\mathbf{x})\}. \quad (\text{B.4})$$

If \mathbf{A} is arbitrary, this problem includes the maximum cut problem as a special case, as is therefore NP-hard [14]. If \mathbf{A} is positive semidefinite, then $f(\mathbf{x})$ is convex, and \mathbf{x}^* can be found in polynomial time using a variety of convex optimization methods. If \mathbf{A} is positive definite, then the global minimum of $f(\mathbf{x})$ can be found using d steps of conjugate gradient descent. If the global minimum happens to be inside the hyperrectangle $[\underline{\mathbf{x}}, \bar{\mathbf{x}}]$, then it must equal \mathbf{x}^* .

We now describe a variant of conjugate gradient descent that always produces a solution inside the hyperrectangle $[\underline{\mathbf{x}}, \bar{\mathbf{x}}]$, while maintaining some desirable guarantees of conjugate gradient descent in the case where \mathbf{A} is positive definite. To explain our method, recall that two vectors $\mathbf{u}, \mathbf{v} \in \mathbb{R}^d$ are said to be *conjugate* with respect to \mathbf{A} if

$$\mathbf{u}^\top \mathbf{A} \mathbf{v} = 0. \quad (\text{B.5})$$

Like the conjugate gradient method, our algorithm will iteratively compute a set of conjugate directions $\{\mathbf{p}_1, \mathbf{p}_2, \dots, \mathbf{p}_d\}$, and will output a linear combination of the conjugate directions. However, this linear combination will be constrained to lie within the hyperrectangle $[\underline{\mathbf{x}}, \bar{\mathbf{x}}]$.

Our algorithm is defined by the following equations:

$$\begin{aligned} \mathbf{x}_0 &= \mathbf{0}_d \\ \mathbf{r}_i &= \nabla f(\mathbf{x}_i) & \forall i \in \{0, 1, \dots, d\} \\ \mathbf{p}_i &= -\mathbf{r}_i + \frac{\mathbf{r}_i^\top \mathbf{r}_i}{\mathbf{r}_{i-1}^\top \mathbf{r}_{i-1}} \mathbf{p}_{i-1} & \forall i \in \{1, 2, \dots, d\} \\ \alpha_i &= \operatorname{argmin}_{\alpha: \mathbf{x}_{i-1} + \alpha_i \mathbf{p}_i \in [\underline{\mathbf{x}}, \bar{\mathbf{x}}]} \{f(\alpha \mathbf{p}_i)\} & \forall i \in \{1, 2, \dots, d\} \\ \mathbf{x}_i &= \mathbf{x}_{i-1} + \alpha_i \mathbf{p}_i & \forall i \in \{1, 2, \dots, d\} \end{aligned} \quad (\text{B.6})$$

The vectors \mathbf{r}_i and \mathbf{p}_i are defined exactly as in the conjugate gradient descent algorithm (see Algorithm 5.2 of [67]). The only difference is that α_i is defined so as to guarantee that \mathbf{x}_i remains in the hyperrectangle.

It is easy to see by inspection that the vectors \mathbf{p}_i and \mathbf{p}_{i-1} are conjugate with respect to \mathbf{A} . With additional work, it can be shown that all \mathbf{p}_i and \mathbf{p}_j with $i \neq j$ are conjugate with respect to \mathbf{A} .

Lemma 8 (Theorem 5.3 of [67]). *For any symmetric matrix \mathbf{A} (not necessarily positive definite), the set of vectors $\{\mathbf{p}_1, \mathbf{p}_2, \dots, \mathbf{p}_d\}$ are conjugate with respect to \mathbf{A} (i.e., $\mathbf{p}_i^\top \mathbf{A} \mathbf{p}_j$ for $i \neq j$).*

With the conjugacy of $\{\mathbf{p}_1, \mathbf{p}_2, \dots, \mathbf{p}_d\}$ established, we can prove the following theorem, which shows that the algorithm always monotonically reduces the loss, while maintaining the good performance of conjugate gradient descent if \mathbf{A} is positive definite and the hyperrectangle is sufficiently large.

Theorem 13. *For any symmetric matrix \mathbf{A} , the sequence of iterates returned by algorithm (B.6) satisfy*

$$f(\mathbf{x}_d) \leq f(\mathbf{x}_{d-1}) \leq \dots \leq f(\mathbf{x}_1) \leq 0.$$

Furthermore, if \mathbf{A} is positive definite, and each \mathbf{x}_i is in the interior of $[\underline{\mathbf{x}}, \bar{\mathbf{x}}]$, then $\mathbf{x}_d = \mathbf{x}^$.*

Proof. First observe that, because \mathbf{p}_a and \mathbf{p}_b are conjugate for $a \neq b$ (by Lemma 8), the objective function decomposes additively:

$$\begin{aligned} f(\mathbf{x}_i) &= f\left(\sum_{a=1}^i \alpha_a \mathbf{p}_a\right) \\ &= \frac{1}{2} \left(\sum_{a=1}^i \alpha_a \mathbf{p}_a\right)^\top \mathbf{A} \left(\sum_{b=1}^i \alpha_b \mathbf{p}_b\right) - \mathbf{b}^\top \left(\sum_{a=1}^i \alpha_a \mathbf{p}_a\right) \\ &= \frac{1}{2} \left(\sum_{a=1}^d \alpha_a \mathbf{p}_a^\top \mathbf{A} \mathbf{p}_a\right) - \mathbf{b}^\top \left(\sum_{a=1}^i \alpha_a \mathbf{p}_a\right) \\ &= \sum_{a=1}^i f(\alpha_a \mathbf{p}_a). \end{aligned} \quad (\text{B.7})$$

This immediately implies

$$f(\mathbf{x}_i) = f(\mathbf{x}_{i-1}) + f(\alpha_i \mathbf{p}_i). \quad (\text{B.8})$$

Furthermore, because $\alpha_i = \operatorname{argmin}_{\alpha \in I_i} \{f(\alpha \mathbf{p}_i)\}$, where I_i is an appropriately-defined interval that includes 0, we have

$$f(\alpha_i \mathbf{p}_i) \leq f(0 \mathbf{p}_i) = 0. \quad (\text{B.9})$$

Combining (B.8) and (B.9) gives $f(\mathbf{x}_i) \leq f(\mathbf{x}_{i-1})$, which completes the first part of the proof.

To prove the second part of the theorem, we first note that, using (B.7),

$$\begin{aligned} \min_{\alpha_1, \alpha_2, \dots, \alpha_d \in \mathbb{R}} \left\{ f \left(\sum_{i=1}^d \alpha_i \mathbf{p}_i \right) \right\} &= \min_{\alpha_1, \alpha_2, \dots, \alpha_d \in \mathbb{R}} \left\{ \sum_{i=1}^d f(\alpha_i \mathbf{p}_i) \right\} \\ &= \sum_{i=1}^d \min_{\alpha_i \in \mathbb{R}} \{f(\alpha_i \mathbf{p}_i)\}. \end{aligned} \quad (\text{B.10})$$

Now suppose that each \mathbf{x}_i is in the interior of $[\underline{\mathbf{x}}, \bar{\mathbf{x}}]$. It follows that for all i , α_i is in the interior of I_i . Because $f(\alpha \mathbf{p}_i)$ is a quadratic function of α , the fact that α_i is in the interior of I_i implies $\alpha_i = \operatorname{argmin}_{\alpha \in \mathbb{R}} \{f(\alpha \mathbf{p}_i)\}$. Using (B.10), this implies

$$\mathbf{x}_d = \operatorname{argmin}_{\alpha_1, \alpha_2, \dots, \alpha_d \in \mathbb{R}} \left\{ f \left(\sum_{i=1}^d \alpha_i \mathbf{p}_i \right) \right\}. \quad (\text{B.11})$$

To complete the proof, we note that if \mathbf{A} is positive definite and the set of vectors $\{\mathbf{p}_1, \mathbf{p}_2, \dots, \mathbf{p}_d\}$ are conjugate with respect to \mathbf{A} , then it is not hard to see that the vectors $\mathbf{p}_1, \mathbf{p}_2, \dots, \mathbf{p}_d$ must be linearly independent, and therefore span \mathbb{R}^d . It follows that the right hand side of (B.11) is the global minimizer, \mathbf{x}^* , and therefore $\mathbf{x}_d = \mathbf{x}^*$, as claimed. \square

In experimenting with this algorithm, we found that it sometimes returns $\mathbf{0}$ in cases where a simpler coordinate descent algorithm is able to make progress. This happens when reducing f by moving along any conjugate direction \mathbf{p}_i results in a violation of the constraint $\mathbf{x} \in [\underline{\mathbf{x}}, \bar{\mathbf{x}}]$, but there exists a Euclidean basis vector \mathbf{e}_i such that, for some $\alpha_i \in \mathbb{R}$, $f(\alpha_i \mathbf{e}_i) < 0$ and $\alpha_i \mathbf{e}_i \in [\underline{\mathbf{x}}, \bar{\mathbf{x}}]$. To improve performance in such cases, we follow (B.6) by a single pass of cyclic coordinate descent in our implementation of SafeCombination.